博士論文

Pharmacological research of a novel selective SGLT2 inhibitor, tofogliflozin

(新規 SGLT2 選択的阻害剤 Tofogliflozin の薬効薬理学的研究)

永田　工

Contents

Abbreviations **5**

General Introduction **7**

Chapter I

Tofogliflozin, a novel sodium–glucose co-transporter 2 inhibitor, improves renal and pancreatic function in *db/db* mice

Introduction **12**

Materials and Methods **14**

Chemicals 14

Animals 14

Long-term administration study 14

Analysis 15

Evaluation of glomerular size and mesangial expansion 16

Measurement of islet β-cell mass 17

Statistical analysis 18

Results **19**

The effect of long-term tofogliflozin administration on hyperglycemia 19

The effect of long-term tofogliflozin administration on renal function 20

The effect of long-term tofogliflozin administration on β-cell function 22

Discussion **23**

Figures **30**

Chapter II

Selective SGLT2 inhibition by tofogliflozin reduces renal glucose reabsorption under hyperglycemic but not under hypo- or euglycemic conditions in rats

Introduction **46**

Materials and Methods **49**

Chemicals 49

Animals 49

Surgical operation 50

Infusion protocols with blood and urine collection 50

Analysis 52
Calculations 53
Statistical analysis 54
Results **55**
UGE under hyperglycemic conditions induced by glucose titration 55
UGE under hypo- and euglycemic conditions induced by glucose clamp 56
The effect of acute urinary glucose excretion induced by tofogliflozin or phlorizin on the plasma glucose levels and endogenous glucose production 57
Discussion **59**
Figures **65**
Tables **73**

Chapter III
Competitive inhibition of SGLT2 by tofogliflozin or phlorizin induces urinary glucose excretion through extending splay in cynomolgus monkeys

Introduction **79**
Materials and Methods **82**
Chemicals 82
Animals 82
Molecular cloning of cynomolgus monkey SGLT1 and SGLT2 83
Inhibition assay of AMG uptake in COS-7 cells transiently expressing cSGLT1/2 84
Glucose titration study in cynomolgus monkeys 84
Analysis 87
Calculations 87
Statistical analysis 89
Results **90**
In vitro characterization of cynomolgus monkey SGLT1 and SGLT2 90
Glucose titration study in cynomolgus monkeys 91
Discussion **96**
Figures **102**
Tables **117**

General Discussion **121**

Acknowledgments **125**

References **127**

Abbreviations

ACE	: angiotensin-converting enzyme
ACR	: albumin concentration corrected by urinary creatinine
AMG	: α-methyl-D-glucopyranoside
ANOVA	: analysis of variance
ARB	: angiotensin II receptor blocker
ATCC	: American Type Culture Collection
BW	: body weight
CKD	: chronic kidney disease
DAB	: diaminobenzidine
DBP	: diastolic blood pressure
DIO	: diet-induced obese
DN	: diabetic nephropathy
EGP	: endogenous glucose production
FRG	: familial renal glucosuria
G-6-PDH	: glucose-6-phosphate dehydrogenase
GFR	: glomerular filtration rate
GGM	: glucose-galactose malabsorption
GluFR	: glucose filtration rates
GluER	: glucose excretion rates
GluRR	: glucose reabsorption rates
Hb	: hemoglobin
HE	: hematoxylin-eosin
IDF	: International Diabetes Federation
IRI	: immunoreactive insulin
MAC	: minimum alveolar concentration
PAS	: periodic acid Schiff
PG	: plasma glucose
PHZ	: phlorizin
PD	: pharmacodynamic
PK	: pharmacokinetic
PPAR	: peroxisome proliferator-activated receptor
RGR	: renal glucose reabsorption
SBP	: systolic blood pressure
SGLT	: sodium/glucose cotransporter

SMIT1 : sodium/myoinositol transporter 1
STZ : streptozotocin
T1D : type 1 diabetes
T2D : type 2 diabetes
TGF : tubuloglomerular feedback
TmG : the transport maximum for glucose
TOFO : tofogliflozin
UGE : urinary glucose excretion
ZDF rats : Zucker diabetic fatty rats

General Introduction

The prevalence of diabetes mellitus is rapidly increasing worldwide due to various risk factors, such as population growth and aging, urbanization, reduced physical activity, and changes in lifestyle patterns. The latest estimate of the International Diabetes Federation (IDF) indicates that 8.3% of adults (approximately 382 million individuals) currently have diabetes, and the number is predicted to rise above 592 millions in less than 25 years. Furthermore, they estimated that 175 million of cases are currently undiagnosed, and these people are developing major unforeseen health complications (International Diabetes Federation 2013).

Diabetes mellitus is classified as insulin-dependent type I diabetes (T1D) or non-insulin-dependent type 2 diabetes (T2D). T2D accounts for 85%–95% of all diabetic patients. A person with T2D can live for several years without showing any symptoms, as hyperglycemia silently damages the body toward diabetic complications. Several studies have shown that many individuals with undiagnosed diabetes already have complications, such as chronic kidney disease (CKD) and heart failure (Plantinga *et al.* 2010; Flores-Le Roux *et al.* 2011). These studies emphasize the critical importance of early diagnosis to correct the hyperglycemia and prevent disease progression.

In mammals including humans, the blood glucose levels are tightly regulated by the intestines, pancreas, liver, skeletal muscles, adipose tissue, kidneys, and central nervous system. Therefore, these organs are major targets for diabetes care. Many antidiabetic agents targeting the intestines, pancreas, liver, skeletal muscles, and adipose tissues are already used to treat diabetic patients, such as biguanides, thiazolidinediones, alpha-glucosidase inhibitors, insulin secretagogues, and recombinant insulin mimetics. On the other hand, until quite recently, there have been no clinically available agents focusing on renal glucose reabsorption (RGR). Urine glucose excretion (UGE) is the net sum of glucose filtration from the glomeruli and reabsorption in the tubules. Glucosuria

occurs when the renal tubular absorptive capacity (the transport maximum for glucose (TmG)) is exceeded. In healthy individuals, 150–180 g glucose is filtered from the glomeruli to the tubules during the day, and completely reabsorbed in the tubules, with negligible glucosuria even in cases of postprandial hyperglycemia.

In humans, two families of glucose transporters were identified. These transporters comprise two structurally and functionally distinct groups, whose members have been identified over the past two decades, namely: (i) Na^+-dependent glucose co-transporters (SGLT, members of a larger family of Na^+-dependent transporters SGLT1-6); and (ii) the facilitative Na^+-independent sugar transporters (GLUT family, GLUT1-13). The SGLT family and sodium myo-inositol cotransporter 1 (SMIT1) catalyze the active transport of glucose using a sodium gradient. The GLUT family catalyzes the passive transport of glucose (Zhao & Keating 2007). Renal tubules express SGLT1, SGLT2, GLUT1, and GLUT2 for glucose reabsorption. SGLT2 is specifically expressed in renal proximal tubules and plays an important role in renal glucose reabsorption (Kanai *et al.* 1994; Wright *et al.* 2011). Familial renal glucosuria (FRG) is characterized by glucose excretion, despite normal blood glucose levels, due to a loss-of-function mutation in SGLT2 (Santer *et al.* 2003).

Mutations in SGLT2 are associated with FRG, a disease characterized by glucosuria in the absence of hyperglycemia and generalized signs of proximal tubular dysfunction. Despite the consistently high levels of UGE, FRG patients live normal healthy lives without no severe clinical consequences (Brodehl *et al.* 1987; Santer & Calado 2010; Santer *et al.* 2003). On the other hand, mutations in SGLT1 are associated with glucose-galactose malabsorption (GGM) syndrome in the gut. GGM is a rare metabolic disease and characterized by severe diarrhea and dehydration in infants on diets containing glucose or galactose. Notably, in GGM patients, little or no glucosuria has been observed (Wright *et al.* 2002). The potential side effects associated with SGLT1

inhibition make the selective inhibition of SGLT2 a more attractive strategy as a therapy for diabetes, even though both SGLT1 and SGLT2 inhibition could increase efficacy.

Evidence for such a beneficial effect comes not only from FRG patients but also from studies of phlorizin, a natural product isolated from the root bark of the apple tree and known to increase glucosuria. The administration of phlorizin could correct the hyperglycemia in partially pancreatectomized rats without changing insulin levels, and both insulin sensitivity (Rossetti, Smith, *et al.* 1987) and insulin secretion (Rossetti, Shulman, *et al.* 1987) were restored to normal. Despite an antidiabetic activity in several rodent models of diabetes, the development of phlorizin as an antidiabetic agent was discontinued, because phlorizin was readily hydrolyzed and poorly absorbed by the intestine, and inhibited SGLT1 equally as well as SGLT2. Furthermore, phloretin, an active metabolite of phlorizin, inhibits nonspecifically other glucose transporters (Ehrenkranz *et al.* 2005).

Because SGLT2 inhibition could potentially stimulate urinary glucose excretion (UGE) with low safety concerns (Han *et al.* 2008; Suzuki *et al.* 2012; Yamamoto *et al.* 2011), several SGLT2 inhibitors were discovered to overcome disadvantages of phlorizin, and are currently being developed in human clinical studies as a therapy for diabetes (Chao & Henry 2010; Ferrannini & Solini 2012). The potential of SGLT2 inhibitors for glycemic control was demonstrated in animal models of diabetes and in humans. However, their characters have been still unexplored as compared with other class of antidiabetic agents.

Studies characterizing the relationship between RGR and SGLT have been also performed with not only FRG patients but also phlorizin treated animals. However, controversial observations were reported in RGR characterization using the glucose titration study between genetic and pharmacological blockades of SGLT. Despite drastically increased glucosuria in both types of blockades of SGLT, the continuous infusion of phlorizin reduced TmG in rats (Bishop *et al.* 1978), while a missense

mutation of SGLT, reducing the affinity of the transporter for glucose in a certain type of FRG, showed no effect on TmG (Santer *et al.* 2003). Considering the non-specificity of phlorizin and phloretin against various glucose transporters, studies using a highly selective SGLT2 inhibitor could reveal the biological function of SGLT2 on RGR more precisely.

Tofogliflozin is a potent and highly selective inhibitor of SGLT2 (Ohtake *et al.* 2012) recently approved in Japan for the treatment of T2D (Poole & Prossler 2014). A single oral administration of this compound lowered blood glucose levels in Zucker diabetic rats with increased renal glucose clearance; moreover, 4-week administration of this compound improved glucose tolerance in *db/db* mice. Notably, tofogliflozin was the highest SGLT2 selective inhibitor against other SGLT family members among recently developed SGLT2 selective inhibitors, and showed no effect on glucose-related physiological processes, such as glucose uptake, glucose oxidation, and glycogen synthesis (Suzuki *et al.* 2012).

This research aimed to characterize the novel SGLT2 inhibitor, tofogliflozin, in terms of efficacy, safety, and pharmacodynamics, which are critical factors in evaluating the usefulness of a novel drug. In addition, this research clarified the role of SGLT1/2 in renal glucose reabsorption. First, efficacy was evaluated by testing the impact of long-term tofogliflozin administration on diabetic complications. Second, safety was evaluated in terms of the risk of developing hypoglycemia. Third, the pharmacodynamic properties of tofogliflzoin were determined by establishing a relationship among drug, glucose concentration, and glycosuric effect *in vivo*.

Chapter I

Tofogliflozin, a novel sodium–glucose co-transporter 2 inhibitor, improves renal and pancreatic function in *db/db* mice

Introduction

Type 2 diabetes (T2D) is characterized by impaired glycemic control as a result of insulin resistance or disturbed insulin secretion. Chronic hyperglycemia itself may impair insulin secretion and cause pancreatic β-cell dysfunction. Therefore, the preservation of β-cells through appropriate glycemic control is important to prevent both the onset of diabetes and the progressive deterioration of the diabetic disease state (Kahn 2003; Marchetti *et al.* 2009).

Renal sodium–glucose co-transporter 2 (SGLT2) is specifically expressed in renal proximal tubules, and plays the dominant role in renal glucose reabsorption (Kanai *et al.* 1994; Wright *et al.* 2011). Studies with T2D animal models have shown SGLT2 inhibitors to have a blood glucose-lowering effect via increased urinary glucose excretion and to have low safety concerns (Han *et al.* 2008; Suzuki *et al.* 2012; Yamamoto *et al.* 2011); consequently, several SGLT2 inhibitors are now being developed in clinical studies (Chao & Henry 2010; Ferrannini & Solini 2012).

Because SGLT2 predominantly functions in the kidney (J. Chen *et al.* 2010; Wright *et al.* 2011), it is important to know the effects of long-term SGLT2 inhibition on renal function, especially under diabetic conditions. As chronic hyperglycemia is also considered to contribute to the progression of diabetic nephropathy (DN)(The DCCT Research Group 1993; UKPDS Group 1998), the glucose-lowering effects that occur with SGLT2 inhibition may prevent the progression of DN by ameliorating glucose toxicity. Although studies with T2D model mice suggest that the long-term inhibition of SGLT2 by remogliflozin, an SGLT2 inhibitor (Fujimori *et al.* 2008), or by SGLT2 genetic deletion (Jurczak *et al.* 2011) preserves β-cells with improved glycemic conditions, no details on the effects of long-term SGLT2 inhibition on renal function have been reported, even in the above-mentioned preclinical studies.

Long-term administration of T-1095, an SGLT inhibitor, suggested that it has renoprotective effects in *db/db* mice together with improved glycemic conditions

(Arakawa *et al.* 2001). However, T-1095 and its metabolized active form T-1095A may inhibit not only SGLT2 but also SGLT1, which also functions in the kidney, due to their lower selectivity toward SGLT2 (Oku *et al.* 1999). Unfortunately, that study showed no comparison of the renal function with any clinically validated drug, such as angiotensin II receptor blocker (Rüster & Wolf 2006). Therefore, the actual effects of long-term SGLT2 inhibition on renal dysfunction in T2D were still unclear.

Tofogliflozin is a potent and highly selective inhibitor of SGLT2 (Ohtake *et al.* 2012) recently approved in Japan for the treatment of T2D (Poole & Prossler 2014). A single oral administration of this compound lowered blood glucose levels in Zucker diabetic rats with increased renal glucose clearance; moreover, 4-week administration of this compound improved glucose tolerance in *db/db* mice (Suzuki *et al.* 2012).

In this chapter, to evaluate the long-term effects of SGLT2 inhibition on renal and pancreatic function under diabetic conditions, it was intended to compare the long-term effects of tofogliflozin for 8 weeks on the renal and pancreatic functions in *db/db* mice, a mouse model of T2D, with those of losartan, an angiotensin II receptor blocker (ARB).

Materials and Methods

Chemicals

Tofogliflozin ((1S,3′R,4′S,5′S,6′R)-6-[(4-ethylphenyl)methyl]-3′,4′,5′,6′-tetrahydro-6′-(hydroxymethyl)-spiro[isobenzofuran-1(3H),2′-[2H]pyran]-3′,4′,5′-triol), was synthesized in laboratories at Chugai Pharmaceutical Co., Ltd. Losartan was purchased from LKT Laboratories Inc. (St. Paul, MN, USA). Laboratory chow (CE2-pellets) containing 0.005% (w/w) tofogliflozin, 0.015% tofogliflozin, or 0.045% losartan was prepared by Clea Japan, Inc. (Tokyo, Japan)

Animals

Female *db/db* mice (BKS.Cg-Dock7^{m} +/+ Lepr^{db}/J; stock no. 000642) and their lean controls (*db/+m* mice) were purchased from Charles River Laboratories Japan, Inc. (Yokohama, Japan) at 6 weeks of age. These animals were housed under a 12-h/12-h light/dark cycle (lights on 7:00 AM–7:00 PM) with controlled room temperature (20°C –26°C) and humidity (35%–75%), and were allowed *ad libitum* access to a diet of standard laboratory chow (CE-2 pellets; Clea Japan) and water. The animals were 8 weeks of age at the beginning of the experiments. All animal care and experiments were performed in accordance with the guidelines for the care and use of laboratory animals at Chugai Pharmaceutical Co., Ltd., and the protocol was approved by the Institutional Animal Care and Use Committee at the company.

Long-term administration study

The *db/db* mice were randomly allocated into 4 dietary treatment groups matched for both 24-h urinary albumin excretion and body weight at 8 weeks of age. The *db/db* mice were kept on the standard diet or on a diet containing 0.005% or 0.015% tofogliflozin or 0.045% losartan for 8 weeks. The tofogliflozin content was determined according to

previous pharmacokinetic (PK) data (Suzuki *et al.* 2012) and the estimated food consumption of *db/db* mice in order to inhibit SGLT2 completely but not SGLT1. The *db/+m* mice were kept on the standard diet. Blood glucose, glycated hemoglobin (Hb), plasma insulin, plasma creatinine, urinary glucose, urinary creatinine, and urinary albumin levels were measured periodically. Blood samples were collected from the tail vein or inferior vena cava to measure blood glucose, glycated Hb, plasma insulin, and plasma creatinine levels. Metabolic cages were used to collect urine to measure urinary glucose, urinary creatinine, and urinary albumin excretion. At the end of 8 weeks' treatment, animals were sacrificed by whole blood collection from the abdominal aorta under anesthesia with isoflurane. The kidneys and pancreas were isolated for the histological analysis described below. As part of these studies a separate group of *db/db* mice (16 weeks of age, n=9) was kept on the diet containing 0.015% tofogliflozin for 4 days, then three mice each were sacrificed at 10:00, 15:00 and 20:00 on day 4 by whole blood collection from the abdominal aorta under anesthesia and the plasma samples were obtained by centrifugation to determine plasma tofogliflozin concentrations. Urine and plasma samples were stored at −80°C until use.

Analysis

Plasma tofogliflozin concentrations were measured with an HPLC–MS/MS system (Shimadzu 20A [Shimadzu, Kyoto, Japan]; API-4000 [AB SCIEX, Framingham, MA, USA]).

Blood glucose levels were determined using a plasma-glucose monitoring system (Accu-Chek Aviva; Roche Diagnostics, Tokyo, Japan). Urinary glucose concentrations were measured by the hexokinase G-6-PDH method (L-Type Glu 2; Wako Pure Chemical Industries, Ltd., Osaka, Japan) with an automated analyzer (TBA-120FR; Toshiba Medical Systems, Tochigi, Japan). Creatinine concentrations in plasma and urine were measured by the creatininase–HMMPS method (L-Type Creatinine M; Wako Pure

Chemical Industries) with the automated analyzer. Glycated Hb levels were measured by turbidimetric inhibition immunoassay (Auto Waco HbA1c; Wako Pure Chemical Industries) with the automated analyzer. Urinary albumin concentrations were measured by turbidimetric immunoassay (Testant Mouse Urinary Microalbumin Assay; TAUNS Laboratories, Inc., Shizuoka, Japan) with the automated analyzer. Urinary albumin excretion was evaluated as urinary albumin concentration corrected by urinary creatinine (ACR).

Renal creatinine and glucose clearance were determined by dividing the rate of urinary creatinine and glucose excretion for each urine collection period (24-h cumulative urine sample) by the plasma creatinine and glucose levels, respectively.

Plasma insulin levels were determined with an insulin ELISA kit (Morinaga Institute of Biological Science, Kanagawa, Japan).

Evaluation of glomerular size and mesangial expansion

The kidneys were fixed in methanol–Carnoy's solution and embedded in paraffin. The blocks were sliced into sections 3 μm thick and stained with an anti-type IV collagen antibody (20441; Novotec, Lyon, France) or with the hematoxylin and periodic acid Schiff (PAS), and the type IV collagen-stained sections were then visualized with biotinylated secondary antibody (K4003; Dako Japan Inc., Tokyo, Japan) and horseradish peroxidase-conjugated streptavidin with diaminobenzidine (DAB) chromogen (K3466; Dako), and finally stained with hematoxylin by Sapporo General Pathology Laboratory Co., Ltd. (Sapporo, Japan).

For the quantification of glomerular size and mesangial type IV collagen-positive area, sections were scanned with the ScanScope and ImageScope imaging and analysis systems (Aperio Technologies, Inc., Vista, CA, USA). Fifty glomeruli per mouse from 2 different sections were randomly selected in the cortex region. The average of glomerular size was calculated by dividing total glomerular area (mm^2) by the number of analyzed

glomeruli for each mouse. The mesangial matrix area was defined as the type IV collagen-positive area and is expressed as the average number of the total numbers of "Positive and Strong Positive" pixels from among each of the analyzed glomeruli for each mouse by using the Positive Pixel Count V9 algorithm on the default setting, and converted to the type IV collagen-positive area (mm^2) from the correlation formula between the total numbers of pixels and the area in analyzed glomeruli as follows (the area = the number of pixels × $2.5139974 \times 10^{-7} + 2.814267 \times 10^{-8}$; $r^2 = 1$).

Mesangial expansion in the PAS-stained sections was evaluated in a blinded manner under a light microscope. A total of 72 to 100 glomeruli were randomly selected from each animal. The mesangial matrix expansion was graded on a semiquantitative scale from 0 to 4+, as described by other investigators (Guo *et al.* 2006; Qi *et al.* 2005), by scoring the PAS-positive area in the glomerulus as follows: 0 indicates no expansion; 1+ indicates matrix expansion occupying up to 25% of a glomerulus; and 2+, 3+, and 4+ indicate matrix expansion occupying 25–50, 50–75, and more than 75% of a glomerulus, respectively. The mesangial matrix score for each animal was shown as the average score of all the glomeruli that had been graded.

Measurement of islet β-cell mass

Collected pancreases were embedded in OCT compound (Sakura Finetek, Tokyo, Japan) in cryomolds and frozen in *n*-hexane chilled with acetone and dry ice, then sliced into sections 5 µm thick and stained with hematoxylin–eosin (HE) by Sapporo General Pathology Laboratory. Pancreas sections adjacent to the above-mentioned HE-stained sections were immunostained with anti-insulin antibody (sc-9168; Santa Cruz Biotechnology, Inc., Dallas, TX, USA) and visualized with biotinylated secondary antibody (BA-1000; Vector Laboratories Inc., Burlingame, CA, USA) and horseradish peroxidase-conjugated streptavidin with DAB chromogen (Discovery DAB Map Kit

760-124; Roche Diagnostics K.K., Tokyo, Japan). For 4 pancreas sections randomly selected from each mouse, the total β-cell area was calculated as the ratio of insulin-positive area/pancreas area with the imaging and analysis systems mentioned above. The insulin-positive area and total pancreas area were determined with the "Strong Positive" and the total ("Positive + Negative") pixel numbers, respectively, using the Positive Pixel Count V9 algorithm with the intensity threshold settings as follows: weak, 220–150; medium, 150–100; strong, 100–0.

Statistical analysis

Data are presented as means ± SEM. Statistical analysis was performed with the SAS System for Windows, Release 8.02 (SAS Institute Japan, Tokyo, Japan). Statistical significance was determined by the parametric Dunnett's multiple comparison test for metabolic parameters in treated versus untreated *db/db* mice, by the non-parametric Dunnett's multiple comparison (joint-ranking) for histological analysis in treated versus untreated *db/db* mice, or by Student's *t*-test in untreated *db/db* versus *db/+m* mice.

Results

The effect of long-term tofogliflozin administration on hyperglycemia

The fed-state plasma glucose (PG) and glycated Hb levels were both significantly higher in untreated diabetic mice than in *db/+m* mice throughout the experiment. The PG and glycated Hb levels after 4 and 8 weeks were significantly lower in the groups of *db/db* mice treated with 0.005% or 0.015% tofogliflozin than in the untreated control group (Figure 1A, B). The plasma tofogliflozin concentrations in the mice kept on the diet containing 0.015% tofogliflozin for 4 days (16 weeks of age, n=3) at 10:00, 15:00 and 20:00 were 364 ± 35, 216 ± 44 and 606 ± 42 ng mL^{-1}, respectively. No improvement in glycemic condition was observed in the group treated with 0.045% losartan.

The urine volume and urinary glucose excretion (UGE) were significantly higher in untreated *db/db* mice than in *db/+m* mice (Figure 1C, D). Tofogliflozin treatment lowered urine volume compared with the untreated control group at 8 weeks of treatment (Figure 1C). Tofogliflozin treatment tended to decrease the UGE compared with the untreated control group at 4 and 8 weeks of treatment, but the differences did not reach statistical significance (Figure 1D). Tofogliflozin treatment increased renal glucose clearance levels compared with untreated *db/db* mice, whereas losartan treatment had no effect on this parameter (Figure 1E).

At baseline (0 weeks of treatment), the UGE became apparent at PG above around 200 mg dL^{-1} and increased depending on the PG levels, suggesting the glucose filtration levels around 200 mg dL^{-1} exceeded the threshold of glucose reabsorption in *db/db* mice (Figure 2A). At 4 and 8 weeks, the UGE in control and losartan groups was also apparent with increases in PG to around 400–600 mg dL^{-1}. In contrast, although tofogliflozin treatment reduced the PG to around 100–250 mg dL^{-1} at 4 and 8 weeks, their daily UGE levels were still higher than those at 0 weeks when the PG was around 100–250 mg dL^{-1} (Figure 2B, C).These results indicate that tofogliflozin treatment reduced the threshold of

glucose reabsorption in *db/db* mice and increased the UGE levels, and then reduced the PG.

The body weight of untreated *db/db* mice increased gradually till 10 weeks of age (2 weeks of treatment) and reached a maximum of about 50 g (Figure 3A). Tofogliflozin treatment increased the body weight and food consumption of *db/db* mice, whereas losartan treatment had no effect on these parameters (Figure 3B). At baseline, there was no clear relationship between the body weight and daily food consumption (Figure 4A). Interestingly, at 4 weeks, when the difference in body weight between the tofogliflozin and the control groups began to be clear (Figure 3A, B), the daily food consumption in tofogliflozin groups was greater than that in the control group, even between animals with similar body weight (Figure 4B). Finally at 8 weeks, there was a clear positive relationship between the body weight and food consumption, suggesting that the levels of food consumption at this stage were closely linked to the body weight of the animals (Figure 4C).

The effect of long-term tofogliflozin administration on renal function

At baseline, the ACR value ($\mu g\ mg^{-1}$) was higher in the untreated *db/db* mice than in the *db/+m* mice (untreated *db/db* mice, 433 ± 50; *db/+m*, 153 ± 19; $P<0.001$). There were no significant differences in the ACR values at baseline among any of the treatment groups in the *db/db* mice. The ACR values in *db/+m* mice at 4 and 8 weeks of treatment were 118 ± 18 $\mu g\ mg^{-1}$ and 99 ± 30 $\mu g\ mg^{-1}$, respectively, which were slightly smaller than the ACR values at baseline (Figure 5A). In contrast, the ACR values in untreated *db/db* mice at 4 and 8 weeks of treatment increased by about 455 $\mu g\ mg^{-1}$ and 766 $\mu g\ mg^{-1}$ from baseline (Figure 5B), resulting in ACR values of 888 ± 170 $\mu g\ mg^{-1}$ and 1199 ± 284 $\mu g\ mg^{-1}$ at 4 and 8 weeks of treatment, respectively (Figure 5A). Both losartan and tofogliflozin treatment significantly prevented the increase of the ACR value by about 50% to 70% (Figure 5A, B).

At baseline, a trend toward a positive correlation between ACR values and PG levels was observed (Figure 5C). At 4 and 8 weeks, although the ACR values of several animals in the control groups exceeded 1,000 μg $mg^{-1}$and 2,000 μg mg^{-1}, respectively, the ACR values in the tofogliflozin and losartan groups were still maintained at levels less than 1,000 μg mg^{-1}, with improved glycemic conditions in the tofogliflozin groups but not in the losartan group (Figure 5D, E).

Creatinine clearance was significantly higher in the untreated *db/db* mice than in the *db/+m* mice (Figure 6A), which is consistent with the reported hyperfiltration in *db/db* mice (Gärtner 1978; Sugaru *et al.* 2006b) or streptozotocin-induced (STZ-induced) diabetic mice (Dunn *et al.* 2004; Vallon *et al.* 2013). Tofogliflozin and losartan treatment slightly ameliorated the increase in creatinine clearance. The plasma creatinine concentrations at 8 weeks of treatment were 0.059 ± 0.005 mg dL^{-1} in the untreated *db/db* mice, 0.064 ± 0.003 mg dL^{-1} in the 0.005% tofogliflozin-treated mice, 0.064 ± 0.003 mg dL^{-1} in the 0.015% tofogliflozin-treated mice, 0.064 ± 0.005 mg dL^{-1} in the 0.045% losartan-treated *db/db* mice, and 0.124 ± 0.012 mg dL^{-1} in the *db/+m* mice (untreated *db/db* mice *vs. db/+m* mice, $P<0.005$). A tendency towards a positive correlation between the PG and the creatinine clearance levels was observed in the tofogliflozin and losartan groups (Figure 6B).

The kidney weight of the *db/db* mice (control group) was significantly greater than that of *db/+m* mice. Neither tofogliflozin nor losartan treatment reduced the kidney weight, and there was no clear relationship between the glucose levels and the kidney weight in *db/db* mice (Figure 6C, D).

The renoprotective effect of tofogliflozin was also assessed by histopathological analysis (Figure 7A, 8A). The mean glomerular area was significantly larger in the untreated *db/db* mice than in the *db/+m* mice. Tofogliflozin treatment significantly attenuated glomerular hypertrophy in a dose-dependent manner, whereas losartan treatment had no effect on the glomerular size (Figure 7B). Both in the PAS- and type IV

collagen-stained sections, the mesangial matrix area was also significantly greater in the untreated *db/db* mice than in the *db/+m* mice. Neither tofogliflozin nor losartan significantly altered the mesangial expansion (Figures 5C, 8B).

The effect of long-term tofogliflozin administration on β-cell function

The levels of plasma immunoreactive insulin (IRI) in the untreated *db/db* mice decreased from 9.9 ± 2.4 ng mL^{-1} at the start of study to 2.0 ± 0.3 ng mL^{-1} at week 8 ($p<0.05$). Tofogliflozin treatment prevented the decrease in IRI levels and resulted in a significant increase in IRI levels as compared with the untreated group at 8 weeks of treatment. Losartan treatment had no effect on IRI level (Figure 9A). To assess the potential for preventing β-cell loss by improving hyperglycemia, the total β-cell mass was determined from the ratio of the anti-insulin positive stained area. The total β-cell mass was significantly larger in the untreated *db/db* mice than in the *db/+m* mice at the start of the study (Figure 9B, C). After 8 weeks, the β-cells of untreated *db/db* mice degraded and the total β-cell mass was significantly reduced compared to that of control lean mice, implying β-cell loss in the *db/db* mice. Tofogliflozin treatment significantly and dose-dependently elevated the total β-cell mass, suggesting that β-cell loss was prevented (Figure 9D, E).

Discussion

Several SGLT inhibitors are being developed as a new class of anti-diabetic agent. Studies in *db/db*-SGLT2$^{-/-}$ mice (Jurczak *et al.* 2011) and studies of SGLT inhibitors, such as T-1095 (Arakawa *et al.* 2001) and remogliflozin (Fujimori *et al.* 2008), in *db/db* mice have suggested that long-term inhibition of SGLT might exert a protective effect on kidneys and β-cells in T2D. However, the actual renoprotective effects exerted via SGLT2 inhibition are unclear owing to the lack of a positive renoprotective compound in the study on the non-selective SGLT1/2 inhibitor T-1095 (Arakawa *et al.* 2001) and the lack of parameters on renal function in the study on long-term SGLT2 inhibition (Jurczak *et al.* 2011).

To evaluate the renoprotective effects of long-term SGLT2 inhibition more precisely, it was intended to compare the effects of tofogliflozin (a highly specific SGLT2 inhibitor) with the effects of losartan (ARB) on renal and β-cell functions, together with a quantitative analysis of glomerular and islet β-cell mass. It was demonstrated that long-term SGLT2 inhibition with tofogliflozin prevented not only loss of islet β-cells but also the progression of renal impairment in *db/db* mice.

In this chapter, sustained blood glucose-lowering effects and stably reduced glycated hemoglobin levels were observed over 4 to 8 weeks of treatment with tofogliflozin together with a significant increase in glucose clearance (Figure 1A, B, E), suggesting that stable long-term glycemic control can be achieved by tofogliflozin treatment.

Based on the measured concentrations of tofogliflozin in plasma in the mice (0.015% tofogliflozin group) and the protein-binding properties of tofogliflozin, it seemed reasonable to estimate the unbound tofogliflozin concentrations to be between 120 and 350 nM. These concentrations are about 24–70 times the IC_{50} value of tofogliflozin against mouse SGLT2 (5.0 nM) and one-fifteenth to one-fifth of its IC_{50} value against mouse SGLT1 (1800 nM) (Suzuki *et al.* 2012). Therefore, the unbound concentrations of

400 tofogliflozin mentioned above are sufficient to inhibit mouse SGLT2 almost completely
401 but not inhibit mouse SGLT1.
402 DN is a major cause of chronic kidney failure and end-stage renal disease in diabetic
403 patients. Renal failure caused by chronic hyperglycemia via metabolic factors, such as
404 increased oxidative stress, renal polyol formation and advanced glycated end-products
405 (Cooper 2001), is a major micro-vascular complication in T2D patients, and intensive
406 glycemic control to prevent the progression of DN is recommended (American Diabetes
407 Association 2013; National Kidney Foundation 2007; The DCCT Research Group 1993;
408 UKPDS Group 1998).
409 In addition to metabolic factors, the hemodynamic factors of increased systemic and
410 intraglomerular pressure are also implicated in the pathogenesis of DN (Dronavalli *et al.*
411 2008; Forbes *et al.* 2007).
412 The *db/db* mouse has been used as an animal model of T2D that develops progressive
413 kidney disease similar to human DN (Breyer *et al.* 2005; Soler *et al.* 2012). In *db/db* mice,
414 glomerular hyperfiltration during the early stage of diabetes has been reported (Gärtner
415 1978; Sugaru *et al.* 2006b), which was also suggested by the increased creatinine
416 clearance in *db/db* mice in this chapter (Figure 6A). Although several discrepancies have
417 been noted between the severity of nephropathy in this mouse strain and that in humans, a
418 number of basic and novel therapeutic agents have been investigated in *db/db* mice and
419 been found to reduce the progression of renal failure with decreased albuminuria (Tesch
420 & Lim 2011).
421 Arakawa *et al.* (2001) reported that albuminuria and mesangial expansion were
422 improved in T-1095-treated *db/db* mice. However, their study did not compare any renal
423 function parameters (including glomerular filtration rate) after treatment with clinically
424 validated anti-nephropathy drugs, such as ARB. Moreover, the selectivity of T-1095
425 toward SGLT2 versus SGLT1 is low (Oku *et al.* 1999) . Therefore, the precise potential
426 of SGLT2 inhibition for the treatment of DN was still unknown. To address this issue, it

was intended to compare the renoprotective effects of tofogliflozin in *db/db* mice with those of losartan, which has been shown to suppress the increase in urinary albumin excretion until 17 weeks of age (Sugaru *et al.* 2006a). It was found that 8-week treatment with either tofogliflozin or losartan equally ameliorated the increase in creatinine-corrected urinary albumin excretion, an important marker of glomerular dysfunction. Considering that the actual plasma concentration of tofogliflozin in the *db/db* mice was sufficient to inhibit only mSGLT2, it is suggested that specific SGLT2 inhibition has the potential to delay the progression of DN. Furthermore, given the concerns with SGLT1 inhibition, such as gastrointestinal side effects, the increased risk of hypoglycemia and unknown effects with long-term inhibition of this ubiquitous transporter (Washburn & Poucher 2013), it is considered that specific SGLT2 inhibitors have potential as anti-diabetic agents without safety concerns in long-term administration.

This chapter confirmed the presence of glomerular hyperfiltration in *db/db* mice as compared with *db/+m* mice and showed that creatinine clearance tended to be suppressed in both tofogliflozin- and losartan-treated *db/db* mice. Therefore, it is suggested that suppression of glomerular hyperfiltration may contribute to ameliorating the increase in urinary albumin excretion. Interestingly, imaging analysis of renal glomeruli revealed that tofogliflozin suppressed glomerular hypertrophy, whereas losartan had no effect on glomerular size. These findings indicate that tofogliflozin and losartan may each suppress the deterioration of renal function via different mechanisms.

Long-term treatment with losartan delayed the progression of nephropathy in *db/db* mice (Sugaru *et al.* 2006a). The renoprotective effects of angiotensin-converting enzyme inhibitors (ACEi) and ARBs are mainly considered to be due to the antihypertensive effects they achieve by inhibiting the renin-angiotensin system (Thomas & Atkins 2006). The blood pressure of *db/db* mice was reported to be higher than that of *db/+m* mice with higher plasma ACE activity and angiotensin II concentration, and the treatment with

losartan reduced the blood pressure of *db/db* mice to the normal range (Senador *et al.* 2009). In addition, both enalapril, an ACEi (Moriyama *et al.* 2004), and valsartan, an ARB (Dong *et al.* 2010), exerted their renoprotective effects in *db/db* mice with blood pressure-lowering effects. Therefore, it is assumed that the renoprotective effect of losartan in this chapter is mainly due to the reduction of intraglomerular pressure.

The mild antihypertensive effect that SGLT inhibitors have on systolic blood pressure has also been reported following phlorizin treatment in a STZ/high salt diet model (Osorio *et al.* 2010) and dapagliflozin treatment in T2D patients (Bailey *et al.* 2010; Wilding *et al.* 2009).

Tofogliflozin showed a sustained blood glucose-lowering effect in *db/db* mice, whereas losartan had no effect on glucose levels (Figure 1A, B). Therefore, amelioration of glucose toxicity by tofogliflozin may contribute to the above-mentioned differences in renoprotective effect between losartan and tofogliflozin. Recently, empagliflozin, an SGLT2 inhibitor, was reported to reduce the inflammatory and fibrotic markers in human kidney proximal tubular cells by blocking glucose entry (Panchapakesan *et al.* 2013). The amelioration of hyperglycemic condition in the proximal tubular cells by SGLT2 inhibition might explain the difference in the renoprotective effects between losartan and tofogliflozin.

The contribution of the tubuloglomerular feedback (TGF) system in early DN has been well investigated in STZ-induced diabetic model rodents (Vallon *et al.* 2003). The enhanced Na^+ reabsorption coinciding with higher reabsorption of filtered glucose through SGLT1/2 that occurs in the diabetic state as compared with that in the normoglycemic state reduces the TGF signal at the macula densa, leading to an increase in single nephron glomerular filtration rate (Vallon & Thomson 2012).

More recently, Vallon et al. showed that the knockout of SGLT2 attenuated hyperglycemia and glomerular hyperfiltration, thus preventing the increase in ACR of STZ diabetic mice, and they suggested that the TGF system contributed to these effects

(Vallon *et al.* 2013). However, in their study, the SGLT2 knock-out showed no effect on kidney growth or on the marker of renal injury.

This chapter also showed that ACR increase was attenuated by tofogliflozin with a long-term improvement of hyperglycemic condition and tendency of amelioration of hyperfiltration without reducing kidney weight. Considering the up-regulation of SGLT2 in the kidney of *db/db* mice (Vallon *et al.* 2013), it is likely reasonable to assume that the TGF system may contribute to hyperfiltration of *db/db* mice.

Taken together, there are at least 2 mechanisms by which SGLT inhibition could possibly ameliorate glomerular hyperfiltration and the increase of ACR: one is the improvement of TGF signaling, the other is the reduction of systolic blood pressure. Further characterization, such as by using the micro-puncture technique, is required to address the precise mechanisms involved in the reduction of glomerular hypertrophy with long-term tofogliflozin treatment.

A reduction in body weight by SGLT2 inhibition through the negative energy balance was confirmed in a human clinical study (Zhang *et al.* 2010) and in diet-induced and genetically obese rodents (Devenny *et al.* 2012; Liang *et al.* 2012). Paradoxically, in this chapter, the body weight in tofogliflozin-treated *db/db* mice increased gradually throughout the study with increased food consumption (Figure 2B), whereas the untreated *db/db* mice showed no weight gain after 10 weeks of age with no increase in food consumption, resulting in a significant increase in body weight in the tofogliflozin groups compared to the untreated group after 4 weeks (Figure 2A). Hyperphagia was induced in rodents by inhibiting SGLT2, both in diet-induced obese rats treated with an SGLT2 inhibitor (Devenny *et al.* 2012) and in SGLT2 knock-out mice (Vallon *et al.* 2013). In addition, similar weight gain and preserved plasma insulin levels were also reported for *db/db* mice treated with other SGLT inhibitors, T-1095 (Arakawa *et al.* 2001) and remogliflozin (Fujimori *et al.* 2008).

Because the plasma IRI levels of the untreated *db/db* mice decreased markedly from 0 to 8 weeks of treatment, the lack of further body weight gain in untreated *db/db* mice may be due to the decreased insulin secretion, which is consistent with the previous reports on the disease progression of *db/db* mice (Gibbs *et al.* 1995; Lenhard *et al.* 1999). On the other hand, plasma insulin secretion was significantly preserved in tofogliflozin-treated *db/db* mice (Figure 9A). These results imply that the preserved insulin levels in tofogliflozin groups would have maintained the insulin's anabolic actions in *db/db* mice, leading to the increased food consumption and body weight (Figure 2A, B).

Although modest but significant body weight reductions by SGLT2 inhibitors, including tofogliflozin, were observed both in T2D patients (Fonseca *et al.* 2013; Kadowaki *et al.* 2012; Schernthaner *et al.* 2013; Wilding *et al.* 2012) and in DIO rats (Devenny *et al.* 2012) and KK-A^y mice, a mouse T2D model without β-cell deprivation with aging (Katsuno *et al.* 2009), further evaluations will be needed to understand the interactions among UGE, appetite and insulin secretion of T2D patients treated with SGLT2 inhibitors.

In an earlier study, it was reported that tofogliflozin had no direct effect on glucose-stimulated insulin secretion by isolated pancreatic islets (Suzuki *et al.* 2012). Imaging analysis revealed that β-cell mass was significantly increased in tofogliflozin-treated *db/db* mice (Figure 9D, E), implying that preserved islet mass may contribute to maintaining the plasma insulin secretion.

The preserved β-cell function of *db/db*-SGLT2$^{-/-}$mice was associated with increased β-cell mass and reduced incidence of β-cell apoptosis (Jurczak *et al.* 2011). The plasma tofogliflozin concentrations measured in the 0.015% tofogliflozin group were sufficient to specifically inhibit mSGLT2. Therefore, it is likely that increased β-cell mass in tofogliflozin-treated *db/db* mice was caused by mechanisms similar to those in SGLT2-deleted *db/db* mice. Since no human clinical studies have directly addressed the

effect of SGLT2 inhibitors on β-cell loss, this beneficial effect remains to be determined in human T2D.

Several study limitations should be considered in this study. First, the lack of hemodynamic data of *db/db* mice means that the mechanisms of the renoprotective effects of losartan and tofogliflozin through their hemodynamic effects discussed above are speculative. Second, although the mechanisms underlying the reduction of ACR with tofogliflozin are considered to be closely related to its blood glucose-lowering effect, the essential mode of action that is dependent on the amelioration of glucose toxicity and independent of glucose remains to be elucidated.

In conclusion, this chapter showed evidence for prevention of kidney and pancreatic dysfunctions in a T2D mice model through long-term SGLT2 inhibition with tofogliflozin. Further studies are required to evaluate the therapeutic usefulness of tofogliflozin for preservation of renal function and β-cells in T2D patients.

Figures

Figure 1 Blood glucose and glycated Hb in db/db mice.

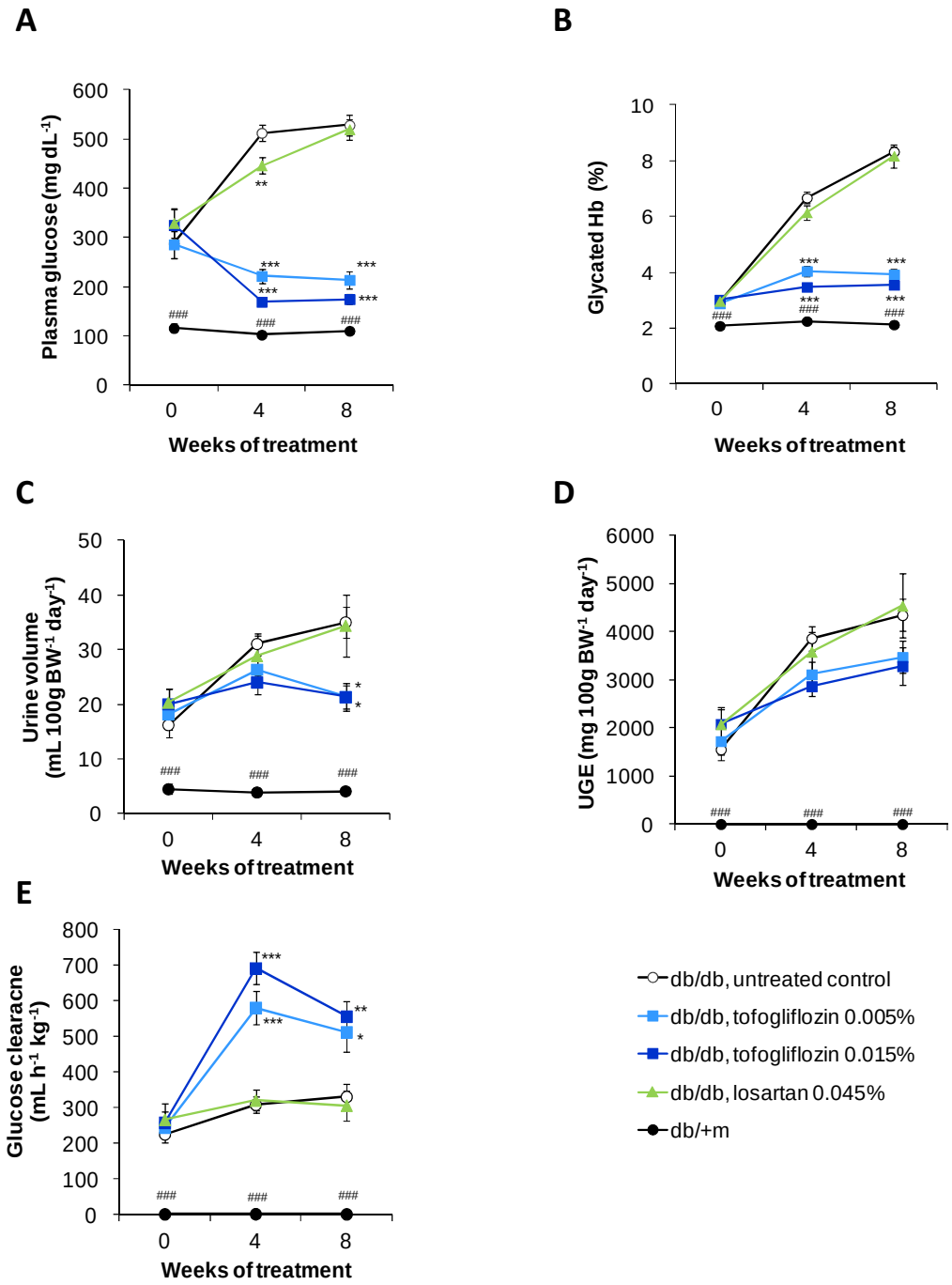

(A–B) Tofogliflozin lowered blood glucose concentration (A) and suppressed glycated Hb (B) in *db/db* mice.

554 **(C–E)** Long-term tofogliflozin administration lowered the urine volume (C), lowered
555 urinary glucose excretion (D), and elevated glucose clearance (E) in *db/db* mice.
556 Symbols represent mean values and vertical lines indicate SEM (*db/db* mice, n=8;
557 *db/+m* mice, n=10).
558 * P<0.05, ** P<0.01, *** P<0.001 versus control group by Dunnett's multiple
559 comparison test. ### P<0.001 versus control group by t-test.
560

Figure 2 Scatter plot of plasma glucose and UGE levels in db/db and db/+m mice.

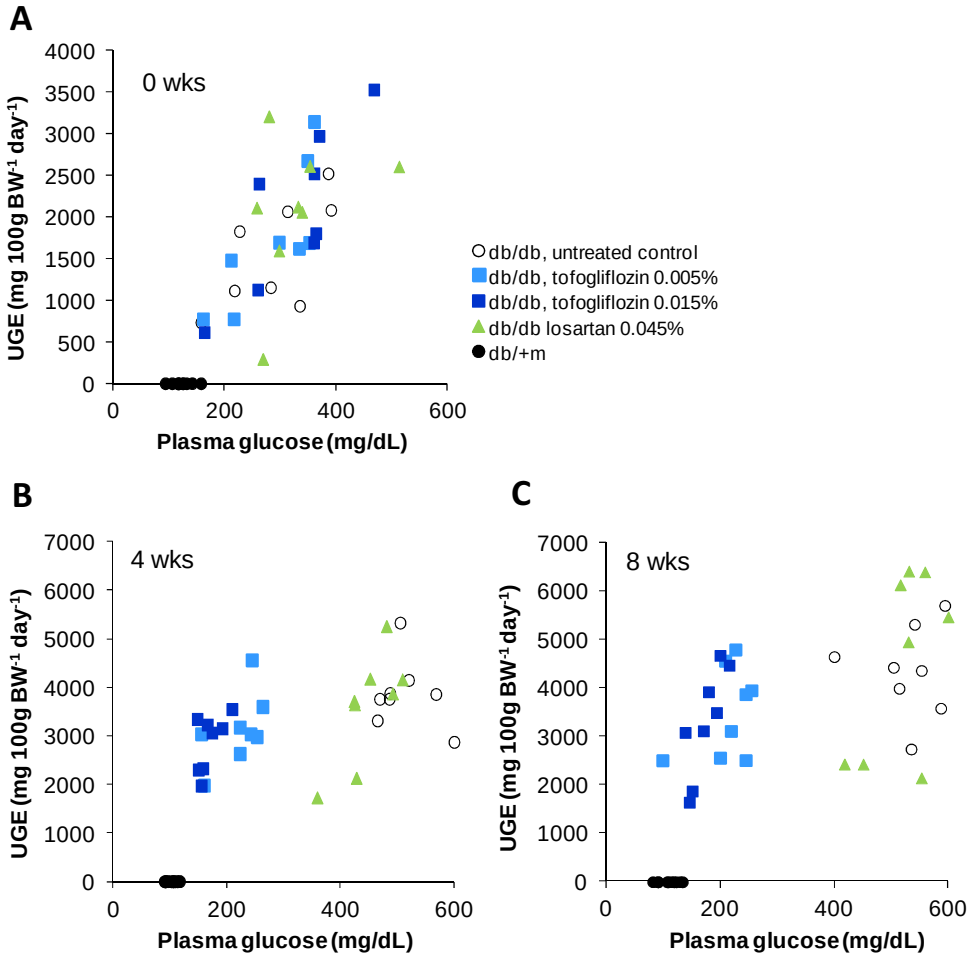

(A) 0 weeks (Baseline value), **(B)** 4 weeks of treatment, **(C)** 8 weeks of treatment

Symbols represent individual values.

Figure 3 Body weight and food consumption in db/db mice.

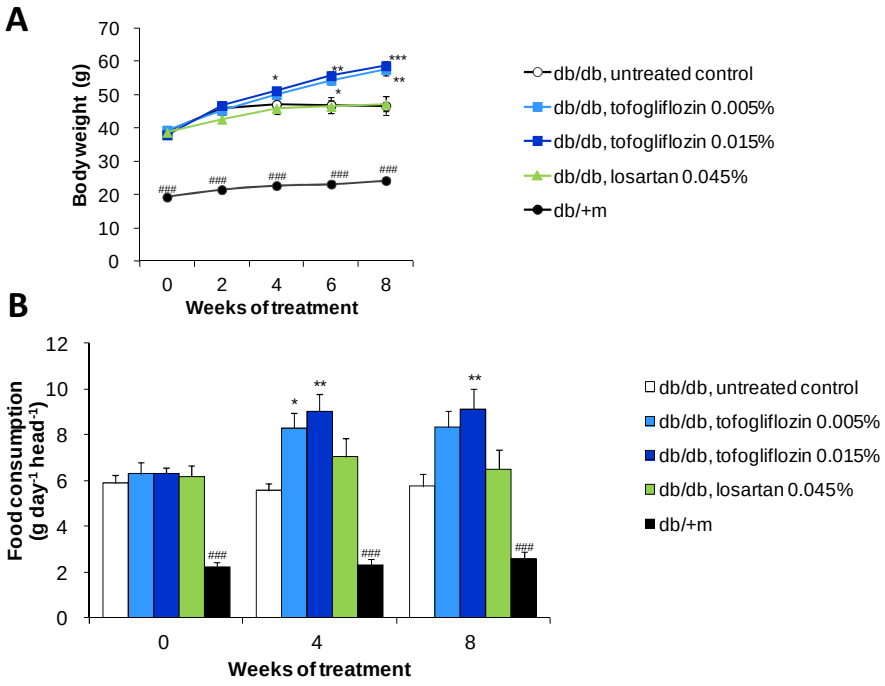

(A–B) Tofogliflozin treatment increased body weight (A) and food consumption (B) in *db/db* mice.

Symbols and columns represent mean values and vertical lines indicate SEM (*db/db* mice, *n*=8; *db/+m* mice, *n*=10).

* *P*<0.05, ** *P*<0.01, *** *P*<0.001 versus control group by Dunnett's multiple comparison test. ### *P*<0.001 versus control group by *t*-test.

Figure 4: Scatter plot of body weight and food consumption in db/db mice.

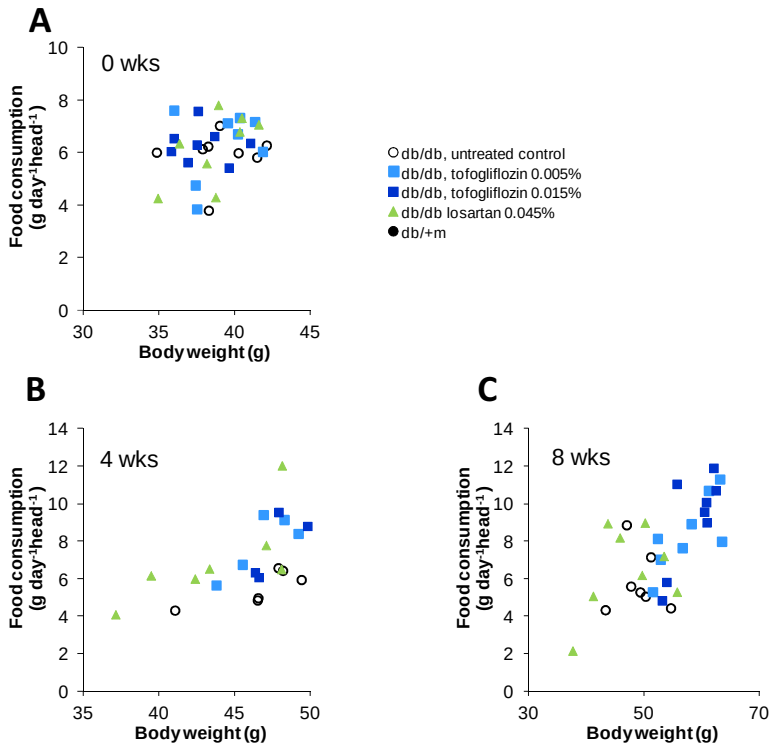

(A) 0 weeks (Baseline value), **(B)** 4 weeks of treatment, **(C)** 8 weeks of treatment Symbols represent individual values.

Figure 5 Urinary albumin excretion in db/db and db/+m mice.

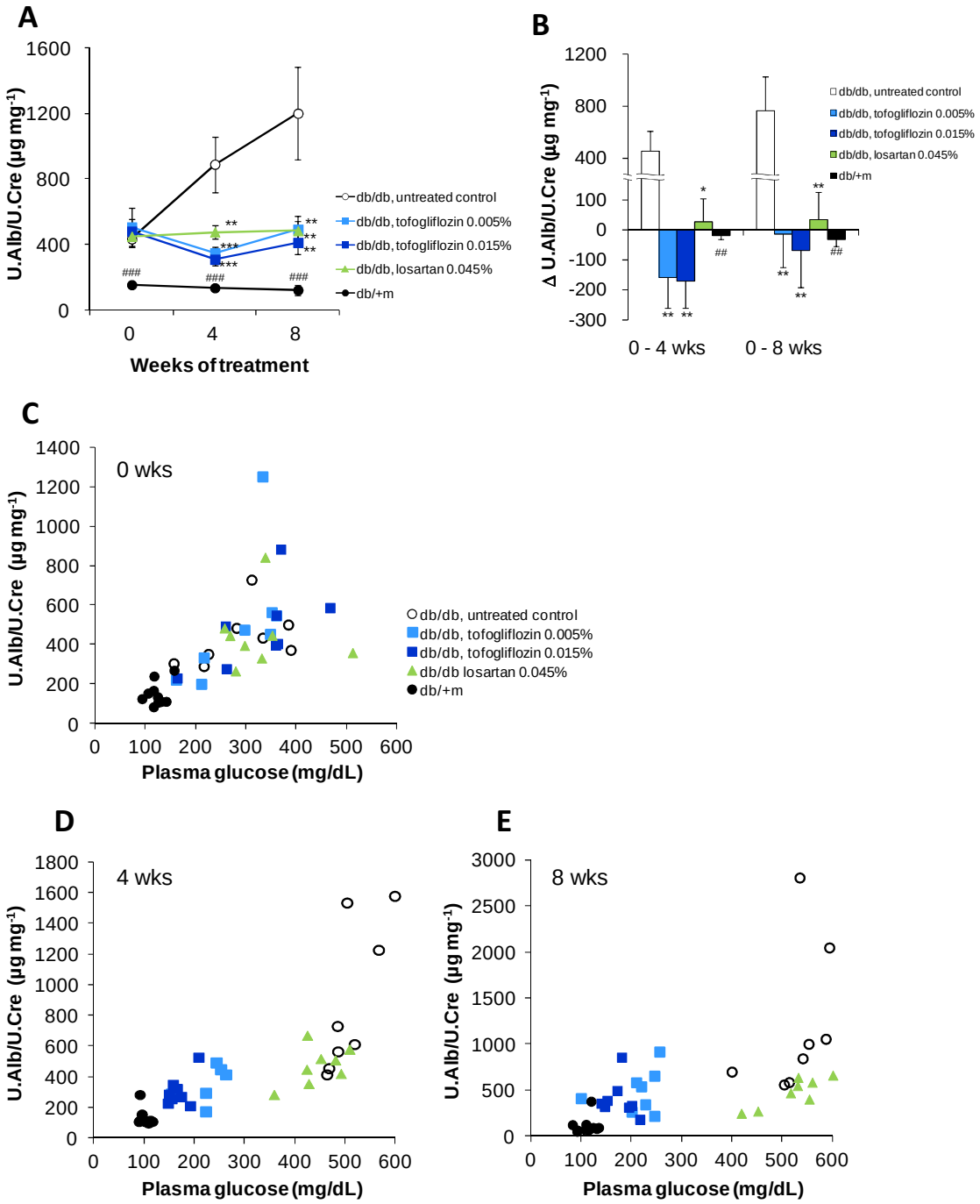

(A–B) Urinary albumin excretion was corrected by urinary creatinine excretion. Tofogliflozin treatment suppressed the 24-hour urinary albumin/creatinine ratio (ACR) in *db/db* mice. ACR was significantly lower in tofogliflozin-treated mice than in control *db/db* mice (A). Changes in ACR values from the start of study in the tofogliflozin-treated groups were comparable to changes in ACR values in the losartan-treated group at 4 and 8 weeks of treatment (B left, 0–4 weeks; B right, 0–8 weeks).

(C-E) Scatter plot of plasma glucose and ACR values in *db/db* and *db/+m* mice

(C) 0 weeks (Baseline value), **(D)** 4 weeks of treatment, **(E)** 8 weeks of treatment

Figure 6 Creatinine clearance and kidney weight in db/db and db/+m mice.

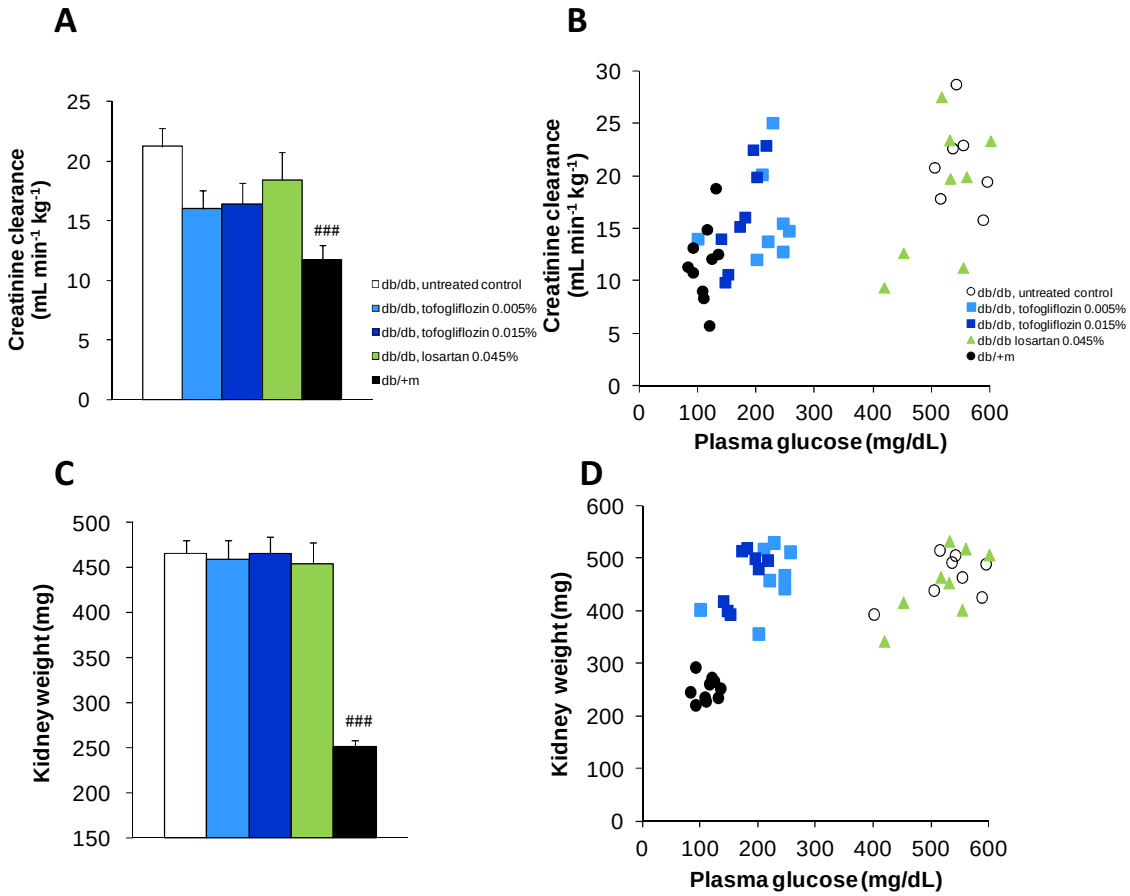

(A) Creatinine clearance in *db/db* mice was not notably affected by 8 weeks' treatment with tofogliflozin or losartan. Creatinine clearance was significantly higher in untreated *db/db* mice than in *db/+m* mice.

Symbols and columns represent mean values and vertical lines indicate SEM (*db/db* mice, n=8; *db/+m* mice, n=10).

P<0.001 versus control group by *t*-test.

(B) Scatter plot of plasma glucose and creatinine clearance in *db/db* and *db/+m* mice

(C) Kidney weight in *db/db* mice was not notably affected by 8 weeks' treatment with tofogliflozin or losartan. Kidney weight was significantly greater in untreated *db/db* mice than in *db/+m* mice.

Symbols and columns represent mean values and vertical lines indicate SEM (*db/db* mice, *n*=8; *db/+m* mice, *n*=10).

P<0.001 versus control group by *t*-test.

(D) Scatter plot of plasma glucose and kidney weight in *db/db* and *db/+m* mice

609 **Figure 7 Histological analysis of glomerulus at 8 weeks of treatment (1)**

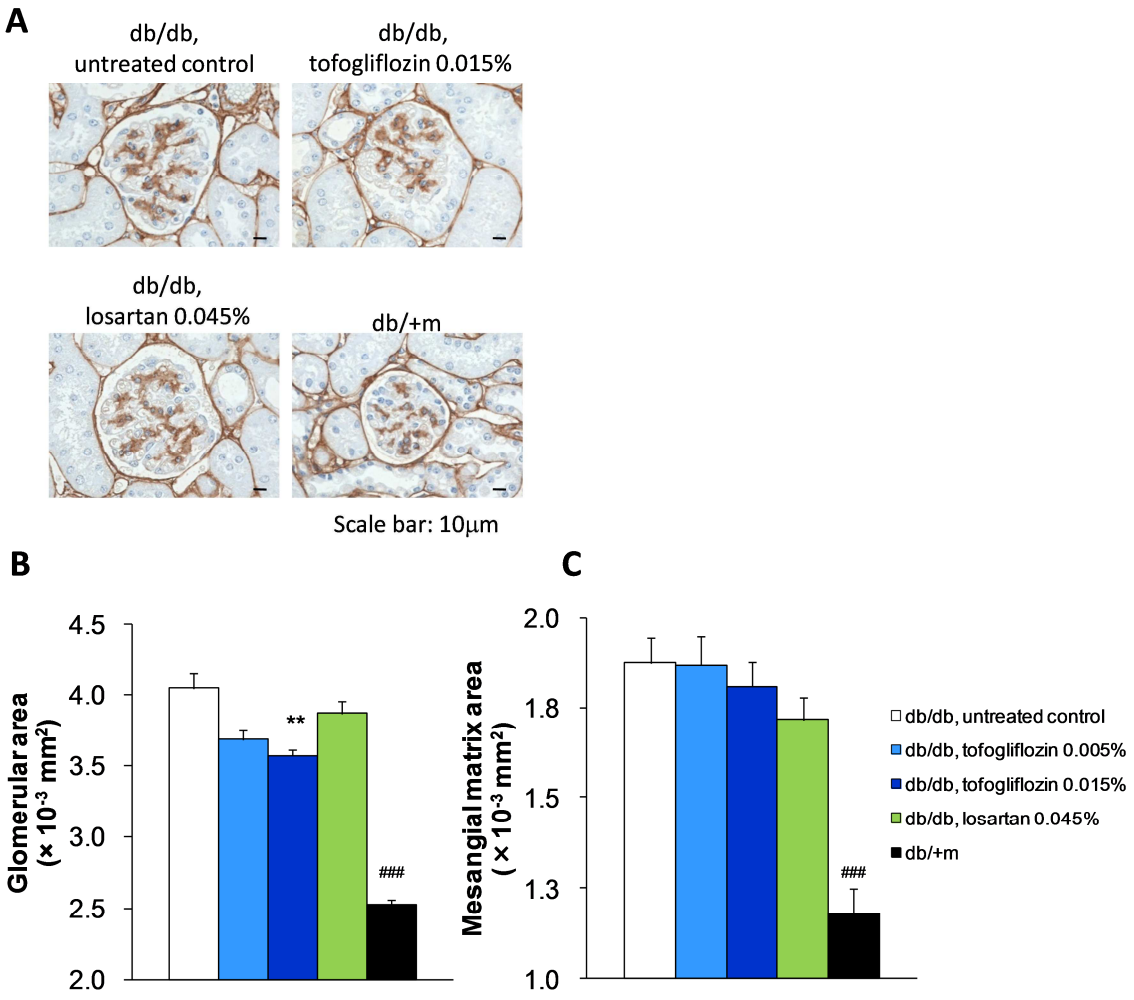

(A) Kidney sections were stained with anti-type IV collagen antibody. Representative images are shown (scale bar, 10 μm).
(B–C) Kidney sections from each mouse were stained with anti-type IV collagen antibody. Glomerular size and mesangial matrix area were determined by imaging analysis. (B) 0.015% tofogliflozin treatment significantly prevented glomerular expansion in *db/db* mice. (C) Mesangial matrix area was significantly lower in *db/+m* mice than in untreated *db/db* mice. Tofogliflozin and losartan treatment had no effect on type IV collagen-positive area.
Columns show mean values and vertical lines indicate SEM (*db/db* mice, n=8; *db/+m* mice, n=10).
** P<0.01 versus control group by Dunnett's multiple comparison test. ### P<0.001 versus control group by *t*-test.

623 **Figure 8 Histological analysis of glomerulus at 8 weeks of treatment (2)**

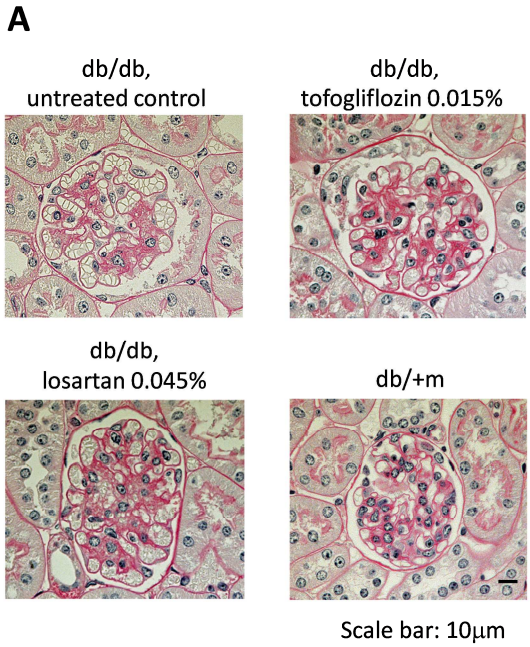

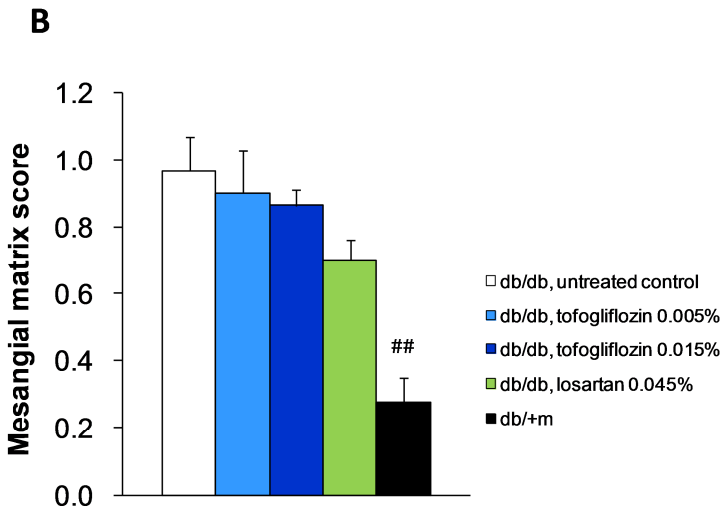

624

(A) Kidney sections were stained with PAS techniques. Representative images are shown (scale bar, 10 μm).
(B) Kidney sections from each mouse were stained with PAS techniques. Mesangial matrix area was determined by scoring. Mesangial matrix area was significantly lower in *db/+m* mice than in untreated *db/db* mice. Tofogliflozin and losartan treatment had no effect on the expansion of mesangial matrix area.
Columns show mean values and vertical lines indicate SEM (*db/db* mice, n=8; *db/+m* mice, n=10).
P<0.001 versus control group by t-test.

635 **Figure 9 Mean plasma insulin concentration and histological analysis of pancreatic β-cell**
636 **mass.**

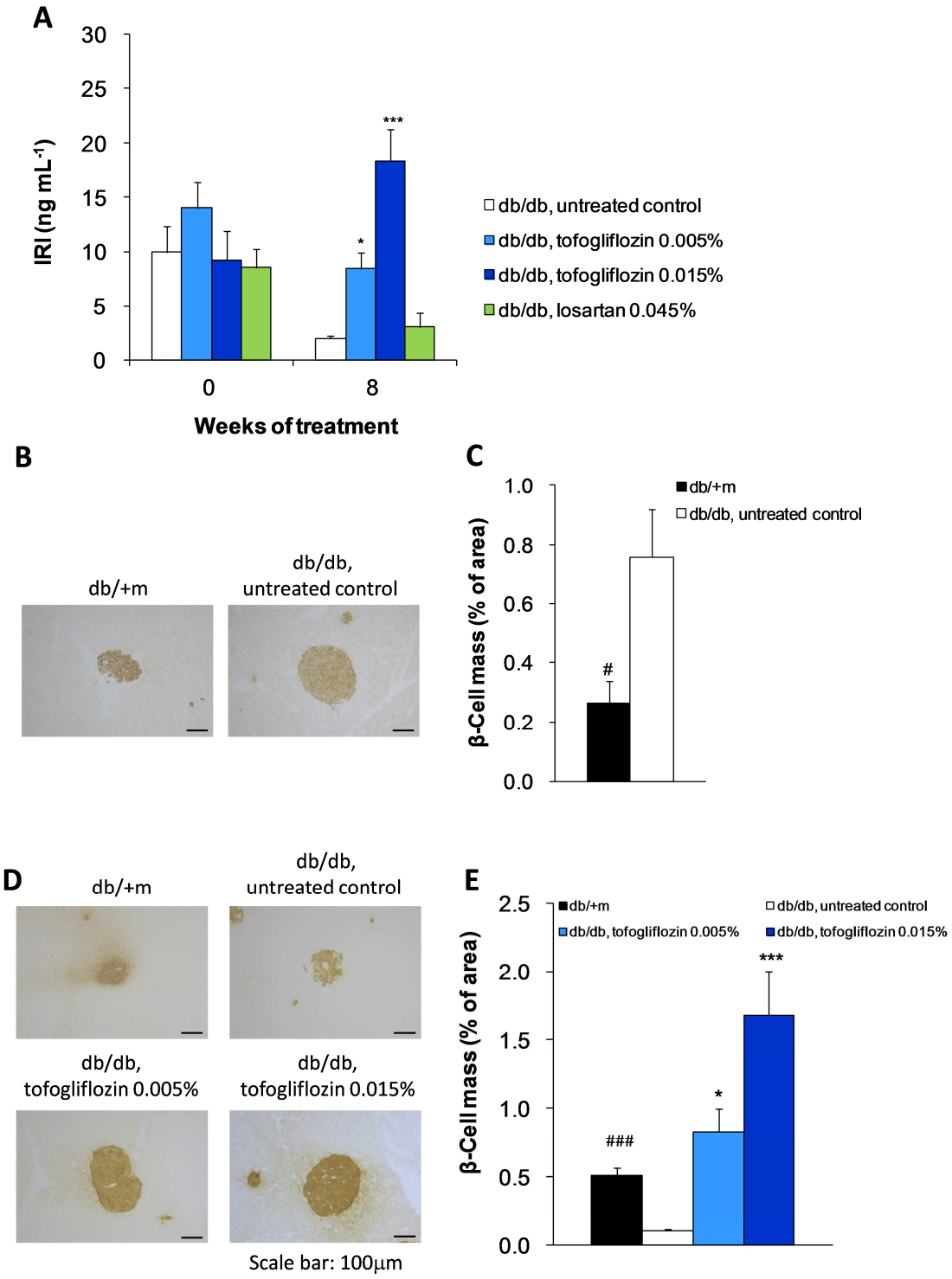

(A) Tofogliflozin treatment increased plasma insulin levels (immunoreactive insulin, IRI) in *db/db* mice.

(B–E) Total β-cell mass was calculated from the insulin-positive area of pancreatic sections. Total β-cell mass (% of area) was significantly smaller in *db/+m* mice than in *db/db* mice at the start of the study (B, C). Total β-cell mass was significantly higher in the tofogliflozin treatment groups than in the control group at the end of the study (D, E).

Columns show mean values and vertical lines indicate SEM (*db/db* mice, n=8; *db/+m* mice, n=10).

* P<0.05, *** P<0.001 versus control group by Dunnett's multiple comparison test.

# P<0.05, ### P<0.001 versus control group by t-test.

Chapter II

Selective SGLT2 inhibition by tofogliflozin reduces renal glucose reabsorption under hyperglycemic but not under hypo- or euglycemic conditions in rats

Introduction

Renal glucose reabsorption (RGR) is mediated by sodium–glucose cotransporters, namely the high-affinity sodium–glucose cotransporter SGLT1 (*SLC5A1*) and the low-affinity sodium–glucose cotransporter SGLT2 (*SLC5A2*), in the proximal tubules (Wright *et al.* 2011). Recently, several SGLT inhibitors have been developed for the treatment of Type 2 diabetes (Chao & Henry 2010; Ferrannini & Solini 2012). Although SGLT1 is reported to be expressed in several organs, such as the intestine, kidney, brain, and heart, SGLT2 is predominantly distributed in the kidney (J. Chen *et al.* 2010; Wright *et al.* 2011). Therefore, because of the concern associated with inhibiting SGLT1 in these organs, it is reasonable that most of the SGLT inhibitors being currently evaluated are SGLT2-specific.

It had been considered that SGLT2 contributes about 90% and SGLT1 contributes about 10% to RGR (Chao & Henry 2010; Wright *et al.* 2011), suggesting that inhibition of renal SGLT1 may have a negligible impact on RGR. However, a recent electrophysiological study using a whole-cell patch-clamp system showed that $K_{0.5}$ (glucose) of human SGLT2 (hSGLT2) (4.9 mM) is greater than that of hSGLT1 (1.8 mM), suggesting that hSGLT2 works at only 50% capacity under euglycemic conditions, whereas hSGLT1 would work more dominantly under hypoglycemic conditions (Hummel *et al.* 2011). These findings are consistent with the percentage inhibition of RGR found in clinical studies with dapagliflozin, a relatively SGLT2-specific inhibitor, which was calculated to be at a maximum of about 50% even at plasma concentrations that were expected to completely inhibit hSGLT2 (Kasichayanula *et al.* 2011; Komoroski, Vachharajani, Boulton, *et al.* 2009; Komoroski, Vachharajani, Feng, *et al.* 2009). In addition, SGLT2 knockout mice showed relatively higher (up to 60%) fractional reabsorption of glucose in the proximal tubules at lower rates of glucose filtration, suggesting that SGLT1 or another glucose transporter may have a higher capacity to reabsorb glucose under euglycemic conditions (Vallon 2011;

688 Vallon *et al.* 2011). These findings imply that the relative contribution of SGLT1 to RGR
689 compared to that of SGLT2 may be greater under hypo- or euglycemic conditions than
690 under hyperglycemic conditions. If this is the case, the selectivity of SGLT inhibitors to
691 SGLT2 versus selectivity to SGLT1 can be critical to determining the hypoglycemic
692 potentials of SGLT inhibitors. Therefore, it is important to determine the relationship
693 between glucose levels *in vivo* and the ratio of contribution of SGLT1 versus SGLT2.
694 One way to more accurately understand the contributions of SGLT1 and SGLT2 to
695 RGR *in vivo* is to evaluate the efficacy of inhibitors specific to certain SGLTs under
696 variable glycemic conditions.
697 Tofogliflozin (Ohtake *et al.* 2012) is a highly specific SGLT2 inhibitor (IC_{50} values
698 against rat SGLT1 [rSGLT1] and rSGLT2 are 8200 and 15 nM, respectively) (Suzuki *et*
699 *al.* 2012) recently approved in Japan for the treatment of T2D (Poole & Prossler 2014).
700 In diabetic animal models, such as ZDF rats, this compound had blood glucose lowering
701 effects accompanied with increased urinary glucose excretion (UGE); on the other hand,
702 it showed no significant hypoglycemic effects in normal rats (Suzuki *et al.* 2012).
703 Phlorizin is an SGLT inhibitor that has shown inhibitory activities against several SGLTs
704 in addition to SGLT1 and SGLT2 (Suzuki *et al.* 2012); however, the contribution of these
705 SGLTs to RGR is considered minimal compared with the contributions of SGLT1 and
706 SGLT2 (Wright *et al.* 2011). Therefore, to understand the contribution of SGLT1 in RGR,
707 it is feasible to compare the efficacies of tofogliflozin with those of phlorizin as an
708 SGLT1/2 inhibitor (IC_{50} values for phlorizin against rSGLT1 and rSGLT2 are 970 and
709 48 nM, respectively) (Suzuki *et al.* 2012). It should be noted that this protocol
710 necessitates stably controlled plasma glucose levels and glomerular filtration rate (GFR),
711 since UGE levels are influenced by plasma glucose levels and GFR (Katsuno *et al.* 2007;
712 Yamaguchi *et al.* 2011).
713 In addition, if SGLT1 has a greater role in glucose reabsorption under hypo- and
714 euglycemic conditions, it also implies that the inhibition of SGLT1 under these

conditions may exacerbate hypoglycemia via induction of excessive UGE as compared with selective SGLT2 inhibition.

In a previous study, repeated subcutaneous injection of phlorizin in streptozotocin-induced diabetic rats showed no severe hypoglycemic effect (Rossetti, Smith, *et al.* 1987); however, the lack of pharmacokinetic data in that study makes interpretation of the results difficult. In addition, in clinical trials of SGLT2 inhibitors, no significant increases in hypoglycemic episodes were reported under euglycemic conditions in healthy volunteers despite the induction of UGE (Komoroski, Vachharajani, Boulton, *et al.* 2009; Sha *et al.* 2011), which is explained as counter-regulation by endogenous glucose production (EGP) accompanying the induction of UGE (Komoroski, Vachharajani, Boulton, *et al.* 2009). However, no detailed studies are available on the relationships between UGE and EGP. To examine the hypoglycemic potentials of UGE with SGLT inhibitors, it is important to evaluate UGE and EGP simultaneously.

This chapter showed the comparison of the inhibitory effects of tofogliflozin and phlorizin on RGR in rats under variable glycemic conditions. In particular, I tried to fix the plasma concentrations of each of the 2 compounds at a constant level that can completely inhibit rSGLT2 and may inhibit rSGLT1 to a certain extent with controlled stable plasma glucose levels and GFR. In addition, I evaluated the EGP and UGE induced by tofogliflozin or phlorizin under euglycemic conditions.

Materials and Methods

Chemicals

Tofogliflozin ((1S,3′R,4′S,5′S,6′R)-6-[(4-ethylphenyl)methyl]-3′,4′,5′,6′-tetrahydro-6′-(hydroxymethyl)-spiro[isobenzofuran-1(3H),2′-[2H]pyran]-3′,4′,5′-triol) (Ohtake *et al.* 2012), was synthesized in laboratories at Chugai Pharmaceutical. Phlorizin was purchased from Sigma-Aldrich (St. Louis, MO, USA). Insulin (Novolin R; 100 U/mL) was purchased from Novo Nordisk Pharma (Tokyo, Japan). Uniformly labeled [U-^{13}C]glucose (99 atom percent excess) was purchased from Cambridge Isotope Laboratories (Andover, MA, USA). Glucose solutions of 20% and 50% were purchased from FUSO Pharmaceutical Industries (Osaka, Japan) and from Otsuka Pharmaceutical Factory (Tokushima, Japan), respectively. Tofogliflozin was dissolved at 0.6 mg/mL in saline and diluted serially. Phlorizin was dissolved at 0.2 mg/mL in saline and diluted serially. Insulin was diluted at 2 U/mL with saline. Glucose solutions (20% or 50%) were diluted with purified water to make concentrations of 10%, 30%, or 40%.

Animals

Male Wistar rats (Jcl:Wistar) were purchased from CLEA Japan (Tokyo, Japan).These animals were housed under a 12-h/12-h light/dark cycle (lights on 7:00 AM–7:00 PM) with controlled room temperature (20–26°C) and humidity (35–75%), and were allowed *ad libitum* access to a diet of laboratory chow (CE-2 pellets [Clea Japan]) and water. All animal care and experiments were performed in accordance with the guidelines for the care and use of laboratory animals at Chugai Pharmaceutical. The protocol was approved by the Institutional Animal Care and Use Committee at Chugai Pharmaceutical.

Surgical operation

Rats at 9–12 weeks of age, weighing 260–370 g, were anesthetized with an intraperitoneal injection of thiobutabarbital sodium salt (120 mg/kg) and placed on a heating pad to maintain body temperature at 36–38°C. The trachea was cannulated with polyethylene tubing for breathing. For infusion of drugs (SGLT inhibitors and insulin) and glucose, the right femoral vein was cannulated with three PE10 polyethylene catheters (V1–V3 in the clamp study) or two PE10 polyethylene catheters (V1–V2 in the titration and infusion study). The right carotid artery was cannulated with PE50 polyethylene catheters for monitoring blood pressure and heart rate. A silicon tube catheter (I.D. = 1 mm) was inserted into urinary bladder for collection of urine. Upon completion of the surgical operation, saline (15 mL/kg) was injected subcutaneously and the animals were stabilized for 30 min.

Infusion protocols with blood and urine collection

UGE under hyperglycemic conditions induced by glucose titration (Protocol 1)

Each animal was infused with saline at a rate of 15 $mL \cdot kg^{-1} \cdot h^{-1}$ through vein catheter V1 and 10 $mL \cdot kg^{-1} \cdot h^{-1}$ through vein catheter V2 for 60 min. Then, the infusion of tofogliflozin or phlorizin solution was started at a rate of 2 mL/kg (bolus) plus 15 $mL \cdot kg^{-1} \cdot h^{-1}$ through vein catheter V1 without changing the constant infusion of saline at 10 $mL \cdot kg^{-1} \cdot h^{-1}$ through vein catheter V2. The concentrations of the tofogliflozin and phlorizin solutions used were determined on the basis of pharmacokinetic parameters obtained from separate pharmacokinetic studies (data not shown) to maintain plasma concentrations of 4, 13.3, 40, 133, or 400 ng/mL for tofogliflozin and 13.3, 40, 133, 400, or 1333 ng/mL for phlorizin. Namely, the infusion rate needed to achieve a target plasma concentration of tofogliflozin of 400 ng/mL was 1.2 mg/kg (bolus) and 0.5 $mg \cdot kg^{-1} \cdot h^{-1}$ (constant), and that to achieve a target plasma concentration of phlorizin of 1333 ng/mL

was 0.15 mg/kg (bolus) and 2.8 mg·kg^{-1}·h^{-1} (constant). After 60 min of tofogliflozin or phlorizin infusion, infusion of glucose solutions (10%, 20%, 30%, 40%, and 50%) was started at 10 mL·kg^{-1}·min^{-1} in a step-wise manner from 10% at 30-min intervals through vein catheter V2 to raise the plasma glucose concentration to above 400 mg/dL. A blood sample (0.25 mL) was collected every 15 min with a heparinized syringe; the plasma glucose level in the sample was checked with a plasma glucose monitoring system (Accu-check Aviva; Roche Diagnostic, Tokyo, Japan), and then a plasma sample was obtained by centrifugation to determine plasma glucose and creatinine levels and tofogliflozin or phlorizin concentrations. Urine was collected at 30-min intervals after glucose infusion to pre-weighed polyethylene sample tubes through the bladder catheter. The catheter was flushed with 0.5 mL saline to minimize the residual urine. Urine volume was determined by subtracting the weight of the pre-weighed sample tube from the sampled urine plus tube weight, with the specific gravity of sampled urine as 1. Urine and plasma samples were stored at −80°C until use.

UGE under hypo- and euglycemic conditions induced by glucose clamp (Protocol 2)

Each animal was infused with saline at the rate of 15 mL·kg^{-1}·h^{-1} through vein catheter V1 and 10 mL·kg^{-1}·h^{-1} through vein catheter V2 for 90 min. Then, insulin (40 mU·kg^{-1}·min^{-1} for 3 min; 20 mU·kg^{-1}·min^{-1}, constant) infusion was started through vein catheter V3. After 30 min of insulin infusion, infusion of tofogliflozin or phlorizin solution was started at a rate of 2 mL/kg (bolus) and 15 mL·kg^{-1}·h^{-1} (constant) through vein catheter V1 without changing the constant infusion of saline at 10 mL·kg^{-1}·h^{-1} through vein catheter V2. The concentrations of tofogliflozin and phlorizin solution used were determined as in Protocol 1. After infusion of tofogliflozin or phlorizin solution for 60 min, glucose (20%) infusion was started through vein catheter V2 at a variable infusion rate based on a formula calculated to raise the plasma concentration to around 100 mg/dL (Furler *et al.* 1986). After this glucose infusion, blood (0.01 mL) was

sampled from the jugular vein every 5–10 min, the plasma glucose levels were measured using Accu-check Aviva, and the glucose infusion rate was adjusted based on the same formula (Furler *et al.* 1986). Additional blood samples (0.25 mL) and urine samples were collected and prepared in the same manner as Protocol 1. In this protocol, the UGE under hypoglycemic conditions was defined as that during the last 30 min of the insulin plus tofogliflozin or insulin plus phlorizin infusion period, and the UGE under euglycemic conditions was defined as that during the last 30 min of insulin plus tofogliflozin or phlorizin with glucose infusion as indicated in Figure 4.

Effects of acute urinary glucose excretion induced by tofogliflozin or phlorizin on plasma glucose levels and endogenous glucose production (Protocol 3)

Each animal was infused with saline at the rate of 25 $mL \cdot kg^{-1} \cdot h^{-1}$ through vein catheter V1 and [U-^{13}C, 99%] D-glucose saline solution at 0.14 $mg \cdot kg^{-1} \cdot min^{-1}$ through vein catheter V2. After a basal infusion period of 150 min, infusion of tofogliflozin (bolus, 1.2 mg/kg; constant, 0.5 $mg \cdot kg^{-1} \cdot h^{-1}$) or phlorizin (bolus, 0.15 mg/kg; constant, 2.8 $mg \cdot kg^{-1} \cdot h^{-1}$) was started at the rate of 2 mL/kg (bolus) and 25 $mL \cdot kg^{-1} \cdot h^{-1}$ (constant) through vein catheter V1. Blood and urine samples were collected and prepared in the same manner as Protocol 1 for 120 min from the start of tofogliflozin or phlorizin infusion.

Analysis

Plasma tofogliflozin concentrations were measured with a HPLC–MS/MS system (Shimadzu 20A [Shimadzu, Kyoto, Japan], API-4000 [AB SCIEX, Framingham, MA, USA]). Plasma phlorizin concentrations were measured with a HPLC–MS/MS system (ACQUITY UPLC [Waters, Milford, MA, USA], API-3200 [AB SCIEX]).

Blood and urinary glucose concentrations were measured by the hexokinase G-6-PDH method (L-Type Glu 2; Wako Pure Chemical Industries, Ltd., Osaka, Japan)

with an automated analyzer (TBA-120FR; Toshiba Medical Systems, Tochigi, Japan). Creatinine concentrations of plasma and urine were measured by the creatininase-HMMPS method (L-Type Creatinine M; Wako Pure Chemical Industries, Ltd.) with the automated analyzer.

Plasma [U-^{13}C]glucose concentrations, together with that of an internal standard (fructose), were determined with a HPLC-MS/MS system (Shimadzu 20A [Shimadzu]), API-4000 [AB SCIEX]) with an improved procedure to increase the sensitivity by Cs^+ attachment to the sugars (18).

Calculations

In Protocols 1 and 2, the following parameters were calculated:

Creatinine clearance (mL/min) = (urine creatinine; mg/dL) × (urine excretion rate; mL/min) / (plasma creatinine; mg/dL)

Urinary glucose excretion (UGE; mg/min) = (urine glucose; mg/dL) × (urine excretion rate; mL/min) / 100

Glucose clearance (mL/min) = (urine glucose; mg/dL) × (urine excretion rate; mL/min) / (plasma glucose; mg/dL)

Percentage inhibition of RGR [RGR inhibition (%)] = glucose clearance / creatinine clearance × 100 (%)

This calculation method was based on formulas used in a clinical study (Kasichayanula *et al.* 2011). In Protocol 1, an apparent increase in UGE was observed with vehicle alone when plasma glucose was above around 300 mg/dL, which may result in the overestimation of percentage RGR inhibition; therefore, the percentage inhibition of RGR in Protocol 1 was defined as the glucose clearance/creatinine clearance ×100 (%), when the plasma glucose levels were within 250 to 350 mg/dL for each rat.

In Protocol 3, the rate of EGP was calculated according to the following equation (Bergeron *et al.* 2001)

$$EGP\ (R_a;\ \text{rate of glucose production}) = f \times ([IE_{\text{infusate}} / IE_{\text{plasma}}] - 1)$$

where f is infusion rate of [U-^{13}C]glucose; IE_{infusate} is isotopic enrichment of [U-^{13}C]glucose in infusate; IE_{plasma} is isotopic enrichment (%) of [U-^{13}C]glucose in plasma = plasma [U-^{13}C]glucose concentration/total plasma glucose concentration × 100.

Statistical analysis

Data are presented as means ± SD. Statistical analysis was performed with SAS System for Windows, Release 8.02 (SAS Institute Japan, Tokyo, Japan). Statistical significance was determined by the parametric Dunnett's multiple comparison or Student's (un-paired) *t*-test.

Results

UGE under hyperglycemic conditions induced by glucose titration

The plasma concentrations of tofogliflozin and phlorizin in the glucose titration protocol are shown in Table 1. The means of the actual plasma tofogliflozin concentrations measured at 3 sampling points (60, 135, and 210 min after start of infusion) were 4.6 to 474 ng/mL, which were 114% to 119% of the target plasma concentrations. Similarly, the means of the actual plasma phlorizin concentrations were 42.6 to1574 ng/mL, which were 106% to 118% of the target plasma concentration.

The plasma glucose concentrations gradually increased from the normal range before glucose titration to over 400 mg/dL after 30 min infusion of 50% glucose solution (Figure 1A, B). During the experiments, the creatinine clearance of each group was stable at around 3 mL/min (Figure 1C, D).

Figure 2 shows the relationship between the plasma glucose concentration and UGE. In both the phlorizin group and the tofogliflozin group, the plasma glucose concentration at which apparent UGE was induced shifted to the left in a dose-dependent manner.

There were no significant differences between the glucose levels at which the maximum percentage inhibition of RGR was calculated (Table 1). The percentage inhibition of RGR increased dose-dependently in both the tofogliflozin group and the phlorizin group (Figure 3). Over 50% inhibition of RGR was observed at ≥133 ng/mL of tofogliflozin (Figure 3A) and at ≥400 ng/mL of phlorizin (Figure 3B). Therefore, it was intended to examine the effects of the SGLT inhibitors on UGE under hypo- and euglycemic conditions at 133 and 400 ng/mL for tofogliflozin and 400 and 1333 ng/mL for phlorizin; at these concentrations, the rSGLT2 will be completely inhibited according to their IC_{50} and protein binding properties (Suzuki *et al.* 2012; Yamaguchi *et al.* 2011).

UGE under hypo- and euglycemic conditions induced by glucose clamp

The means of actual plasma tofogliflozin concentrations at 3 sampling points (30, 90, and 150 min after infusion) in the 133 and 400 ng/mL groups were 245 and 599 ng/mL, which were 184% and 150% of the target plasma concentration, respectively. The means of actual plasma phlorizin concentrations at the 3 sampling points in the 400 and 1333 ng/mL groups were 378 and 1143 ng/mL, which were 95% and 86% of the target plasma concentration, respectively (Table 2).

By the continuous infusion of insulin for 30 min, the plasma glucose concentrations decreased from the normal range to nearly 50 mg/dL. Even with additional infusion of tofogliflozin or phlorizin for 60 min, plasma glucose concentrations remained above 40 mg/dL. Thereafter, with the glucose infusion at around 10–25 $mg \cdot kg^{-1} \cdot min^{-1}$ for 30 min and around 25–35 $mg \cdot kg^{-1} \cdot min^{-1}$ for 60 min, the plasma glucose concentration increased to the normal range and remained around 100 mg/dL for 60 min (Figure 4).

The UGE under hypoglycemic conditions was defined as that during the last 30 min of the insulin plus tofogliflozin or insulin plus phlorizin infusion period, and the UGE under euglycemic condition was defined as that during the last 30 min of insulin plus tofogliflozin plus glucose or insulin plus phlorizin plus glucose infusion as indicated in Figure 4. There were no differences in plasma glucose concentration (Table 3) or in creatinine clearance (Table 4) between the five groups under either the hypo- or euglycemic conditions.

Under hypoglycemic conditions, significant increases in UGE were observed in the phlorizin groups both at 400 and 1333 ng/mL. In contrast, no significant increase in UGE was observed in tofogliflozin at 133 and 400 ng/mL under hypoglycemic conditions. Under euglycemic conditions, significant increases in UGE were also observed in the phlorizin groups both at 400 and 1333 ng/mL. In contrast, no significant increase in UGE was observed with tofogliflozin at 133 ng/mL under euglycemic conditions, although a slight increase in UGE was induced with tofogliflozin at 400 ng/mL (Figure 5).

922 Phlorizin inhibited RGR under hypo- and euglycemic conditions by about 25 and
923 35%, respectively at 400 ng/mL and by about 50% and 60%, respectively at 1333 ng/mL.
924 In contrast, tofogliflozin (133 and 400 ng/mL) showed no apparent RGR inhibition under
925 hypoglycemic conditions. In addition, even under euglycemic conditions, tofogliflozin
926 showed only about 5% RGR inhibition at 133 ng/mL and about 20% inhibition at
927 400 ng/mL (Figure 6).

928 ***The effect of acute urinary glucose excretion induced by tofogliflozin or phlorizin on***
929 ***the plasma glucose levels and endogenous glucose production***

930 Finally, it was intended to evaluate the effects on plasma glucose of continuous
931 infusion of tofogliflozin (400 ng/mL) and phlorizin (1333 ng/mL) under euglycemic
932 conditions by simultaneously comparing UGE and EGP. The actual plasma tofogliflozin
933 and phlorizin concentrations after 120 min infusion were 574 ± 80 and
934 1514 ± 243 ng/mL, respectively.

935 Although tofogliflozin (400 ng/mL) induced UGE of about 2 $mg \cdot kg^{-1} \cdot min^{-1}$
936 (Figure 7A) and slightly decreased plasma glucose levels, the plasma glucose levels were
937 maintained above 100 mg/dL (Figure 7C).

938 The calculated EGP levels ($mg \cdot kg^{-1} \cdot min^{-1}$) at the end of the basal infusion period did
939 not differ between the 3 groups (8.4 ± 1.4 in the vehicle group, 8.6 ± 1.2 in the
940 tofogliflozin group, and 8.7 ± 1 .6 in the phlorizin group). The calculated EGP in the
941 steady-state period 60–120 min after the initiation of tofogliflozin infusion increased by
942 1–2 $mg \cdot kg^{-1} \cdot min^{-1}$ (Figure 7B, Table 5), resulting in no difference in Δ(EGP − UGE)
943 between the vehicle and tofogliflozin groups (Table 5). Thus, the increased UGE level
944 induced with tofogliflozin may be almost compensated for by the increase in EGP.

945 Phlorizin (1333 ng/mL) induced not only a significantly greater increase in UGE (to
946 about 6 $mg \cdot kg^{-1} \cdot min^{-1}$) as compared with both the vehicle and tofogliflozin groups
947 (Figure 7A, Table 5) but also a greater reduction in plasma glucose levels than

948 tofogliflozin (Figure 7C, Table 5). The minimum plasma glucose concentration during
949 the steady-state period 60–120 min after start of phlorizin infusion was significantly
950 lower than that in the tofogliflozin group (Table 5). The calculated EGP in the
951 steady-state period (60–120 min) in the phlorizin group was increased by about
952 4 $mg \cdot kg^{-1} \cdot min^{-1}$ which was greater than that in tofogliflozin group (Figure 7B, Table 5).
953 However, there was a significant reduction in the Δ(EGP-UGE) value in the phlorizin
954 group as compared with that in the vehicle group and in the tofogliflozin group (Table 5),
955 suggesting that the UGE induced with phlorizin may not be fully compensated for by the
956 increase in EGP.
957

Discussion

Although it had been generally believed that SGLT2 mediated 90% of RGR in humans (Chao & Henry 2010; Wright *et al.* 2011), recent clinical studies with SGLT2 inhibitors have shown only about 30–50% inhibition of RGR, provoking debate on the mechanisms underlying this discrepancy (Hummel *et al.* 2011; Liu *et al.* 2012; Vallon 2011).

Liu *et al.* (Liu *et al.* 2012) proposed several explanations for the discrepancy and denied the possibility that SGLTs/GLUTs other than SGLT2 were responsible for a much greater fraction of the RGR than previously reported. However, the electrophysiological studies and the titration study with SGLT2 knockout mice suggest the possibility of the increased contribution of SGLT1 under hypoglycemic conditions (Hummel *et al.* 2011) or euglycemic conditions, especially with SGLT2 deficiency (Vallon *et al.* 2011). If this is the case, inhibition of SGLT1 with SGLT2 inhibitors under hypoglycemic conditions or normalized glycemic conditions may have a significant impact on the physiological conditions of Type 2 diabetes patients. Therefore, it is important to confirm the capacity of SGLT1 in RGR under hypoglycemic conditions and to know the relationship between the ratio of contribution of SGLT1 versus SGLT2 and the glucose levels *in vivo*.

Although it is a feasible approach to use SGLT inhibitors in order to understand the roles of SGLT subtypes in RGR *in vivo*, there are limitations to the understanding that can be gained from comparisons of data from separate clinical studies of SGLT inhibitors. Intravenous infusion of phlorizin to humans was reported for the first time in 1933 by Chasis *et al.* (Chasis *et al.* 1933) They reported that “tubular reabsorption of glucose was completely blocked” by phlorizin (11.8–65.2 mg/kg, i.v.). Hummel *et al.* (Hummel *et al.* 2011) proposed the greater (>50%) contribution of SGLT1 to tubular glucose reabsorption under normal conditions by comparing these results for phlorizin and the estimated percentage inhibition (about 50%) of glucose reabsorption in the clinical studies with dapagliflozin (Komoroski, Vachharajani, Boulton, *et al.* 2009; Komoroski,

Vachharajani, Feng, *et al.* 2009). However, it is difficult to estimate the contribution of SGLT1 to tubular glucose reabsorption from these results for the following reasons: First, since the plasma phlorizin concentrations were not determined in the i.v. infusion studies with phlorizin in humans (Chasis *et al.* 1933), it is impossible to examine the precise relationships between the inhibition of SGLT1/2 and UGE. In addition, although the plasma concentrations of dapagliflozin were determined in the clinical studies (Komoroski, Vachharajani, Boulton, *et al.* 2009; Komoroski, Vachharajani, Feng, *et al.* 2009), it is possible that fluctuations of plasma drug concentration caused by oral administration may impose limitations on the interpretation of the relationship between the drug concentrations in plasma and the efficacy. Moreover, the SGLT1 and SGLT2 contributions under different glycemic levels remain unknown.

In this chapter, it was intended to examine the contributions of SGLT2 and SGLT1 under different glycemic conditions by comparing the inhibitory effects of tofogliflozin, a highly specific SGLT2 inhibitor and phlorizin, an SGLT1/2 inhibitor, on RGR with glucose titration and clamp protocols in normal rats. In particular, I conducted these experiments under fixed plasma concentrations of each SGLT inhibitor to evaluate the relationship between the inhibitory activities estimated from the plasma concentration and the inhibition of RGR.

Under hyperglycemic conditions (Protocol 1), over 50% inhibition of RGR was achieved by tofogliflozin (≥133 ng/mL) and phlorizin (≥400 ng/mL) (Figure 3). Based on the actual plasma concentrations (Table 1) and the protein binding properties of tofogliflozin (Suzuki *et al.* 2012), it seemed reasonable to estimate the unbound tofogliflozin concentrations at 133 ng/mL (actual mean concentration: 168 ng/mL) and at 400 ng/mL (actual mean concentration: 474 ng/mL) to be 70 nM and 196 nM, respectively. Considering the IC_{50} values of tofogliflozin against rSGLT1 and rSGLT2 (rSGLT1, 8200 nM; rSGLT2, 15 nM) calculated from its inhibitory activities on the sodium-dependent uptake of alpha-methyl-D-glucopyranoside (AMG) , a

nonmetabolizable glucose analogue, in COS-7 cells overexpressing rSGLT1 or rSGLT2 (Suzuki *et al.* 2012), the unbound concentrations of tofogliflozin mentioned above are relevant concentrations to inhibit rSGLT2 almost completely but not rSGLT1.

Similarly, based on the actual plasma concentrations (Table 1) and the reported protein binding properties of phlorizin (Yamaguchi *et al.* 2011) , it seemed reasonable to estimate the unbound phlorizin concentrations at 400 ng/mL (actual concentration: 433 ng/mL) and 1333 ng/mL (actual concentration: 1574 ng/mL) to be 309 nM and 1123 nM, respectively. Considering the IC_{50} values of phlorizin against rSGLT2 in the AMG uptake assay (48 nM) (Suzuki *et al.* 2012), and the reported IC_{50} values against rSGLT2 of phlorizin (Han *et al.* 2008; Tahara *et al.* 2012), the unbound phlorizin concentrations mentioned above are also relevant concentrations to inhibit rSGLT2 almost completely.

As the inhibition of rSGLT1 at the estimated unbound phlorizin concentration (309 nM and 1123 nM) in the AMG uptake assay (Suzuki *et al.* 2012) was estimated to be about 30–50%, the inhibitory activity of phlorizin on RGR in this experiment is expected to be mainly due to the partial inhibition of rSGLT1 and complete inhibition of rSGLT2. Recently, SGLT3 has been identified in the human kidney as a novel Na^+ transporter sensitive to phlorizin (Kothinti *et al.* 2012). Although mRNA for SGLT3b, an ortholog of human SGLT3 (hSGLT3), has been found in rat kidney (GenBank DQ054787), its function in rat kidney is still unknown. Even if the SGLT3b functions as a glucose transporter in rat kidney, as the sugar-transport activity of mouse SGLT3b is estimated to be 60 times lower than that of mouse SGLT1 (Aljure & Díez-Sampedro 2010) and the inhibitory activity of phlorizin against hSGLT3 is about 100 times lower than that against hSGLT1 in the sodium-dependent AMG uptake assay (Suzuki *et al.* 2012), the inhibitory activity of phlorizin against the glucose transport of rat kidney via SGLT3b may has a negligible impact on the results of this chapter.

The inhibitory effect of tofogliflozin on RGR was saturated at about 60% at 133–400 ng/mL under hyperglycemic conditions (Figure 3A), where rSGLT2 was expected to be inhibited almost completely but not rSGLT1. In contrast, no saturation was observed in the inhibitory effect on RGR by phlorizin at 400–1333 ng/mL (Figure 3B), resulting in greater RGR inhibition at 1333 ng/mL phlorizin than at 400 ng/mL tofogliflozin (73 ± 5%, phlorizin 1333 ng/mL, 61 ± 5%, tofogliflozin 400 ng/mL; $p < 0.05$). At 1333 ng/mL phlorizin, rSGLT2 was expected to be inhibited almost completely with a substantial rSGLT1 inhibition by about 50%. Therefore, the difference in RGR inhibition (%) between phlorizin (1333 ng/mL) and tofogliflozin (400 ng/mL) was attributed to the partial inhibition of rSGLT1 by phlorizin. Taken together, the contribution of rSGLT2 to the RGR under hyperglycemic conditions was assumed to be about 60% in rats.

Under hypo- and euglycemic conditions with glucose clamp (Protocol 2), phlorizin reduced RGR by about 25–35% and 50–60% at 400 ng/mL and 1333 ng/mL, respectively, where rSGLT2 is almost totally inhibited and rSGLT1 is partially inhibited. In contrast, tofogliflozin minimally (1–5%) reduced RGR under hypoglycemic conditions even at the concentrations supposed to inhibit rSGLT2 almost completely (Figure 6). As the actual concentrations of phlorizin and tofogliflozin were maintained at the same levels (Table 2) and the plasma glucose levels and creatinine clearance were stable during the measurement of RGR inhibition (Tables 3 and 4), the minimal inhibition of RGR with tofogliflozin is due to the absence of rSGLT1 inhibition. In SGLT2 knockout mice, a greater contribution of SGLT1 to RGR under euglycemic conditions has been proposed (Vallon 2011; Vallon *et al.* 2011). The results of this chapter not only strongly support these suggestions but also suggest the dominant role of SGLT1 in RGR under hypoglycemic conditions. To evaluate whether this dominant role of SGLT1 is observed only under complete SGLT2 inhibition or not, it will be necessary to measure the actual glucose concentration gradient along the different segments of the proximal tubules.

Finally, it was intended to compare the UGE and EGP simultaneously to evaluate the hypoglycemic potentials of the SGLT inhibitors. Under euglycemic conditions, tofogliflozin-induced UGE and EGP were increased together with a slight decrease in plasma glucose concentration. Even after 120 min of tofogliflozin infusion at 400 ng/mL, the plasma glucose levels were maintained above 100 mg/dL. The increased EGP (1–2 $mg \cdot kg^{-1} \cdot min^{-1}$) was nearly the same as the UGE level induced with tofogliflozin. These results suggest that UGE induction with tofogliflozin under euglycemic condition can be fully compensated for by the increase of EGP.

In contrast, compared with tofogliflozin, phlorizin induced greater UGE under euglycemic conditions, which may be due to the dual inhibition of both SGLT1 and SGLT2. In the phlorizin group, although the EGP was also increased (by about 4 $mg \cdot kg^{-1} \cdot min^{-1}$, which was greater than in the tofogliflozin group), the plasma glucose was decreased more than in the tofogliflozin group. As the level of UGE induced with phlorizin (about 6 $mg \cdot kg^{-1} \cdot min^{-1}$) was apparently greater than the increased level of EGP, it is suggested that the induction of UGE with the dual inhibition of both SGLT1 and SGLT2 was not fully compensated for by the increase in EGP. The actual blood glucose lowering effects have not been mentioned in studies in rats (Rossetti, Smith, *et al.* 1987) or humans (Chasis *et al.* 1933) treated with phlorizin under euglycemic conditions. Even in this experiment, actual hypoglycemia was not observed with continuous infusion of phlorizin for 120 min. However, the level of UGE observed with phlorizin, which was comparable to about 75% of the basal EGP (Figure 7), suggests that dual inhibition of both SGLT1 and SGLT2 may pose a risk of excessive UGE under hypo- and euglycemic conditions which may lead to sustained hypoglycemia. Further studies are required to understand the mechanisms of compensatory EGP increase and the long-term effects of sustained UGE induction by SGLT inhibitors.

In this chapter, it was intended to examine the potential risk of hypoglycemia due to SGLT1 inhibition accompanying SGLT2 inhibition in normal rats. Although the results

of this chapter suggest the better profile of highly specific SGLT2 inhibition, experiments under diabetic conditions will be needed to precisely examine the potential risk of these compounds. Moreover, the mechanism that regulates the differential contributions of SGLT1 and SGLT2 to RGR under different glycemic conditions will need to be clarified.

In conclusion, the contribution of SGLT1 to RGR was found to be greater under lower glycemic conditions than under hyperglycemic conditions, and selective SGLT2 inhibition by tofogliflozin exhibited greater reduction of RGR preferentially under hyperglycemic conditions. This suggests that SGLT2-selective inhibitors, such as tofogliflozin, carry a lower risk of causing hypoglycemia than SGLT1/2 inhibitors.

Figures

Figure 1

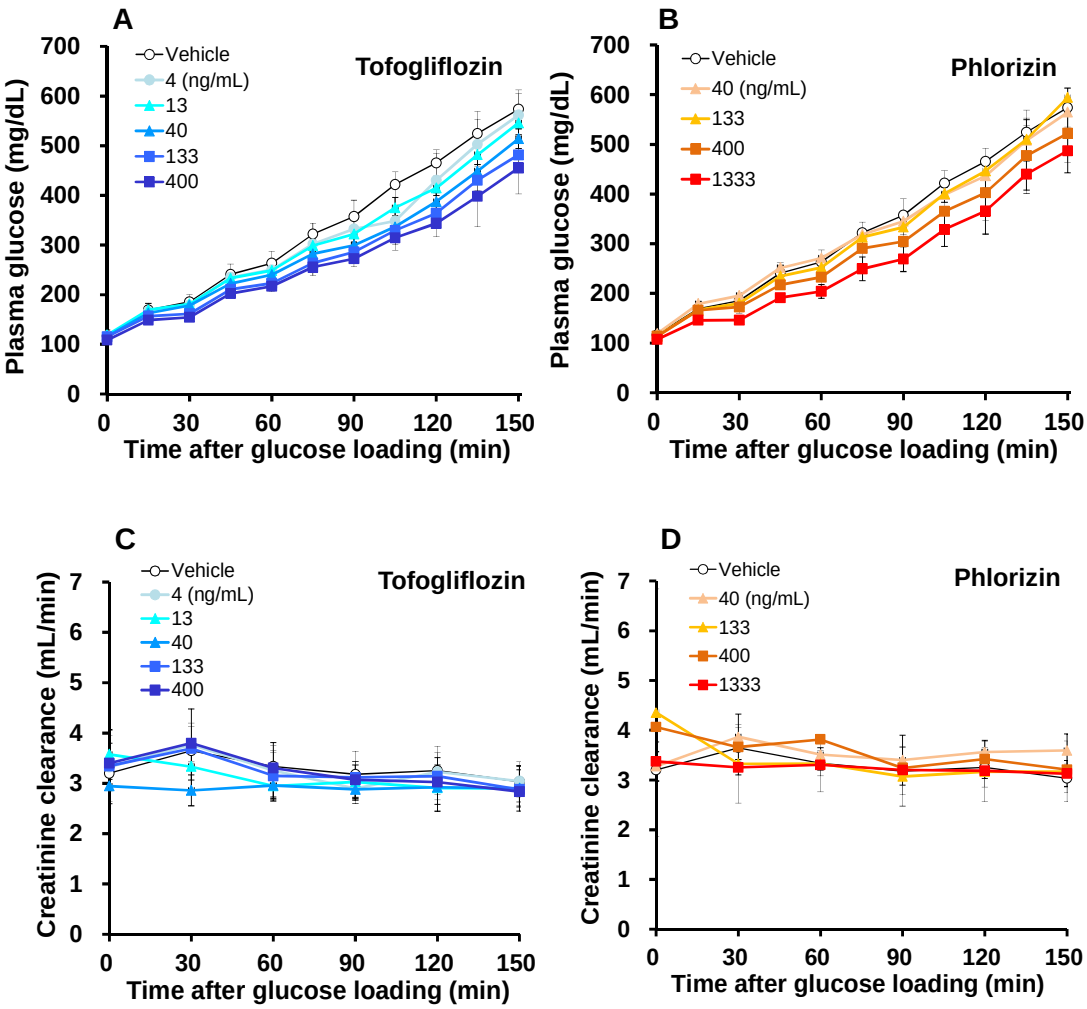

Time-course of (A, B) plasma glucose and (C, D) creatinine clearance of Wistar rats after glucose loading and infusion with (A, C) tofogliflozin or (B, D) phlorizin in the glucose titration protocol. Data are shown as means ± SD, n = 3–7. The concentrations (4–1333 ng/mL) indicated are target plasma concentrations. The actual plasma concentrations of the two SGLT inhibitors are shown in Table 1. After 60 min of tofogliflozin or phlorizin infusion, infusion (10 $mL \cdot kg^{-1} \cdot min^{-1}$) of glucose solution (10%) was started (time = 0) and increased in a step-wise manner (20%, 30%, 40%, and 50%) at 30-min intervals with the constant infusion of tofogliflozin or phlorizin.

Figure 2

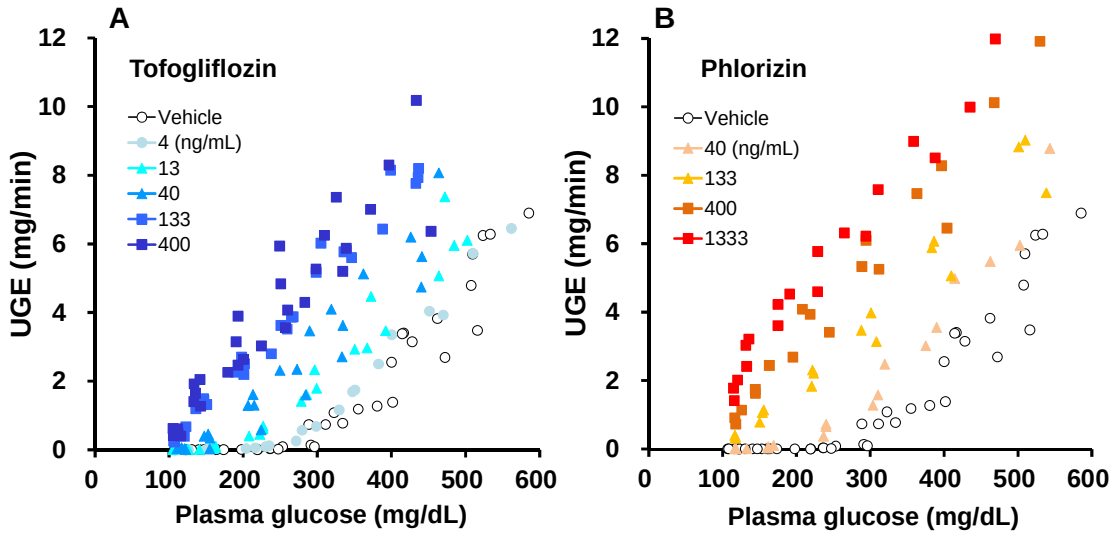

Scatter plot of plasma glucose and urinary glucose excretion (UGE) levels in Wistar rats infused with (A) tofogliflozin or (B) phlorizin. The concentrations (4–1333 ng/mL) indicated are target plasma concentrations. The actual plasma concentrations of the two SGLT inhibitors are shown in Table 1.

Figure 3

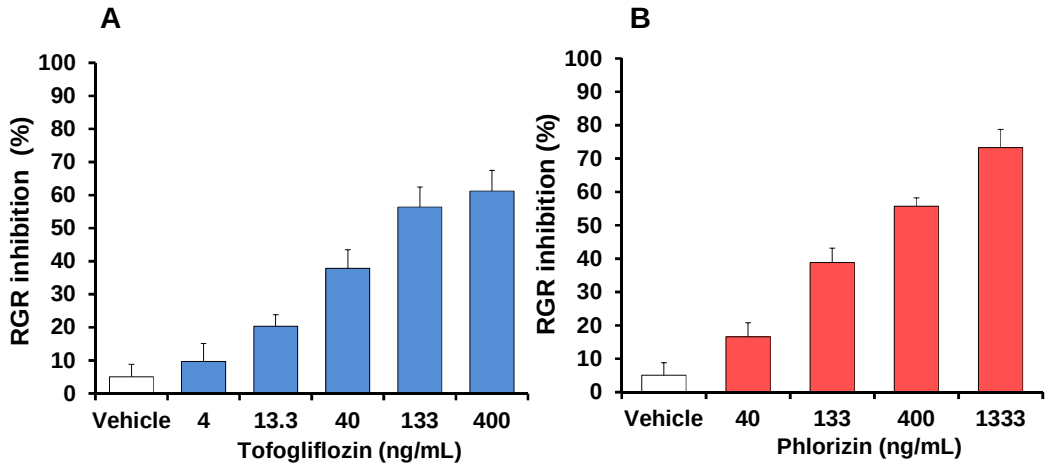

Maximum percentage inhibition of renal glucose reabsorption (RGR) in hyperglycemic Wistar rats infused with (A) tofogliflozin or (B) phlorizin. The concentrations (4–1333 ng/mL) indicated are target plasma concentrations. The actual plasma concentrations of the two SGLT inhibitors are shown in Table 1. The plasma glucose levels at which the maximum percentage RGR inhibition was calculated are shown in Table 1.

Figure 4

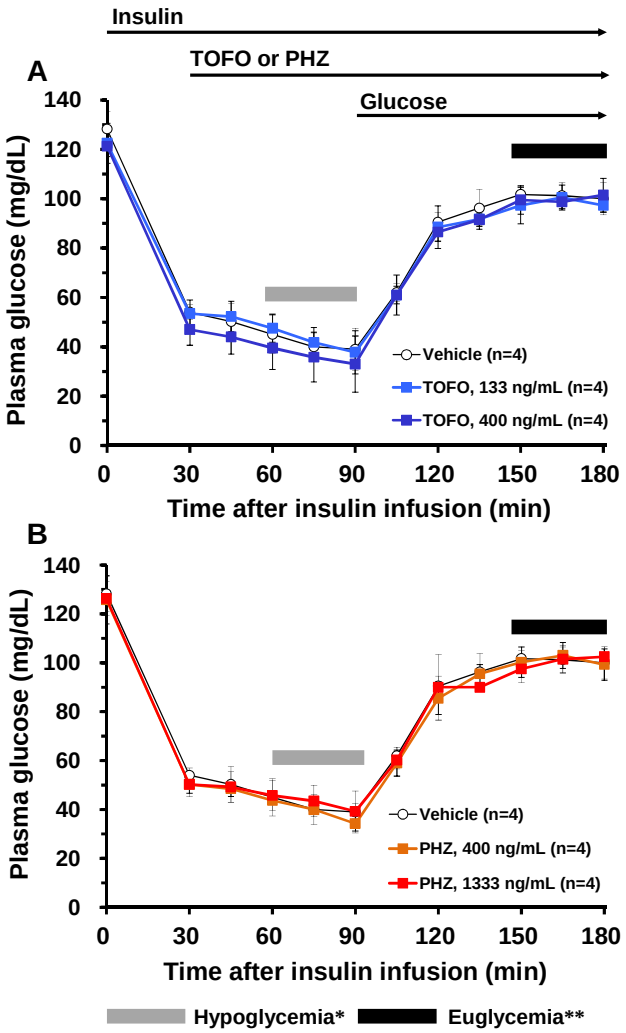
Insulin
TOFO or PHZ
Glucose
A
Plasma glucose (mg/dL)
Time after insulin infusion (min)
Vehicle (n=4)
TOFO, 133 ng/mL (n=4)
TOFO, 400 ng/mL (n=4)
B
Plasma glucose (mg/dL)
Time after insulin infusion (min)
Vehicle (n=4)
PHZ, 400 ng/mL (n=4)
PHZ, 1333 ng/mL (n=4)
Hypoglycemia*
Euglycemia**

Time-course of plasma glucose levels in Wistar rats infused with insulin, glucose, and (A) tofogliflozin (TOFO) or (B) phlorizin (PHZ) in the glucose clamp protocol. Data are shown as means ± SD, $n = 4$. The concentrations indicated (133–1333 ng/mL) are target plasma concentrations. The actual plasma concentrations of the two SGLT inhibitors are shown in Table 2. *, ** Hypo- and euglycemic periods defined for the comparison of UGE (Figure 5) and percentage RGR inhibition (Figure 6). After insulin (2 U/mL, 40 $mU \cdot kg^{-1} \cdot min^{-1}$ for 3 min; 20 $mU \cdot kg^{-1} \cdot min^{-1}$, constant) was infused for 30 min, tofogliflozin or phlorizin was infused at 2 mL/kg (bolus) and 15 $mL \cdot kg^{-1} \cdot h^{-1}$ (constant) for 60 min, and then glucose (20%) was infused at a variable infusion rate based on the calculation formula (Furler *et al.* 1986) to raise the concentration of glucose in plasma to around 100 mg/dL.

Figure 5

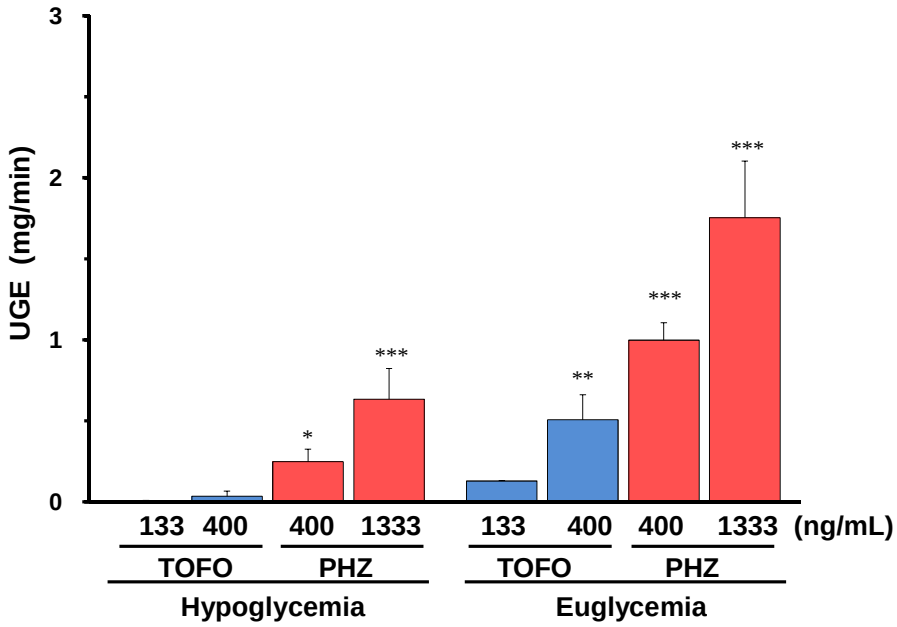

Differential effects of tofogliflozin (TOFO) and phlorizin (PHZ) on the urinary glucose excretion (UGE) of Wistar rats under hypoglycemic or euglycemic conditions in the glucose clamp protocol. Data are shown as means + SD, n = 4. The concentrations (133–1333 ng/mL) indicated are target plasma concentrations. The actual plasma concentrations of the two SGLT inhibitors are shown in Table 2. *p <0.05, ** p <0.01, *** p <0.001 *vs.* vehicle group by Dunnett's multiple comparison test. The UGE levels (mg/min) of the vehicle group under hypoglycemic and euglycemic conditions were 0.0013 ± 0.0007 and 0.0026 ± 0.0014, respectively.

Figure 6

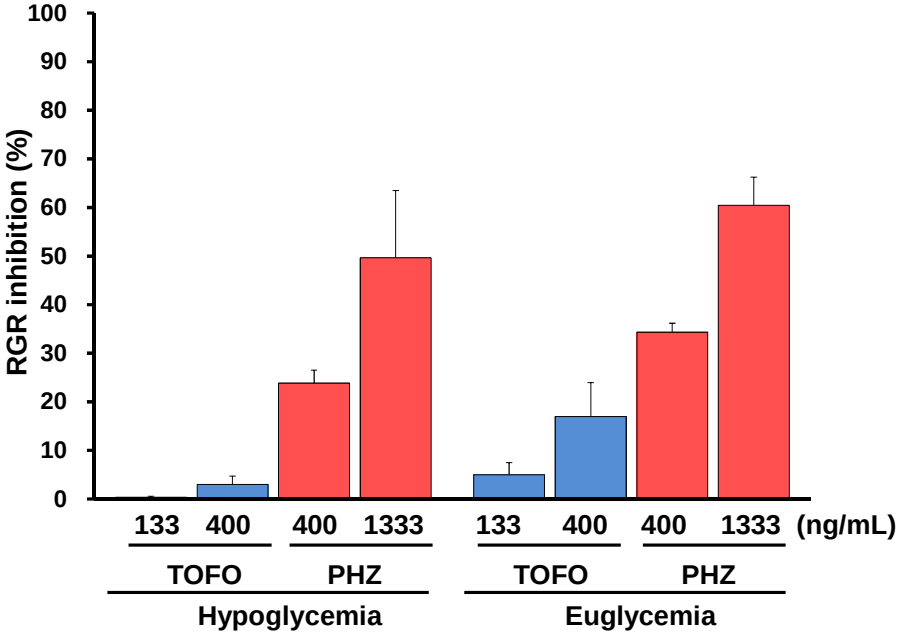

Effect of tofogliflozin (TOFO) or phlorizin (PHZ) on the percentage inhibition of renal glucose reabsorption (RGR) under hypo- and euglycemic conditions of Wistar rats in the glucose clamp protocol. Data are shown as means + SD, *n* = 4–5. The concentrations (133–1333 ng/mL) indicated are target plasma concentrations. The actual plasma concentrations of the two SGLT inhibitors are shown in Table 2.

Figure 7

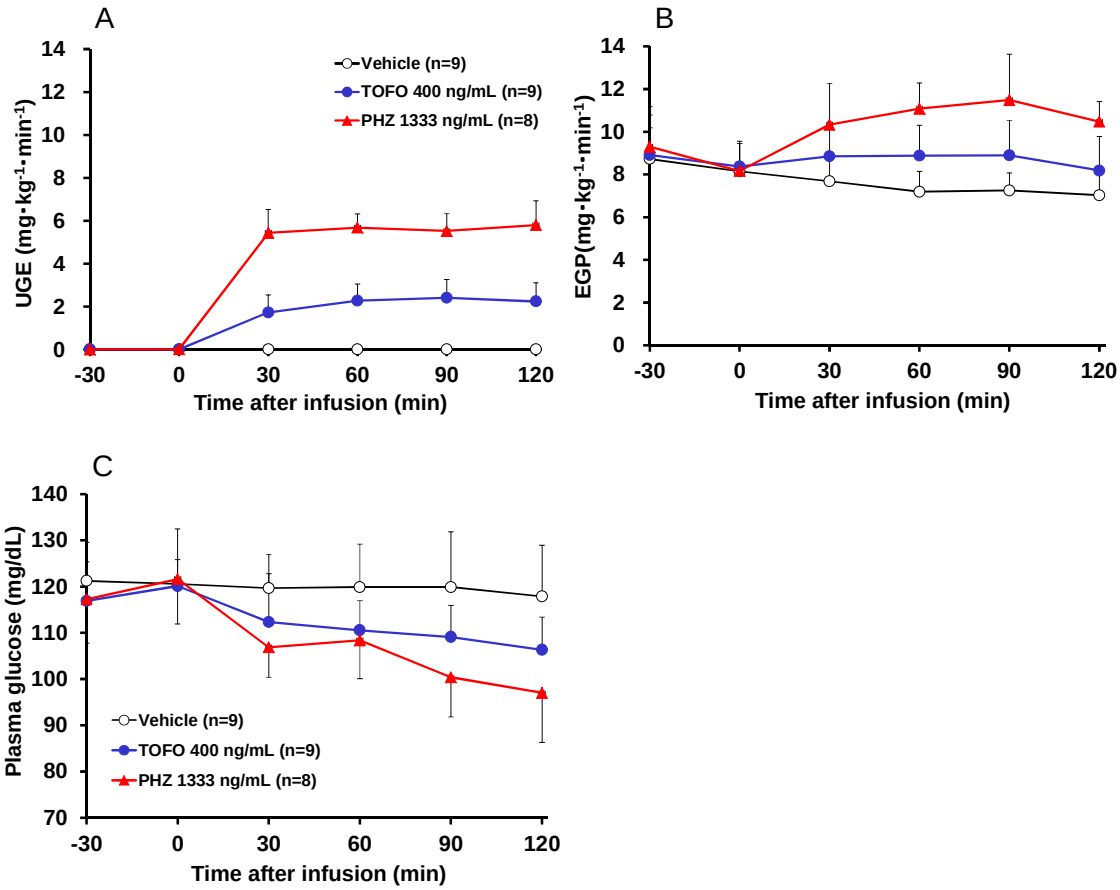

Time-course of (A) urinary glucose excretion (UGE), (B) endogenous glucose production (EGP), and (C) plasma glucose of euglycemic Wistar rats infused with tofogliflozin (TOFO) or phlorizin (PHZ). Data are shown as means + SD, *n* = 8–9. The concentrations (400, 1333 ng/mL) indicated are target plasma concentrations. The actual plasma tofogliflozin and phlorizin concentrations after 120 min infusion were 574 ± 80 and 1514 ± 243 ng/mL, respectively. After 150 min infusion of [U-^{13}C, 99%] D-glucose (time = 0), the infusion of tofogliflozin (bolus, 1.2 mg/kg; constant, 0.5 mg·kg^{-1}·h^{-1}) or phlorizin (bolus, 0.15 mg/kg; constant, 2.8 mg·kg^{-1}·h^{-1}) was started at 2 mL/kg (bolus) and 25 mL·kg^{-1}·h^{-1} (constant).

Tables

Table 1 Plasma glucose levels and actual plasma concentrations of SGLT inhibitors in the rat glucose titration protocol

Group	Target plasma conc. (ng/mL)	n	Plasma glucose (mg/dL)		Actual plasma concentration of SGLT inhibitor (ng/mL)		
			Basal	Max. % inhibition of RGR*	Time after the start of infusion (min)		
					60	135	210
Vehicle	-	7	120 ± 9	300 ± 26			
Tofogliflozin	4	4	116 ± 9	312 ± 31	5.0 ± 0.5	4.2 ± 0.6	4.5 ± 0.4
	13	4	120 ± 10	290 ± 29	17.0 ± 0.7	13.9 ± 0.6	14.2 ± 1.0
	40	5	119 ± 5	319 ± 31	57.9 ± 2.6	43.8 ± 2.2	42.7 ± 1.7
	133	5	114 ± 8	325 ± 33	196.9 ± 9.1	153.1 ± 8.1	151.5 ± 10.3
	400	5	111 ± 6	321 ± 36	570.1 ± 34.7	446.0 ± 40.1	407.2 ± 94.1
Phlorizin	40	3	127 ± 11	312 ± 18	40.2 ± 10.5	44.4 ± 4.8	43.1 ± 8.5
	133	3	121 ± 4	299 ± 17	145.0 ± 13.1	167.0 ± 13.0	153.7 ± 14.6
	400	3	127 ± 4	303 ± 18	436.0 ± 24.0	434.7 ± 29.1	428.3 ± 42.7
	1333	3	127 ± 8	290 ± 19	1593.3 ± 83.3	1463.3 ± 228.1	1666.7 ± 100.2

* Plasma glucose levels (<350 mg/dL) when the maximum % inhibition of renal glucose reabsrption (RGR) was defined.

Table 2 Plasma concentration of SGLT inhibitors in the glucose clamp protocol.

Group	Target plasma conc.	n	Actual plasma concentration of SGLT inhibitor (ng/mL)		
			Time after the start of infusion (min)		
	(ng/mL)		30	90	150
Tofogliflozin	133	4	260.3 ± 24.0	193.8 ± 19.8	181.5 ± 20.8
	400	4	718.5 ± 27.8	556.5 ± 48.5	521.5 ± 48.5
Phlorizin	400	4	364.8 ± 36.1	381.5 ± 18.3	387.0 ± 42.1
	1333	4	1052.0 ± 67.3	1177.5 ± 86.6	1200/0 ± 87.6

Values are means ± SD.

Table 3 Plasma glucose levels under basal, hypoglycemic, and euglycemic conditions in the glucose clamp protocol.

Group	Plasma conc. (ng/mL)	n	Plasma glucose (mg/dL)		
			Basal	Hypoglycemia*	Euglycemia**
Vehicle	-	4	134 ± 7	46 ± 7	99 ± 3
Tofogliflozin	133	4	130 ± 9	48 ± 7	95 ± 5
	400	4	128 ± 4	40 ± 9	96 ± 3
Phlorizin	400	4	131 ± 11	43 ± 2	97 ± 4
	1333	4	131 ± 4	46 ± 5	97 ± 2

Values are means ± SD.

* Mean values during the last 30 min of the insulin plus vehicle plus tofogliflozin, or phlorizin infusion period, as indicated in Figure 4.

** Mean values during the last 30 min of the insulin plus vehicle plus tofogliflozin, or phlorizin plus glucose infusion period, as indicated in Figure 4.

Table 4 Creatinine clearance under basal, hypoglycemic, and euglycemic conditions in the glucose clamp protocol.

Group	Plasma conc. (ng/mL)	n	Creatinine clearance (mL/min)		
			Basal	Hypoglycemia*	Euglycemia**
Vehicle	-	4	2.33 ± 0.40	2.55 ± 1.22	3.34 ± 1.08
Tofogliflozin	133	4	2.67 ± 0.41	2.81 ± 0.35	2.52 ± 0.76
	400	4	1.95 ± 0.32	2.76 ± 0.74	3.11 ± 0.50
Phlorizin	400	4	2.81 ± 0.47	2.62 ± 0.76	2.88 ± 0.21
	1333	4	2.64 ± 0.44	3.01 ± 0.43	2.94 ± 0.77

Values are means ± SD.

* Mean values during the last 30 min of the insulin plus vehicle plus tofogliflozin, or phlorizin infusion period, as indicated in Figure 4.

** Mean values during the last 30 min of the insulin plus vehicle plus tofogliflozin, or phlorizin plus glucose infusion period, as indicated in Figure 4.

Table 5 Plasma glucose, EGP and UGE at steady-state in infusion protocol

	Vehicle (n=9)	Tofogliflozin (n=9)	Phlorizin (n=8)
Plasma glucose (mg/dL)	119 ± 11	109 ± 7 *	102 ± 9 **
Minimum plasma glucose (mg/dL) †	117 ± 11	106 ± 7	96 ± 9 *** #
EGP ($mg \cdot kg^{-1} \cdot min^{-1}$)	7.3 ± 1.0	8.8 ± 1.5*	11.0 ± 1.3***##
UGE ($mg \cdot kg^{-1} \cdot min^{-1}$)	0.0071 ± 0.0019	2.3 ± 0.7***	5.7 ± 0.7***###
ΔEGP-UGE ($mg \cdot kg^{-1} \cdot min^{-1}$)	7.3 ± 1.0	6.5 ± 1.1	5.3 ± 1.0***#

Values are means ± SD during the last 60 min of vehicle, tofogliflozin, or phlorizin-infusion period.

* p <0.05, ** p <0.01, *** p <0.001 *vs.* vehicle group by Dunnett's multiple comparison test.

# p <0.05, ## p <0.01, ### p <0.001 *vs.* tofogliflzoin group by unpaired *t*-test test.

†Means ± SD of the minimum value of three sampling times (60, 90, and 120 min after infusion) for each rat.

Chapter III

Competitive inhibition of SGLT2 by tofogliflozin or phlorizin induces urinary glucose excretion through extending splay in cynomolgus monkeys

Introduction

Sodium–glucose cotransporter 2 (SGLT2) is specifically expressed in renal proximal tubules and plays an important role in renal glucose reabsorption (Kanai *et al.* 1994; Wright *et al.* 2011). Since SGLT2 inhibition is expected to have a high potential to induce urinary glucose excretion (UGE) with low safety concerns (Han *et al.* 2008; Suzuki *et al.* 2012; Yamamoto *et al.* 2011), several SGLT2 inhibitors are currently being developed in human clinical studies (Chao & Henry 2010; Ferrannini & Solini 2012).

The substantial role that SGLT2 plays in renal glucose handling in rodents has been demonstrated by the increased UGE in SGLT2 knock-out mice (Vallon *et al.* 2011), the improvement of hyperglycaemic conditions in db/db mice with SGLT2 deletion (Jurczak *et al.* 2011), and the improvement of hyperglycemic conditions accompanied by markedly increased UGE in diabetic rats treated with SGLT2 inhibitors (Han *et al.* 2008; Katsuno *et al.* 2007; Liang *et al.* 2012; Suzuki *et al.* 2012).

In humans, genetic and functional analyses of familial renal glucosuria (FRG), a disorder caused by mutations of SLC5A2 (SGLT2), have revealed the predominant role that SGLT2 plays in the handling of glucose by the kidney (Calado *et al.* 2011). FRG affects key parameters of glucose titration studies, including the tubular transport maximum for glucose (TmG), the threshold of renal glucose excretion, and splay (DeFronzo *et al.* 2012). Patients with FRG type A exhibit increased UGE with a low threshold and TmG, but with normal splay, suggesting that a loss in the amount of functional SGLT2 contributes to their increased UGE. In contrast, patients with FRG type B exhibit increased UGE with a low threshold and exaggerated splay, but with a normal TmG, suggesting that reduced affinity of SGLT2 for glucose due to a missense mutation contributes to their increased UGE (Brodehl *et al.* 1987; Santer & Calado 2010; Santer *et al.* 2003). Of note, the term ‘splay’ has been generally defined as “the deviation from a linear relationship between the filtered and reabsorbed glucose encountered during glucose titrations” (McPhaul & Simonaitis 1968) or “the difference between the actual

and theoretical thresholds"(DeFronzo *et al.* 2012). However, there have been few reports on the quantitative evaluation on the magnitude of splay (McPhaul & Simonaitis 1968; Shankel *et al.* 1967).

From the observations on the glucose titration curves of FRG mentioned above, SGLT inhibitors are thought to induce UGE *in vivo* by two inhibition mechanisms. One is the suppression of TmG through non-competitive inhibition of SGLT2 activity, and the other is the extension of splay through competitive inhibition. Although there are a few reports from glucose titration studies in dogs (Lotspeich & Woronkow 1958; Ueta *et al.* 2006) and rats (Katsuno *et al.* 2007) that examine the effect of SGLT2 inhibitors on TmG and the threshold of glucosuria, there is no report to quantitatively examine their effects on splay.

Moreover, with the method previously used to determine threshold in rats and humans using non-linear regression between the blood glucose and UGE (Liang *et al.* 2012; Polidori *et al.* 2013; Sha *et al.* 2011), the fitted UGE line lacks the splay curve, implying that the threshold value estimated in their studies may vary from the actual threshold, which would also affect the accuracy of the estimated splay value.

Considering the importance of splay as an indicator of the homogeneity of nephron function in patients with chronic progressive renal diseases (McPhaul & Simonaitis 1968; Rieselbach *et al.* 1967; Usberti & Andreucci 1976) and in certain types of FRG patients (Brodehl *et al.* 1987; Santer & Calado 2010; Santer *et al.* 2003), I believe that it is also necessary to evaluate the effect of SGLT2 inhibitors on splay, in order to predict their efficacy precisely.

Recently, DeFronzo *et al.* reported that dapagliflozin, a selective SGLT2 inhibitor, produces its glucosuric effect in type 2 diabetes (T2D) patients and healthy subjects by reducing the TmG and threshold for glucosuria together with a reduction of splay (Defronzo *et al.* 2013). However, they started the glucose titration from normal plasma glucose concentration with a single dose of dapagliflozin, suggesting the human glucose

titration study had several limitations, such as a narrow range of plasma glucose and dapagliflozin concentrations, which may affect the accuracy of the estimated drug's effect on TmG, threshold, and splay.

Non-human primates are more closely related to humans than are rodents. Therefore, they are currently considered the primary model for evaluating diabetic drugs (H. Chen *et al.* 2010; Kharitonenkov *et al.* 2007; Wagner *et al.* 2010). In fact, cynomolgus monkeys have been used to evaluate the efficacy and toxicity of a second-generation antisense nucleotide targeting human SGLT2 (Zanardi *et al.* 2012). In that report, 13-week administration of ISIS 388626 reduced the expression of SGLT2 mRNA in the kidneys and promoted UGE in cynomolgus monkeys, suggesting that using cynomolgus monkeys is relevant for predicting the effects of SGLT2 inhibition in humans.

However, there are no previous reports about the molecular cloning of non-human primate SGLT1 or SGLT2 or about the *in vitro* and *in vivo* activities of SGLT inhibitors in non-human primates, indicating that the properties of cynomolgus monkey SGLT1 and SGLT2 and their contribution to renal glucose handling have yet to be fully characterized.

In this chapter, first, it was tried to clone the SGLT1 and SGLT2 cDNAs of cynomolgus monkeys and express cSGLT1 and cSGLT2 in COS-7 cells. Then, it was intended to confirm the properties of tofogliflozin, a highly selective SGLT2 inhibitor in humans (Ohtake *et al.* 2012; Suzuki *et al.* 2012), and phlorizin, a non-selective SGLT1/2 inhibitor (Pajor *et al.* 2008), in the inhibition of cSGLT1 and cSGLT2. Next, it was intended to evaluate the effect of these SGLT inhibitors on renal glucose handling in cynomolgus monkeys with a glucose titration study, in which TmG, glucosuria threshold, and splay were quantatively estimated using a newly introduced method for fitting the titration curve.

Materials and Methods

Chemicals

Tofogliflozin ([1*S*, 3′*R*, 4′*S*, 5′*S*, 6′*R*]-6-[(4-ethylphenyl)methyl]-3′, 4′, 5′, 6′-tetrahydro-6′-[hydroxymethyl]-spiro[isobenzofuran-1(3*H*), 2′-(2*H*) pyran]-3′, 4′, 5′-triol) was synthesized in laboratories at Chugai Pharmaceutical Co. Phlorizin and α-methyl-D-glucopyranoside (AMG) were purchased from Sigma-Aldrich (St. Louis, MO, USA), and α-methyl-D-[^{14}C] glucopyranoside ([^{14}C]-AMG) was purchased from General Electronic Company (Tokyo, Japan). Glucose solutions (20% and 50%) were purchased from Fuso Pharmaceutical Industries Ltd. (Osaka, Japan) and Otsuka Pharmaceutical Factory Inc. (Tokushima, Japan), respectively. Tofogliflozin was dissolved at 0.34 mg/mL in lactated Ringer's solution and diluted serially. Phlorizin was dissolved at 1.93 mg/mL in lactated Ringer's solution and diluted serially. Glucose solution (20% or 50%) was diluted with purified water to make concentrations of 10%, 30%, or 40%.

Animals

Male cynomolgus monkeys (*Macaca fascicularis*) were purchased from Hamri Co., Ltd. (Tsukuba, Japan). These animals were kept under a 12-h/12-h light/dark cycle (lights on 7:00 AM–7:00 PM) with controlled room temperature (20–26°C) and humidity (35–75%), and were allowed *ad libitum* access to a certified primate diet (5048; LabDiet, St. Louis, MO, USA), fruit as supplementary food, and water. No cynomolgus monkeys were euthanized specifically for the experiment in this chapter. All animal experiments were performed in accordance with the Guidelines for the Care and Use of Laboratory Animals at Chugai Pharmaceutical under the approval of the company's Institutional Animal Care and Use Committee and also in compliance with the "Act on Welfare and Management of Animals" in Japan. The company is fully accredited by the Association for Assessment and Accreditation of Laboratory Animal Care International, a non-profit

organization that promotes the humane treatment of animals in science through voluntary accreditation and assessment programs (http://www.aaalac.org/). The experiments using cynomolgus monkeys was conducted, adhering to the principles stated in the US National Research Council's *Guide for the Care and Use of Laboratory Animals*. Every effort was made to minimize the number of animals used.

Molecular cloning of cynomolgus monkey SGLT1 and SGLT2

In vitro inhibition studies using cells expressing cynomolgus monkey SGLT1 (cSGLT1) and cynomolgus monkey SGLT2 (cSGLT2) were performed as follows by a method reported previously (Suzuki *et al.* 2012). Cynomolgus monkey SGLT1 and SGLT2 cDNAs were amplified by RT-PCR from total RNA isolated from the kidney of a cynomolgus monkey. The sequences of the PCR primers used were 5′-CGCTGCCACCATGGACAGTA-3′ and 5′-CTAGTGGGAAATAACAACTC-3′ for cSGLT1 and 5′-CGCTGCCACCATGGACAGTA-3′ and 5′-CCACTTCCTGTGAGGCTGTG-3′ for cSGLT2. Experimental conditions for PCR with KOD Plus (Toyobo Co., Osaka, Japan) were as follows: 94°C for 2 min; 35 cycles of 94°C for 15 s, 58°C for 30 s, and 68°C for 3 min. Expression plasmids containing cSGLTs were prepared by ligating amplified cDNA fragments into the multi-cloning site of pcDNA3.1(–) (Life Technologies Co. [Invitrogen], Grand Island, NY, USA). The expression plasmid containing cSGLT1 or cSGLT2 cDNA fragments or empty vector (pcDNA3.1(-)) was transfected into African green monkey SV40-transfected kidney fibroblast cells (COS-7) obtained from the American Type Culture Collection (ATCC, Manassas, VA, USA), and the cells transiently expressing each cSGLT were used for the AMG uptake assay.

Inhibition assay of AMG uptake in COS-7 cells transiently expressing cSGLT1/2

For the AMG uptake assay, cells expressing each cSGLT were cultured in 96-well plates for 2 or 3 days and washed twice with sodium-free buffer containing 140 mM choline chloride, 2 mM KCl, 1 mM $CaCl_2$, 1 mM $MgCl_2$, and 10 mM Hepes/Tris (pH 7.4). The cells were then incubated in sodium-free buffer or sodium buffer containing 140 mM NaCl, 2 mM KCl, 1 mM $CaCl_2$, 1 mM $MgCl_2$, and 10 mM Hepes/Tris (pH 7.4) with 1 mM AMG mixture (non-radiolabeled AMG and [^{14}C]-AMG) at 37°C for 45 min. Sodium-dependent AMG uptake was calculated by subtracting the radioactivity detected in cells incubated in the sodium-free buffer from the radioactivity detected in the cells incubated in the sodium buffer. IC_{50} values of the SGLT inhibitors were calculated with the empirical four-parameter model fitting of XLfit (IDBS, Guildford, UK). To measure K_m , V_{max}, and K_i values, the AMG uptake assays were performed in sodium buffer or sodium-free buffer containing various concentrations of AMG. K_m , V_{max}, and K_i values of inhibitors were calculated from Lineweaver–Burk plots. K_m and V_{max}, IC_{50} and K_i values were indicated as mean values of two independent experiments.

Glucose titration study in cynomolgus monkeys

Study design

Three male cynomolgus monkeys, 4 to 6 years of age and weighing 3.5 to 5 kg, were used and allocated to treatment using a randomized block design. Two monkeys were allocated to receive all six treatments consisting of vehicle, tofogliflozin (13.3 or 133 ng/mL), and phlorizin (133, 1333, or 13 333 ng/mL) treatment. The other monkey was given four treatments consisting of vehicle, two dose levels of tofogliflozin (13.3 and 133 ng/mL), and phlorizin (13 333 ng/mL) treatment. For each animal, the titration experiments with drug and glucose infusion were conducted over approximately

6 months, and the mean interval between two titration studies for each animal was 32 days (11-68 days).

Surgical operation

Animals were fasted overnight before each experiment. Pre-anesthetic was given as an intramuscular injection of atropine sulfate (0.15 mg/animal), and anesthetic induction was performed with an intramuscular injection of ketamine (0.5 mg/animal). Intubated animals were maintained with isoflurane inhalation at a minimum alveolar concentration (MAC) of 1% to 3%. Isoflurane concentration was adjusted using an anesthesia apparatus (NS-5000A; Acoma Medical Industry Co., Tokyo, Japan) according to vital signs, including heart rate, blood pressure, respiratory rate, oxygen saturation (SPO_2), and rectal temperature. Respiratory rate was maintained spontaneously or controlled using a respirator (PRO-45Va; Acoma Medical Industry Co.) at 20 to 30 breaths per minute. Vital signs were monitored using a bed-side monitor (BP-88S; Omron Colin Co., Tokyo, Japan). Heart rates were maintained at 130 to 160 beats per minute. Mean blood pressure was maintained at about 40 mmHg. SPO_2 was maintained at over 95%. Rectal temperature was maintained at 36.5°C to 37.5°C.

An indwelling venous catheter (V1) was placed in the left saphenous vein for infusion of drugs or Ringer's solution, and another indwelling venous catheter (V2) was placed in the right saphenous vein for infusion of glucose solution. An indwelling venous needle was placed in the left cephalic vein for blood sampling. A Foley catheter was placed in the bladder for urine sampling.

After completion of the study, the bladder catheter and venous needles were removed, and bleeding was prevented by bandages and applying pressure. Tracheal extubation was performed after recovery of the swallowing reflex, and animals were carefully monitored until complete recovery from anesthesia.

Infusion protocol of SGLT inhibitor and glucose

The infusion of tofogliflozin or phlorizin solution was started at 2 mL/kg (bolus) and continued at 5 $mL \cdot kg^{-1} \cdot h^{-1}$ through the left saphenous vein catheter (V1). The concentrations of tofogliflozin and phlorizin solution infused were determined on the basis of pharmacokinetic parameters obtained from separate PK studies (data not shown) so as to maintain a target plasma concentration of 13.3 or 133 ng/mL for tofogliflozin and 133, 1333, or 13 333 ng/mL for phlorizin. The infusion rate to achieve a target plasma concentration of 133 ng/mL tofogliflozin was 226 μg/kg (bolus) and 53.5 $\mu g \cdot kg^{-1} \cdot h^{-1}$ (constant), and the infusion rate to achieve a target plasma concentration of 13 333 ng/mL phlorizin was 1.9 mg/kg (bolus) and 965 $\mu g \cdot kg^{-1} \cdot h^{-1}$ (constant).

After 120 min of tofogliflozin or phlorizin infusion, infusion of 10% glucose solution through the right saphenous vein catheter (V2) was started at 5 $mL \cdot kg^{-1} \cdot h^{-1}$ and increased in a stepwise manner (20%, 30%, 40%, and 50%) at 60-min intervals to raise the plasma glucose concentrations to above 8 mg/mL. Thereafter, the infusion rate of 50% glucose solution was increased to 10 $mL \cdot kg^{-1} \cdot h^{-1}$ to achieve about 10 mg/mL plasma glucose within 60 min. A blood sample (0.5 mL) was collected every 20 min with a heparinized syringe; the plasma glucose level of the sample was checked with a plasma-glucose monitoring system (Accu-Chek Aviva; Roche Diagnostics, Tokyo, Japan), and then a plasma sample was obtained by centrifugation to determine plasma glucose, creatinine, and tofogliflozin or phlorizin concentrations.

Urine was collected at 30-min intervals beginning 60 min after the start of drug infusion and at 20-min intervals after glucose infusion by injecting 10 mL saline into the bladder catheter to flush urine into pre-weighed polyethylene sample tubes. The weight of the sampled urine plus sample tube was recorded, and urine volume was determined by subtracting the weight of the pre-weighed sample tube from sampled urine and tube weight, with the specific gravity of sampled urine taken as 1. Urine and plasma samples were stored at −80°C until use.

Analysis

Plasma tofogliflozin concentrations were measured with an LC–MS/MS system (high performance liquid chromatography: Shimadzu 20A [Shimadzu Co., Kyoto, Japan]; mass spectrometry: API-4000 [AB Sciex, Foster City CA, USA]). Plasma phlorizin concentrations were measured with an LC–MS/MS system (high performance liquid chromatography: Acquity UPLC [Waters, Milford, MA, USA]; mass spectrometry: API-3200 [AB Sciex]).

Plasma glucose and urinary glucose concentrations were measured by the hexokinase/G-6-PDH method (L-Type Glu 2; Wako Pure Chemical Industries, Ltd., Osaka, Japan) with an automatic analyzer (TBA-120FR; Toshiba Medical Systems Corporation, Tochigi, Japan). Creatinine concentrations of plasma and urine were measured by the creatininase/HMMPS method (L-Type Creatinine M; Wako Pure Chemical Industries) with an automatic analyzer.

Calculations

The following parameters were calculated:

Creatinine clearance (mL/min) = (urine creatinine; mg/mL) × (urine excretion rate; mL/min) / (plasma creatinine; mg/mL)

Glucose clearance (mL/min) = (urinary glucose; mg/mL) × (urine excretion rate; mL/min) / (plasma glucose; mg/mL)

Percent inhibition of renal glucose reabsorption (RGR) [RGR inhibition (%)] = glucose clearance / creatinine clearance × 100 (%)

This calculation method was based on the formula used to calculate the percent inhibition of RGR in a clinical study with dapagliflozin (Kasichayanula *et al.* 2011).

Glucose filtration rates (GluFR), glucose excretion rates (GluER), and glucose reabsorption rates (GluRR) were determined by the following formulas:

GluFR = (plasma glucose; mg/mL) × (creatinine clearance; mL/min)

GluER = urinary glucose excretion (mg) / sampling period (min)

GluRR = GluFR (mg/min) – GluER (mg/min)

The titration curves were plotted as GluFR versus GluER or GluRR. Glucose reabsorption rates were fitted by the following single exponential equation developed by Martin (Martin L. 1961) as follows:

(1) $$\mathrm{GluRR}\ (x) = x_b + (\mathrm{TmG} - x_b) \times (1 - \exp[-k(x - x_b)])$$

where x is glucose filtration rate, x_b is the threshold indicating the GluFR at which glucose first appears in the urine, and k is a coefficient of glucosuric effect.

The threshold (x_b) was defined as the GluFR at which the measured percentage inhibition of RGR exceeded 5% in each experiment for the first time. TmG is defined as the mean GluRR at a GluFR of above 90 mg/min for each experiment, and is designated as observed TmG. This definition is based on the saturated GluRR observed at a GluFR of above 90 mg/min in the vehicle treatment of this chapter.

Splay values (S1 and S2 regions illustrated in Figure 1) were determined from the following formula, in which the first term is the area under the GluER curve ranging from x_b to TmG and the second term is the area between the GluER curve and the (x − TmG) line from TmG to positive infinity:

(2) $$\mathrm{Splay} = \int_{x_b}^{\mathrm{TmG}} \mathrm{GluER}(x)\mathrm{d}x + \int_{\mathrm{TmG}}^{+\infty} \{\mathrm{GluER}(x) - (x - \mathrm{TmG})\}\mathrm{d}x$$

$$= (\mathrm{TmG} - x_\mathrm{b})/k - 1/2 \times (\mathrm{TmG} - x_b)^2$$

where x_b and k are the parameters determined in the above-mentioned formula (1).

The glucose transport rate through cSGLT2 *in vivo* at x_b was estimated from Michaelis-Menten equation for competitive inhibition as follows.

(3) $$\mathrm{V}x_b = V_{\max} \times [\mathrm{S}] / ([\mathrm{S}] + K_\mathrm{m} \times (1 + [\mathrm{SGLTi}] / K_\mathrm{i}))$$

where [S] represents plasma glucose levels at x_b in the above-mentioned titration curve, and [SGLTi] represents the estimated free SGLT inhibitor concentration corrected to

reflect the protein-binding properties (Suzuki *et al.* 2012; Yamaguchi *et al.* 2011). The plasma glucose levels at x_b are the actual ones from the above-mentioned titration study using cynomolgus monkeys with 2 or 3 replications for each treatment. V_{max} and K_m values of cSGLT2 and K_i values of inhibitors were calculated from a Lineweaver-Burk plot of the AMG uptake assay. This estimation was based on the equipotent affinity of AMG and D-glucose to human SGLT2 (Wright *et al.* 2011).

All parameters were calculated with Microsoft Excel 2007 (Microsoft Corporation, Redmond, WA, USA), and GluER was fitted with Prism 5.0 (GraphPad Software Inc., San Diego, CA, USA). The coefficient of determination was calculated from the following formula:

(4) $R^2 = 1 - \text{RSS (residual sum of squares)} / \text{TSS (total sum of squares)}$

Statistical analysis

Data are presented as mean ± SD or SEM. To examine the effects of drug treatment upon the parameters (maximum percentage inhibition of RGR, observed TmG, threshold, and splay) in the titration study, statistical analyses were performed by randomized block analysis of variance (ANOVA). Post-hoc comparisons were performed using Tukey's HSD test (JMP 9.02; SAS Institute Japan, Tokyo, Japan).

Results

In vitro characterization of cynomolgus monkey SGLT1 and SGLT2

The amino acid sequences deduced from the cloned cSGLT1 and cSGLT2 cDNA sequences were perfectly matched to the predicted amino acid sequences of rhesus monkey SGLT1 (XM_001112212) and SGLT2 (XM_001113206), respectively, in the RefSeq protein product database. The nucleotide sequence homologies in cynomolgus monkey, rodent, rhesus monkey, and human SGLTs are shown in Table 1. The amino acid sequence similarities between cSGLT1/2 against rhesus monkey and human SGLT1/2 were higher than those of cSGLT1/2 against rodent SGLT1/2.

The inhibitory activity of tofogliflozin or phlorizin against cSGLT2 was examined in COS-7 cells over-expressing cSGLT2 by evaluating sodium-dependent AMG uptake. Substantial sodium-dependent AMG uptake was confirmed in COS-7 cells over-expressing cSGLT1/2 above background levels (Figure 2), and fold-change values in AMG uptake for cSGLT1/2 relative to the background levels seen in cells with a transfected vector were 186 and 307 times, respectively, indicating that cSGLT1/2 are functionally active, as shown in a similar protocol (Pajor *et al.* 2008).

Analysis using Lineweaver–Burk plots showed that both compounds inhibited AMG uptake in a substrate-competitive manner (Figure 3), and K_i value of phlorizin for cSGLT2 inhibition was 26.1 ± 6.1 nM. Tofogliflozin inhibited cSGLT2 more strongly than did phlorizin: K_i value of tofogliflozin for cSGLT2 inhibition was 5.0 ± 0.6 nM. In addition, from the Lineweaver-Burk plot (Figure 3), K_m and V_{max} values of cSGLT2 were 1.63 ± 0.17 mM and 0.97 ± 0.09 nmol/h, respectively. V_{max} value of cSGLT2 was not altered by either tofogliflozin or phlorizin (phlorizin at 40 and 80 nM: 1.08 ± 0.12 and 1.08 ± 0.41 nmol/h; tofogliflozin at 6 and 12 nM: 0.97 ± 0.26 and 0.99 ± 0.22 nmol/h, respectively).

The IC_{50} values of phlorizin and tofogliflozin against cSGLT2 were 35.8 ± 4.9 and 8.9 ± 0.5 nM, respectively (Table 2). In addition, tofogliflozin was more selective than phlorizin: the selectivity of tofogliflozin toward cSGLT2 was 1,000 times that toward cSGLT1, and the IC_{50} values of tofogliflozin and phlorizin against cSGLT1 were 8875 ± 390 and 309 ± 81 nM, respectively (Table 2). These results suggest that tofogliflozin inhibits SGLT2 more selectively than phlorizin does in cynomolgus monkeys, as well as in rodents and humans (Suzuki *et al.* 2012).

Glucose titration study in cynomolgus monkeys

In both tofogliflozin and phlorizin treatments, plasma drug concentrations were maintained at a stable level during the whole study. Briefly, actual plasma drug concentrations of tofogliflozin were maintained at 132% and 142% of the targeted plasma concentrations of 13.3 and 133 ng/mL, respectively (Figure 4A). On the other hand, actual plasma drug concentrations of phlorizin were maintained at 72%, 69%, and 43% of the targeted plasma concentrations of 133, 1333, and 13 333 ng/mL, respectively (Figure 4B).

The individual data of body weight, treatment, TmG, and creatinine clearance are shown in Table 3. During the course of the repeated titration experiments over approximately 6 months, there were no remarkable changes in body weight or creatinine clearance (Table 3).

The plasma glucose levels continuously increased from about 0.5 to 10 mg/mL with increasing glucose load (Figure 5A and B). At the final sampling point, plasma glucose levels for each treatment were as follows: vehicle, 9.030 ± 0.432 mg/mL; tofogliflozin (13.3 ng/mL), 9.300 ± 0.664 mg/mL; tofogliflozin (133 ng/mL), 8.938 ± 0.566 mg/mL; phlorizin (133 ng/mL), 10.303 ± 0.323 mg/mL; phlorizin (1333 ng/mL), 8.825 ± 0.235 mg/mL; and phlorizin (13 333 ng/mL), 9.112 ± 0.449 mg/mL.

GluER increased with increasing plasma glucose levels (Figure 5C and D). In both tofogliflozin and phlorizin treatment, compared with the vehicle treatment, a clear increase in GluER was observed under normoglycemic conditions. Interestingly, these differences in GluER between vehicle and the inhibitor treatments tended to disappear under hyperglycemic conditions.

The creatinine clearance values in all treatments were maintained at a stable level of around 15 mL/min during the experiment (Figure 5E and F). The creatinine clearance values in this chapter were similar to those in conscious cynomolgus monkeys (Weekley *et al.* 2003).

The time course of the percentage inhibition of RGR is shown in Figure 6A and B. In both tofogliflozin and phlorizin treatments, a dose-dependent increase in the percentage inhibition of RGR was observed even under normal plasma glucose levels before and after the start of glucose infusion. Then, the percentage inhibition of RGR increased to around 50% in both tofogliflozin and phlorizin treatments. Although the percentage inhibition of RGR in the vehicle treatment group was negligible before and until 60 min after the start of glucose infusion, the percentage inhibition of RGR in the vehicle treatment group began to increase when the plasma glucose levels exceeded 2 mg/mL and gradually increased up to 50% at the end of the titration study, when the plasma glucose levels were around 10 mg/mL.

From the percentage inhibition of RGR in the vehicle treatment in this experiment (Figure 6A and B), the threshold of glucose reabsorption in cynomolgus monkeys was assumed to be around 2.5 to 3.5 mg/mL which is similar to that in rats (Chapter II). Accordingly, it was aimed to compare the percentage inhibition of RGR at plasma glucose levels ranging from 2.5 to 3.5 mg/mL to estimate the maximum inhibitory effects of SGLT inhibitors on RGR (maximum percentage inhibition of RGR). The maximum percentage inhibition of RGR was significantly influenced by treatment with SGLT inhibitors (drug treatment effect $F_{5,8} = 51.5544$, $P < 0.0001$). The maximum percentage

inhibition of RGR increased in a dose-dependent manner in both tofogliflozin and phlorizin treatment compared with vehicle treatment (tofogliflozin 13.3 ng/mL, P = 0.0002; tofogliflozin 133 ng/mL, $P < 0.0001$; phlorizin 1333 ng/mL, P = 0.0014; phlorizin 13 333 ng/mL, $P < 0.0001$; *vs.* vehicle treatment; Tukey's HSD test; Figure 6C).

The representative relationships between the calculated GluFR and GluER and between GluFR and GluRR for cynomolgus monkey #2 are shown in Figure 7. Compared with vehicle treatment, both tofogliflozin and phlorizin treatment began to induce GluER at lower GluFR levels (Figure 7A, B). With vehicle treatment, the GluRR increased with increasing GluFR, but levels began to plateau when GluFR was around 90 mg/min. In contrast, although the GluRR with both tofogliflozin treatment (13.3 and 133 ng/mL) and phlorizin treatment (1333 and 13 333 ng/mL) also increased depending on the GluFR, no clear plateau in GluRR was observed, even when the GluFR exceeded 90 mg/min (Figure 7C, D). From these titration curves, it was intended to determine the TmG and threshold of UGE according to the criteria mentioned in the *Methods* section. Splay values were then calculated according to formula (2).

The TmG values observed in all experiments are listed in Table 3 and summarized in Table 4. Although a marginal difference was detected with ANOVA (drug treatment effect $F_{5,8}$ = 3.8039, P = 0.0463), post-hoc comparison detected no significant differences in the TmG values between SGLT2 inhibitor and vehicle treatment (tofogliflozin 13.3 ng/mL, P = 0.9945; tofogliflozin 133 ng/mL, P = 0.7405; phlorizin 133 ng/mL, P = 0.2255; phlorizin 1333 ng/mL, P = 0.9860; phlorizin 13 333 ng/mL, P = 0.6285; *vs.* vehicle treatment; Tukey's HSD test; Figure 8A).

The mean threshold value with vehicle treatment was 37.01 ± 3.96 mg/min, at which the mean plasma glucose level was 2.54 ± 0.50 mg/mL. The threshold was significantly influenced by treatment with SGLT inhibitors (drug treatment effect $F_{5,8}$ = 24.1356, P = 0.0001). The threshold values observed with tofogliflozin 13.3 and 133 ng/mL treatment were respectively decreased to about 36% and 27% of vehicle treatment (tofogliflozin

13.3 ng/mL, P = 0.0016; tofogliflozin 133 ng/mL, P = 0.0007; *vs.* vehicle treatment, Tukey's HSD test). Although no significant difference in the threshold was detected between phlorizin 133 ng/mL and vehicle treatment (P = 0.9574), with phlorizin at higher doses (1333 and 13 333 ng/mL) the threshold was significantly decreased to about 53% and 11%, respectively, of vehicle treatment (phlorizin 1333 ng/mL, P = 0. 0281; phlorizin 13 333 ng/mL, P = 0.0002; *vs.* vehicle treatment, Tukey's HSD test) (Figure 8B).

Clear extensions of splay were observed in the glucose titration curves of animals treated with SGLT inhibitors (Figure 7). To evaluate the splay quantitatively for each treatment in each animal, it first was intended to estimate the parameter k by constructing the fitting equations for the GluRR curve according to formula (1) using the observed TmG (Table 3) and each threshold (data not shown). Then, the splay area was calculated in the titration curve according to formula (2). The mean splay area of vehicle treatment was 640 ± 157 mg^2/min^2. The splay was influenced by treatment with an SGLT inhibitor (drug treatment effect $F_{5,8}$ = 9.1088, P = 0.0037). There were significant increases in the splay values with tofogliflozin 13.3 ng/mL (P = 0.0148), tofogliflozin 133 ng/mL (P = 0.0057), and phlorizin 13 333 ng/mL (P = 0.0038) treatments as compared with vehicle treatment (Tukey's HSD test; Figure 8C).

Next, to confirm the validity of the method, the fitting equations for GluRR was constructed according to formula (1) by using the pooled GluER and GluFR data with the observed TmG of the vehicle treatment and the mean threshold of each treatment. The measured GluRR values were well predicted from GluFR by using the fitting equations, with a coefficient of determination ranging from 0.8547 to 0.9342 (Figure 9A–F). The parameters of the equation and the coefficients of determination are summarized in Table 4.

Finally, to assess the relationship between SGLT2 inhibition and glucose excretion *in vivo*, it was intended to estimate the transport rates at the threshold of glucosuria (Vx_b) by assigning the actual plasma glucose concentration at x_b as the substrate concentration, and

by assigning V_{max} and K_m values of cSGLT2, K_i values of each SGLT2 inhibitor and the estimated free SGLT inhibitor to the Michaelis-Menten equation with competitive inhibition as shown in formula (3). The actual plasma glucose levels (mean ± SD) at x_b for each treatment were as follows: vehicle, 14.01 ± 4.79 mM (n = 3) ; tofogliflozin (13.3 ng/mL), 5.80 ± 0.65mM (n = 3); tofogliflozin (133 ng/mL), 6.75 ± 3.28 mM (n = 3); phlorizin (133 ng/mL), 11.85 ± 0.57 mM (n = 2); phlorizin (1333 ng/mL), 7.92 ± 2.91 mM (n = 2); and phlorizin (13 333 ng/mL), 3.08 ± 0.68 mM (n = 3).The estimated Vx_b value of the vehicle treatment group was similar to the V_{max} value of cSGLT2 for AMG uptake in COS-7 cells (0.86 ± 0.02 nmol/h). The Vx_b values of the tofogliflozin and phlorizin treatment groups decreased in a dose-dependent manner (Figure 10).

Discussion

In this chapter, to understand the contributions of SGLT1/2 to renal glucose handling in cynomolgus monkeys, first, it was intended to examine the inhibition kinetics and activity of tofogliflozin, a SGLT2-specific inhibitor, and phlorizin, a SGLT1/2 non-specific inhibitor, against cynomolgus monkey SGLT1/2 *in vitro*. This chapter then clarified the *in vivo* effects of tofogliflozin and phlorizin on TmG, threshold, and splay, the main parameters of renal glucose reabsorption.

First of all, it was performed to clone cSGLT1/2 cDNAs and investigate the inhibitory effects of tofogliflozin and phlorizin in cells overexpressing cSGLT1/2. As expected, tofogliflozin and phlorizin competitively inhibited the uptake of substrates by cSGLT2, which is consistent with results found for human, mouse, and rat SGLT2 (Suzuki *et al.* 2012). The IC_{50} of tofogliflozin against cSGLT2 was similar to that against human SGLT2 and lower than against both mouse and rat SGLT2s. These differences in inhibitory activity among species may reflect the higher similarity of the cynomolgus monkey SGLT1/2 amino acid sequence to human SGLT1/2 than to rodent SGLT1/2 (Table 1).

Although it had been generally believed that SGLT2 mediated 90% of RGR in humans (Chao & Henry 2010; Wright *et al.* 2011), recent clinical studies with SGLT2 inhibitors have shown only about 30%–50% inhibition of RGR, provoking debate on the mechanisms underlying this discrepancy (Hummel *et al.* 2011; Liu *et al.* 2012; Vallon 2011). In this glucose titration study using cynomolgus monkeys, both tofogliflozin and phlorizin increased the maximum percentage inhibition of RGR up to about 50%, suggesting that the maximum inhibitory effects of these SGLT inhibitors on RGR in cynomolgus monkey are nearly the same as those in rats (Chapter II). A recent human glucose titration study with the selective SGLT2 inhibitor dapagliflozin also showed about 50%–70% inhibition of RGR (Defronzo *et al.* 2013). The results of this chapter

suggest that the contribution of SGLT2 to RGR in cynomolgus monkeys is comparable to that in other species, including rats and humans.

This chapter has newly introduced a detailed fitting method for the titration curve to evaluate the threshold and splay with the equation for glucose reabsorption (formula (1)) that Martin (Martin L. 1961) proposed. To my knowledge, this is the first report of a splay analysis based on Martin's equation using this glucose titration technique.

In previous reports using non-linear regression as the method for determining threshold (Liang *et al.* 2012; Polidori *et al.* 2013; Sha *et al.* 2011), the fitted GluER line lacks the splay curve, implying that the threshold value estimated in those studies may vary from the actual threshold, which would also affect the accuracy of the estimated splay value. To avoid this variability in the estimation, the experimentally determined TmG and threshold values was used to estimate coefficient *k*. In this way, this approach could successfully express the splay curve using three parameters, TmG, threshold, and *k*, with a good coefficient of determination. As a result, it was able to estimate the area of splay, and the splay was expressed by a simple equation using the three parameters mentioned above.

It is notable that the decreased threshold levels and extended splay were quite similar between the tofogliflozin and phlorizin treatments. Based on the actual plasma concentrations of tofogliflozin (Figure 4A) and its protein-binding properties (Suzuki *et al.* 2012), it seemed reasonable to estimate the unbound tofogliflozin concentrations to be 10 nM at 13.3 ng/mL (actual mean concentration, 18 ng/mL) and 113 nM at 133 ng/mL (actual mean concentration, 189 ng/mL). Considering the IC_{50} values of tofogliflozin against cSGLT1 and cSGLT2 (cSGLT1, 8875 nM; cSGLT2, 8.9 nM) calculated from its inhibitory activity on the uptake of AMG (Table 2), the unbound concentrations of tofogliflozin mentioned above are relevant concentrations for inhibiting 50% and 100% of cSGLT2 activity, but scarcely affect cSGLT1 activity.

Similarly, based on the actual plasma concentrations of phlorizin (Figure 4B) and its protein-binding properties (Yamaguchi *et al.* 2011), it seemed reasonable to estimate the unbound phlorizin concentrations to be 698 nM at 1333 ng/mL (actual mean concentration, 924 ng/mL) and 4314 nM at 13 333 ng/mL (actual mean concentration, 5706 ng/mL). Considering the IC_{50} values of phlorizin against cSGLT1/2 in the AMG uptake assay (cSGLT1, 309 nM; cSGLT2, 35.8 nM; Table 2), the unbound phlorizin concentrations mentioned above are also relevant concentrations for inhibiting cSGLT2 completely at 1333 ng/mL (actual mean concentration, 924 ng/mL), and both cSGLT1 and cSGLT2 completely at 13 333 ng/mL (actual mean concentration, 5706 ng/mL).

Phlorizin 13 333 ng/mL treatment may inhibit both cSGLT1 and cSGLT2 completely, and tofogliflozin 133 ng/mL may inhibit only cSGLT2 completely. Therefore, any difference between these two treatments would highlight the contributions of cSGLT1 in glucose handling in cynomolgus monkeys. However, no remarkable differences were observed between the two treatments in terms of the maximum RGR inhibition (Figure 6C), TmG, threshold, or splay (Figure 8A, B, and C). Therefore, it is suggested that inhibiting SGLT2 with SGLT inhibitors in this chapter contributes to RGR inhibition mainly under hyperglycemic conditions by decreasing threshold and extending splay.

In contrast to the percentage inhibition of RGR with tofogliflozin 133 ng/mL treatment, greater percentage inhibition of RGR (ca. 30%) was evident with phlorizin 13 333 ng/mL treatment under the hypoglycemic conditions before the start of glucose loading (Figure 6A and B). This may suggest the greater contribution of cSGLT1 in renal glucose handling under hypoglycemic conditions as has been shown in rats (Chapter II). Further studies are required to understand the actual balance between cSGLT1 and cSGLT2 in their contributions to renal glucose handling in cynomolgus monkeys.

This chapter showed that both tofogliflozin and phlorizin inhibit renal glucose reabsorption in cynomolgus monkeys by extending splay and reducing threshold without any significant change in TmG. In particular, as the plasma glucose levels of cynomolgus

monkey were around 0.5 mg/mL after overnight fasting, it was able to detect the threshold value very precisely. In addition, the glucose titration curve (Figure 9C, D, E, and F) shows that the difference between the actual GluER with both tofogliflozin and phlorizin treatment (solid line) and the theoretical GluER (=glucose filtration rate - TmG) was gradually decreased as GluFR increased, implying that both tofogliflozin and phlorizin inhibit renal glucose reabsorption in a competitive manner, which is consistent with the *in vitro* inhibition kinetics of the two compounds in this chapter and in other species (Pajor *et al.* 2008; Suzuki *et al.* 2012). In this connection, Ferrannini and Solini suggested that SGLT2 inhibitors predominantly reduce the affinity of the transporter for glucose, implying that SGLT2 inhibitors mainly expand splay rather than decrease TmG (Ferrannini & Solini 2012), which was supported by their recent findings in urinary glucose absorption and excretion in T2D patients with chronic kidney disease (Ferrannini *et al.* 2013).

Furthermore, this estimation of the transport rates at the threshold of glucosuria (Vx_b) (Figure 10) suggests a close relationship between the *in vitro* kinetic parameters of SGLT inhibitors and the three critical *in vivo* factors (TmG, threshold and splay) in renal glucose reabsorption as follows.

First, the unchanged TmG values in tofogliflozin and phlorizin treatments *in vivo* are consistent with their negligible effects on the V_{max} values of cSGLT2 in the *in vitro* AMG uptake assay. Next, in the vehicle treatment group, the nearly identical values of V_{xb} and *in vitro* V_{max} suggest that transport activity can be saturated at plasma glucose levels around the threshold. However, as the V_{max} of cSGLT2 in COS-7 cells would be influenced with its protein expression levels, the *in vitro* V_{max} values are independent of *in vivo* V_{max} values, indicating the limitations to the above-mentioned interpretation on the relationship between V_{xb} and *in vitro* V_{max}. Nevertheless, the plasma glucose level at the threshold (x_b) of vehicle treatment was around 14 mM, approximately 9-fold of K_m value

of cSGLT2 (1.63 mM), suggesting that SGLT2 was almost saturated at x_b of vehicle treatment.

In addition, dose-dependent decrease of Vx_b in both the SGLT2-inhibitor treatment groups (Figure 10) suggests that a decrease of threshold coincided with reduced transport activity by SGLT2 inhibitors. From the formula (Calado *et al.* 2011), the changes of threshold are expected to mainly contribute to the splay extension in this chapter, because the TmG is unchanged. Therefore, the reduced transport rate of substrates at the lower plasma glucose concentration created by SGLT2 inhibitors is closely related to the splay extension that occurs as the threshold of UGE decreases.

In contrast, non-competitive SGLT2 inhibitors may reduce the apparent V_{max}, which may lead to reduced TmG. Although a non-competitive SGLT2 inhibitor will not affect the K_m value, the apparent transport rate at a lower plasma glucose concentration will be reduced when the apparent V_{max} is reduced, which may decrease the threshold of UGE. As a result, it is expected from formula (2) that a reduction in both TmG and x_b will reduce splay.

In distinct contrast with the results in this chapter, DeFronzo *et al.* have recently reported that dapagliflozin exerts its glucosuric effect in T2D patients and healthy subjects by reducing both TmG and splay (Defronzo *et al.* 2013) .

At present, it is likely to assume the reasons for the discrepancy between dapagliflozin and tofogliflozin in terms of the effects on the TmG and splay are as follows. First, dapagliflozin may inhibit human SGLT2 with different kinetics from ordinary competitive inhibitors, which is suggested by the remarkably slow dissociation of dapagliflozin from human SGLT2, even with high (100 mM) glucose concentration, in contrast to the rapid dissociation of phlorizin (Hummel *et al.* 2012). Second, the titration study with dapagliflozin was conducted at plasma glucose levels of between around 5 mM (0.9 mg/mL) to 30 mM (5.4 mg/mL), whereas those of experiments in this chapter were from around 0.5 mg/mL to nearly 10 mg/mL. The relatively narrow range of plasma

glucose levels in the titration study with dapagliflozin might lead to underestimating the TmG value, especially after dapagliflozin treatment. The reduced TmG may also affect the degree of splay extension, because the TmG value itself is a critical determinant of splay area in the glucose titration curves (Figure 1).

There are several limitations in this chapter. First, although a randomized block design was used to test the efficacy of tofogliflozin and phlorizin as much as possible and to minimize the number of animals, the number of cynomolgus monkeys for each treatment was relatively small. Second, although the GluRR in treatment with both tofogliflozin (13.3 and 133 ng/mL) and phlorizin (1333 and 13 333 ng/mL) showed no clear plateau within the GluFR ranges in this chapter, the observed TmG was defined as the mean GluRR at GluFR above 90 mg/min, which may influence the accuracy of observed TmG. Nevertheless, it is evident that neither tofogliflozin nor phlorizin showed any remarkable inhibition of TmG. Third, the effect of anesthesia on the actual filtered glucose remains to be assessed, although the creatinine clearance levels were not reduced compared with values reported in the literature, suggesting that filtered glucose load in proximal tubules would be maintained normally due to the autoregulation of glomerular filtration. Finally, creatinine clearance was used to estimate GFR, which may affect the accuracy of the estimated GluFR.

In conclusion, this chapter determined the inhibitory activity of tofogliflozin and phlorizin in cells expressing cSGLT1 or cSGLT2 and suggests that the contribution of SGLT2 in RGR in cynomolgus monkeys is similar to the contribution in humans and rodents and that the competitive inhibition of SGLT2 exerts a glucosuric effect by mainly extending splay without affecting TmG. Further studies are required, before these results can be extrapolated to diabetic patients.

Figures

Figure 1. Schematic diagram of the splay area in the glucose titration curve.

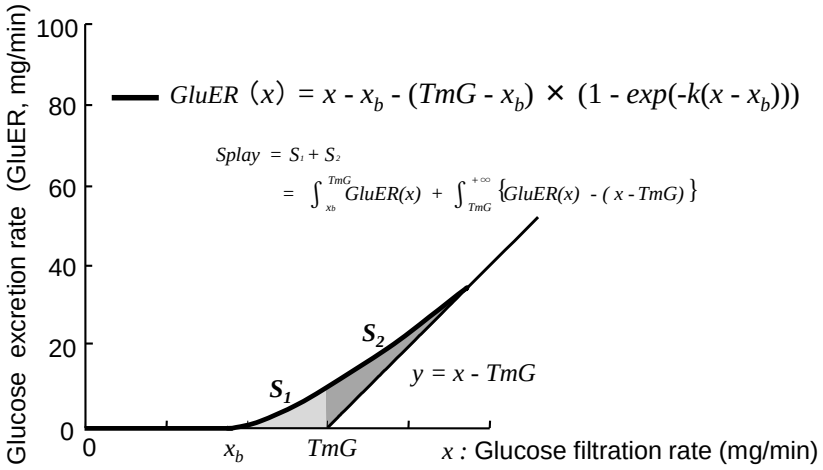

Figure 2. Functional validation in COS-7 cells expressing cSGLT1/2.

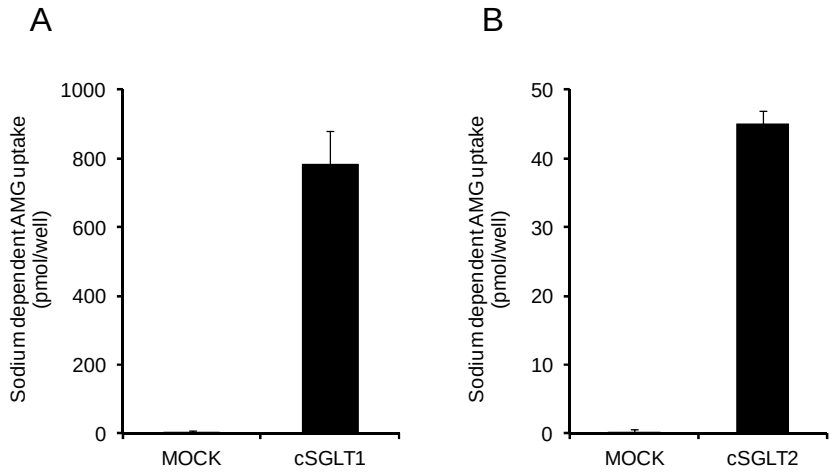

Na^+-dependent AMG uptake was compared in COS-7 cells expressing cSGLT1 (**A**) or cSGLT2 (**B**) with an empty vector (MOCK). Data are mean ± SD.

Figure 3. Lineweaver–Burk plots for inhibition of cynomolgus monkey SGLT2 by tofogliflozin and phlorizin.

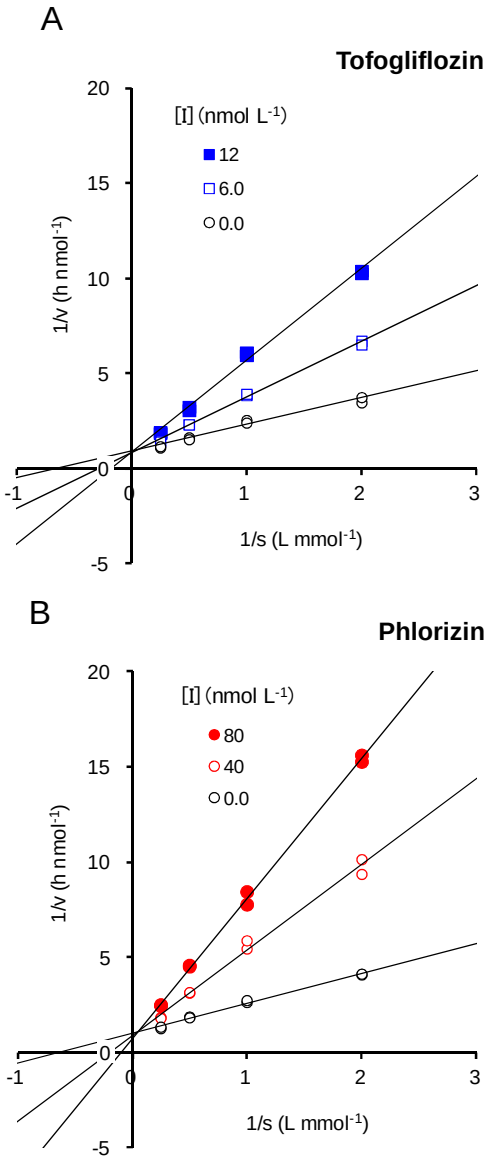

Na^+-dependent and -independent AMG uptake was measured with COS-7 cells expressing cSGLT2 in the presence or absence of tofogliflozin **(A)** or phlorizin **(B)** with various concentrations of AMG (s). Na^+-dependent AMG uptake velocity (v) was calculated and used for the Lineweaver–Burk plots against 1/s. [I] indicates

concentration of tofogliflozin or phlorizin. Experiments were performed twice, independently.

Figure 4. Actual plasma drug concentration in cynomolgus monkeys.

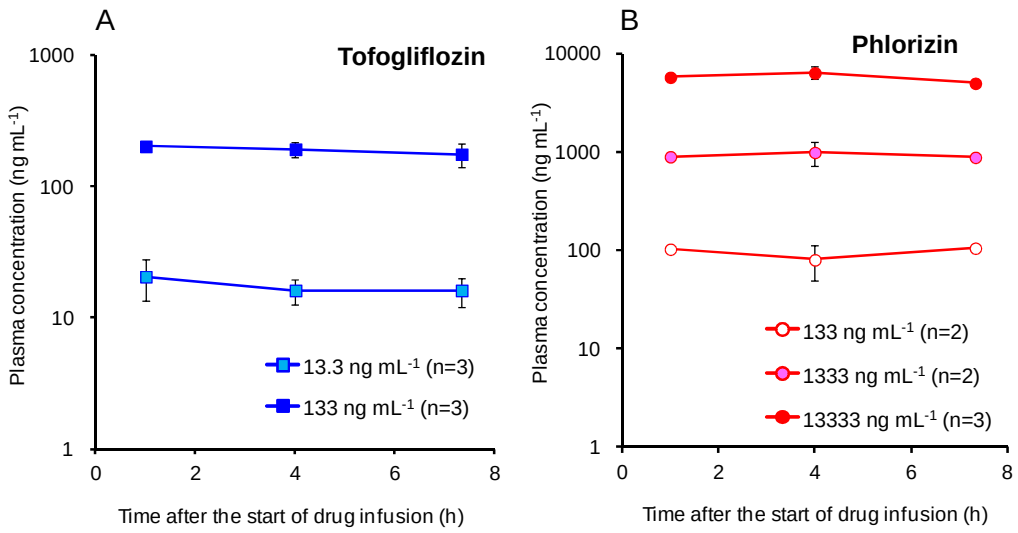

Tofogliflozin **(A)** or phlorizin **(B)** was administered by i.v. bolus followed by continuous infusion. The concentrations indicated (13.3-13 333 ng/mL) are target plasma concentrations. Data are mean ± SEM. *n* = 2-3.

Figure 5. Time course of plasma glucose, glucose excretion rate, and creatinine clearance of cynomolgus monkeys.

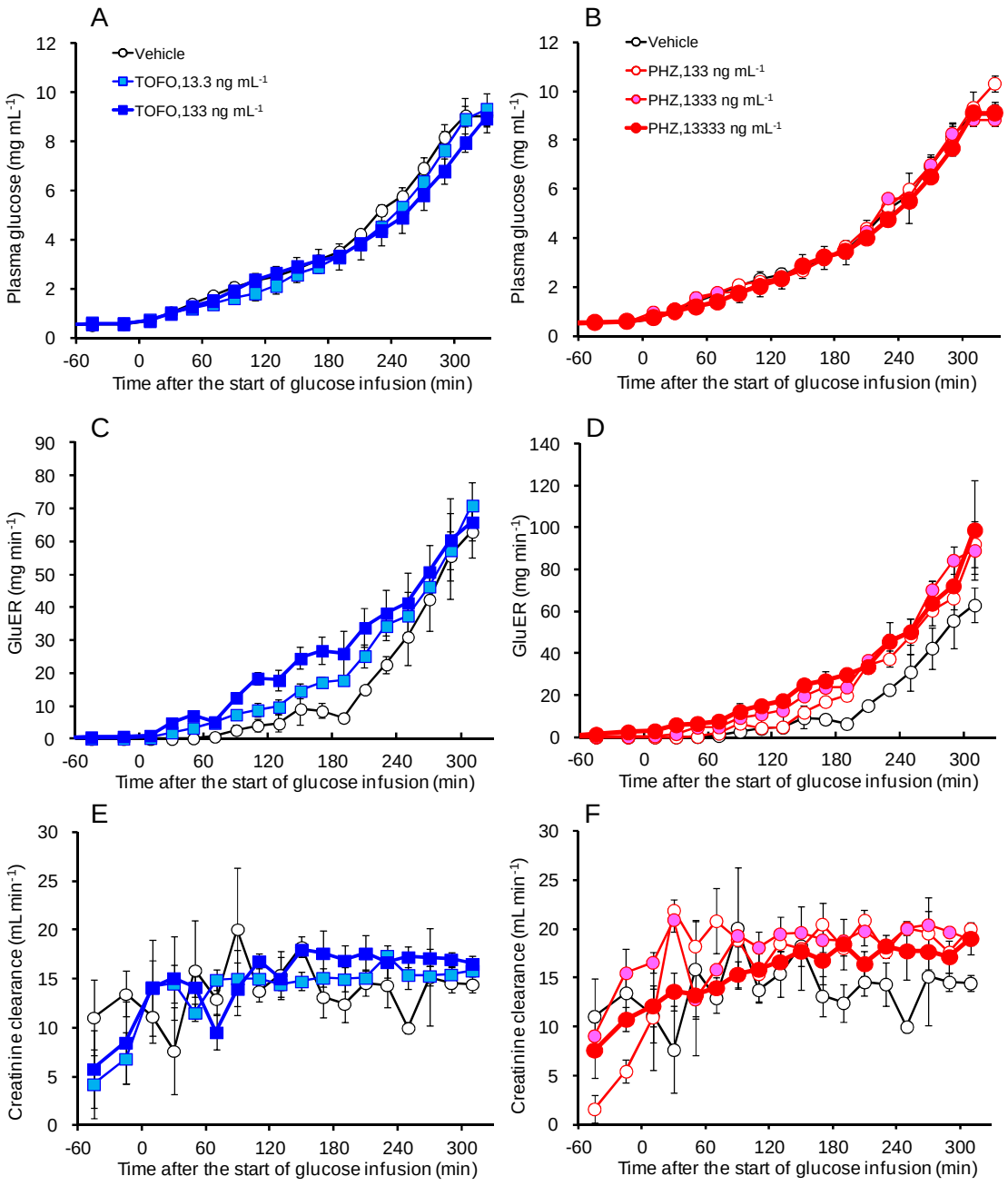

A and **B**: Time course of plasma glucose before and after glucose loading and infusion with tofogliflozin (TOFO, **A**) or phlorizin (PHZ, **B**).

C and **D**: Time course of glucose excretion rate (GluER) before and after glucose

loading and infusion with tofogliflozin (**C**) or phlorizin (**D**).

E and **F**: Time course of creatinine clearance before and after glucose loading and infusion with tofogliflozin (**E**) or phlorizin (**F**).

After 120 min of tofogliflozin or phlorizin infusion, infusion (5 $mL \cdot kg^{-1} \cdot h^{-1}$) of glucose solution (10%) was started (time 0) and increased in a stepwise manner (20%, 30%, 40%, and 50%) at 60-min intervals followed by 60-min infusion of 50% glucose at 10 $mL\ kg^{-1}\ h^{-1}$ with the constant infusion of tofogliflozin or phlorizin. The concentrations indicated (13.3-13 333 ng/mL) are target plasma concentrations. Data are mean ± SEM. n = 2-3.

Figure 6. Effects of tofogliflozin or phlorizin on the percentage inhibition of renal glucose reabsorption in cynomolgus monkeys.

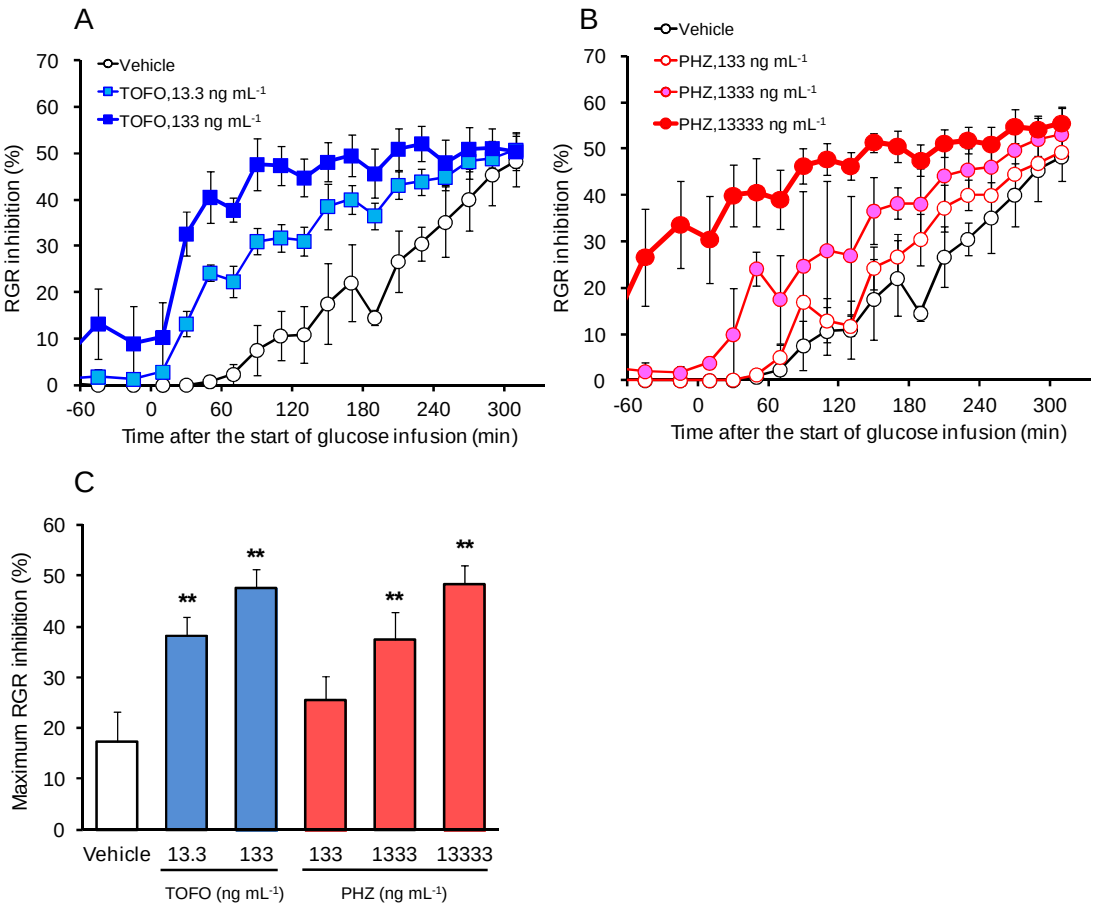

A and **B**: Time course of the percentage inhibition of renal glucose reabsorption (RGR) before and after glucose loading and infusion with tofogliflozin (TOFO, **A**) or phlorizin (PHZ, **B**). After 120 min of tofogliflozin or phlorizin infusion, infusion (5 $mL \cdot kg^{-1} \cdot h^{-1}$) of glucose solution (10%) was started (time 0) and increased in a stepwise manner (20%, 30%, 40%, and 50%) at 60-min intervals followed by 60-min infusion of 50% glucose at 10 $mL \cdot kg^{-1} \cdot h^{-1}$ with the constant infusion of tofogliflozin or phlorizin.

C: Maximum percentage inhibition of RGR under hyperglycemic condition (plasma glucose level; 2.5–3.5 mg/mL) of cynomolgus monkeys infused with tofogliflozin (TOFO) or phlorizin (PHZ).

The concentrations indicated (13.3-13 333 ng/mL) are target plasma concentrations. Data are mean ± SEM. n = 2-3. **P < 0.01 versus vehicle treatment by Tukey's HSD test.

Figure 7.

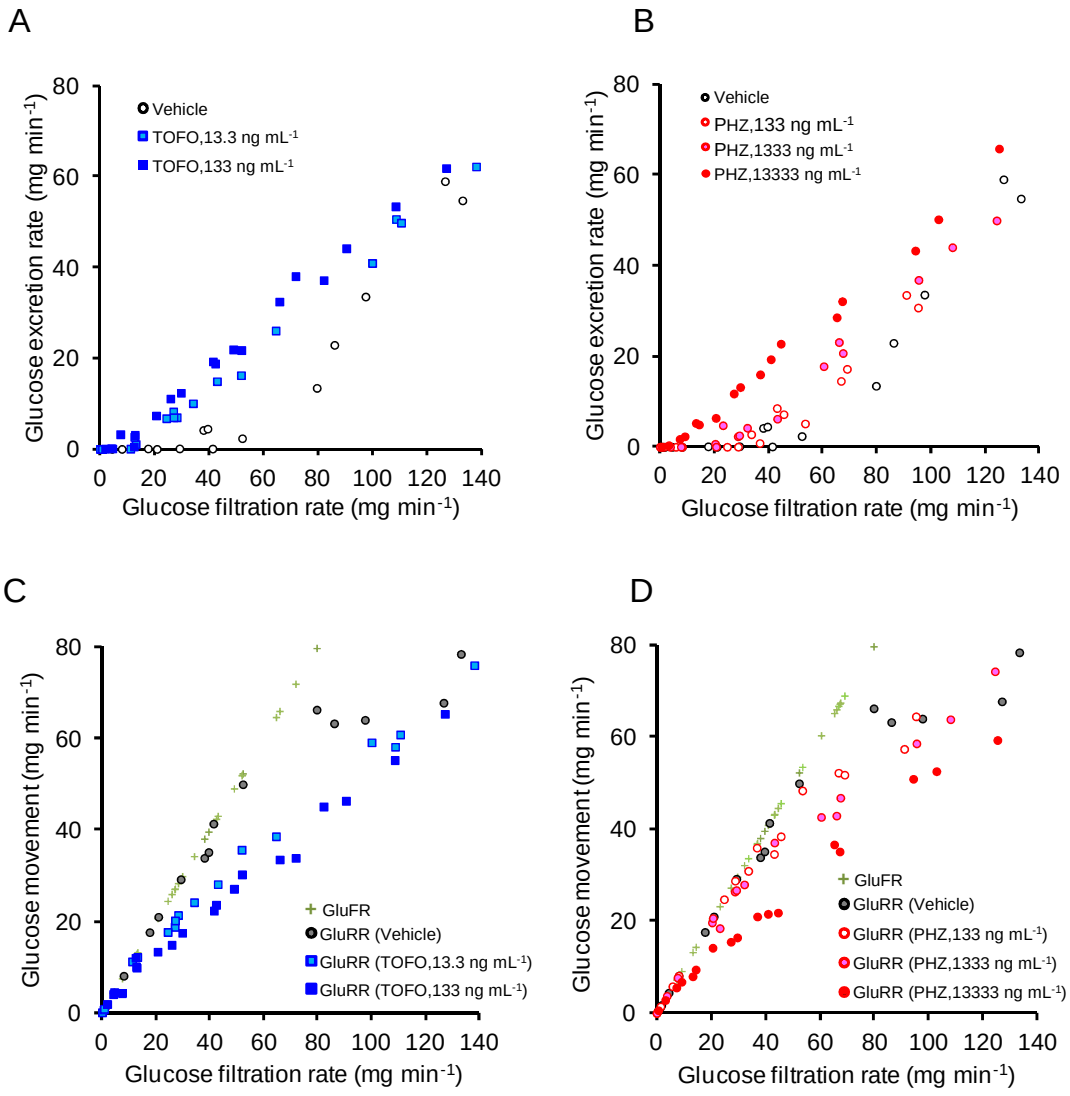

Glucose filtration rate (GluFR) plotted against glucose excretion rate. (GluER; **A, B**), or against GluFR and glucose reabsorption rate (GluRR; **C, D**) in cynomolgus monkey #2 treated with vehicle, tofogliflozin (TOFO), or phlorizin (PHZ).

Vehicle and tofogliflozin **(A, C)** or phlorizin **(B, D)** infusion. Symbols represent individual values.

Figure 8. Effects of SGLT2 inhibitors on observed TmG, threshold, and splay values in cynomolgus monkeys.

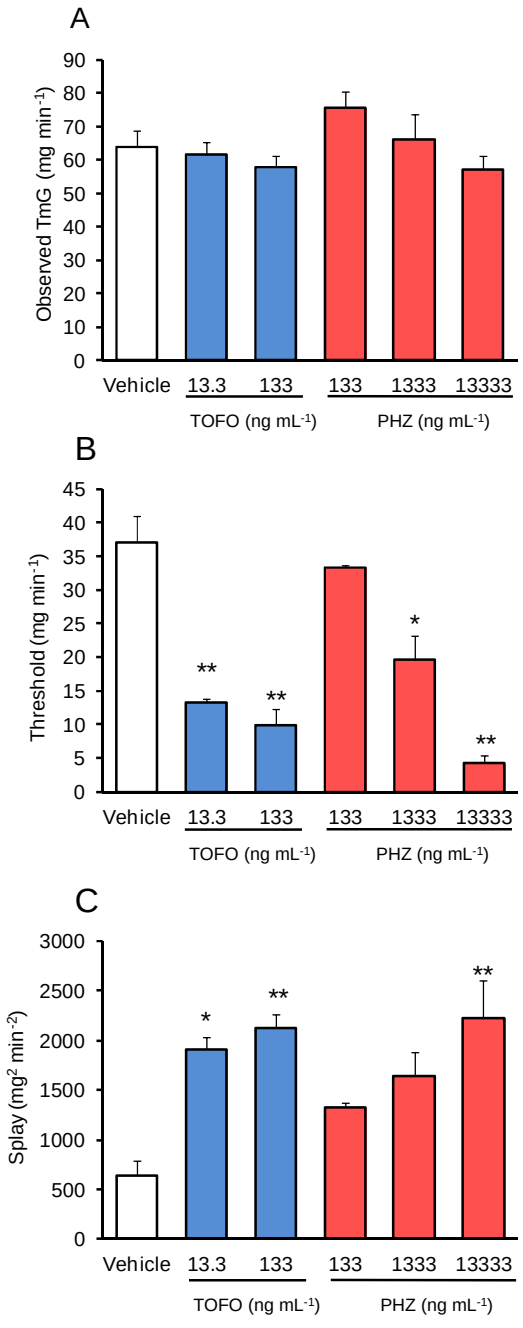

Observed TmG (**A**), threshold (**B**), and splay (**C**) of cynomolgus monkeys infused with vehicle, tofogliflozin (TOFO), or phlorizin (PHZ). The concentrations indicated

(13.3-13 333 ng/mL) are target plasma concentrations. Observed TmG was calculated by averaging the glucose filtration rates under hyperglycemic conditions (GluFR > 90 mg/min). Threshold was defined as the GluFR at which the measured percentage inhibition of RGR exceeded 5% for the first time in each experiment. Splay values were determined from formula (2). Data are mean ± SEM. n = 2-3. *P < 0.05, **P < 0.01 versus vehicle treatment by Tukey's HSD test.

Figure 9. Glucose titration curve analysis in cynomolgus monkeys.

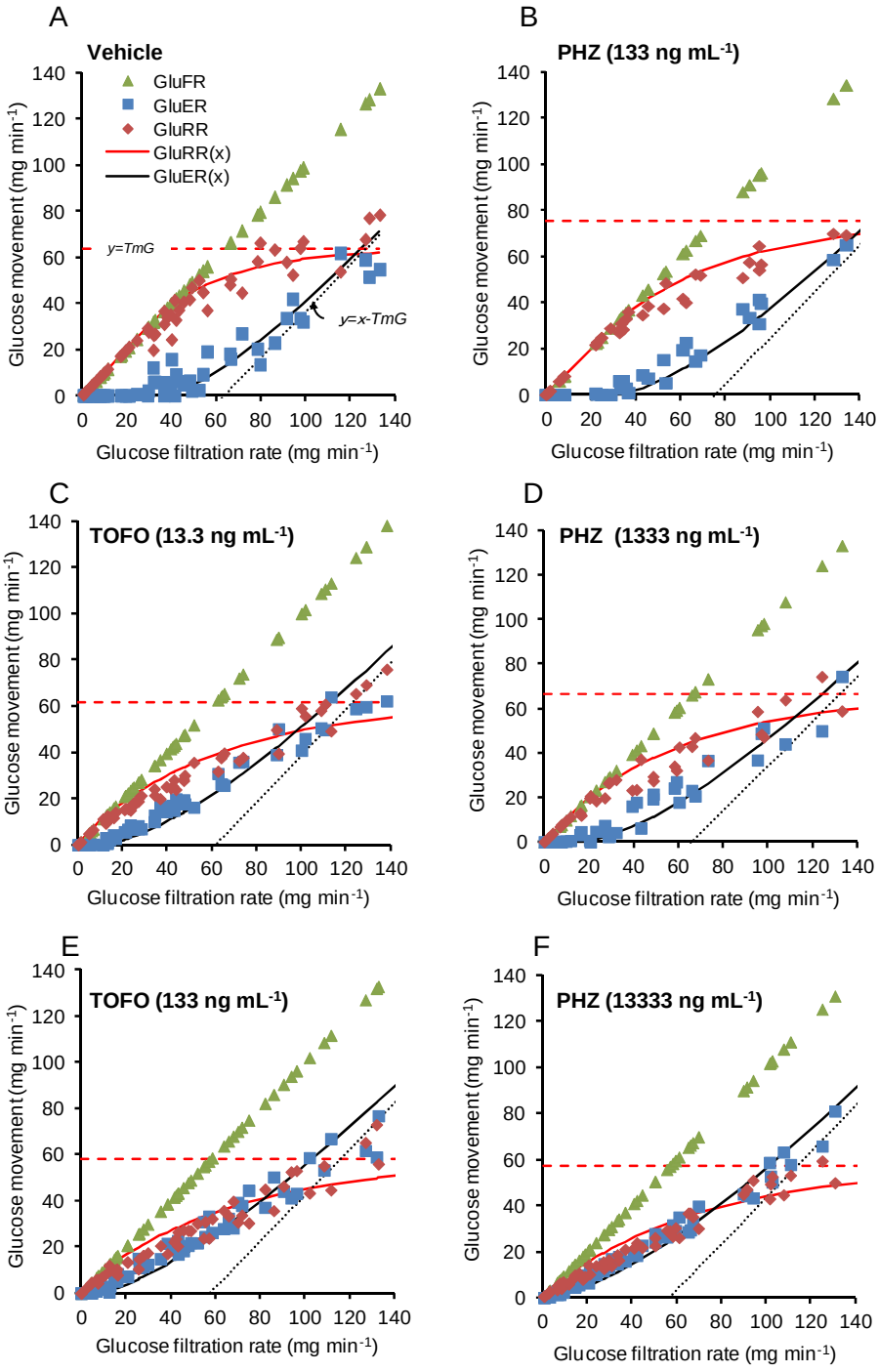

Glucose titration curves of cynomolgus monkeys infused with vehicle (**A**), phlorizin (PHZ; **B, D,** and **F**), or tofogliflozin (TOFO; **C** and **E**). The concentrations indicated

(13.3-13 333 ng/mL) are target plasma concentrations. The fitted curves for glucose excretion rate (GluER) and glucose reabsorption rate (GluRR) were determined using the pooled glucose filtration rates (GluFR) and mean threshold and observed TmG value for each treatment. Symbols represent pooled individual values of GluFR, GluER, and GluRR at each GluFR.

Figure 10. The estimated glucose transport rates in cynomolgus monkeys in the absence or presence of SGLT2 inhibitors.

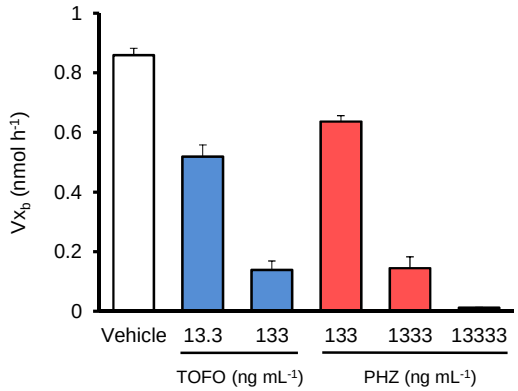

V values (Vx_b) of cynomolgus monkeys infused with vehicle, tofogliflozin (TOFO) or phlorizin (PHZ) were estimated using *in vitro* kinetic parameters of cSGLT2. The concentrations indicated (13.3-13 333 ng/mL) are target plasma concentrations. Data are mean ± SEM. n = 2-3.

Tables

Table 1 Nucleotide sequence homology of cynomolgus monkey SGLT1 and SGLT2 against other species.

Species	SGLT1		SGLT2	
	RefSeq	Homology (%)	RefSeq	Homology (%)
M. fascicularis				
vs. Homo sapiens	NM_000343	96.9	NM_003041	96.9
vs. Macaca mulatta	XM_001112212	99.9	XM_001113206	99.8
vs. Rattus norvegicus	NM_013033	85.6	NM_022590	85.1
vs. Mus musculus	NM_01981	86.1	NM_133254	84.7

The percentages of homology of SGLT1/2 among species were calculated from the nucleotide global homology program in Genetyx ver. 10.0.3 (Genetyx Corporation)

Table 2 IC_{50} values of phlorizin and tofogliflozin against cynomolgus monkey SGLT1/2

	IC_{50} (nM)		IC_{50} ratio
	cSGLT1	cSGLT2	(cSGLT1/cSGLT2)
Phlorizin	309 ± 81	35.8 ± 4.9	8.6
Tofogliflozin	8875 ± 390	8.9 ± 0.5	997

Data are expressed as mean ± SD from 2 independent experiments

Table 3 Individual data of body weight, treatment, TmG, and creatinine clearance for each cynomolgus monkey

		Cyno Monkey ID	Number of Experiment 1	2	3	4	5	6
Body weight (kg)		#1	4.78	4.78	5.00	5.03	5.00	5.20
		#2	4.45	4.35	4.65	4.70	4.58	4.38
		#3	3.52	3.70	3.72	3.80		
Treatment		#1	TOFO 133	TOFO 13.3	PHZ 13333	PHZ 133	PHZ 1333	Vehicle
		#2	Vehicle	TOFO 133	PHZ 133	PHZ 1333	PHZ 13333	TOFO 13.3
		#3	TOFO 13.3	TOFO 133	Vehicle	PHZ 13333		
Observed TmG ($mg\ min^{-1}$)	Mean	#1	49.2	62.3	59.7	76.4	69.2	67.9
		#2	46.2	43.2	64.3	55.2	52.1	42.4
		#3	52.9	54.9	59.8	38.4		
	SEM	#1	2.4	2.5	3.1	2.9	2.6	1.2
		#2	2.6	1.6	2.2	2.2	3.1	1.7
		#3	2.2	3.0	1.8	1.1		
Creatinine clearance ($mL\ min^{-1}$)	Mean	#1	17.6	16.2	18.5	19.9	19.0	14.9
		#2	14.0	16.0	18.2	19.7	20.3	15.6
		#3	15.6	16.8	14.9	14.3		
	SEM	#1	0.3	0.4	0.3	0.4	0.2	0.4
		#2	0.5	0.1	0.2	0.2	0.4	0.2
		#3	0.2	0.2	0.2	0.2		
Number of averaged points		#1	5	6	6	7	6	5
		#2	5	9	8	6	6	6
		#3	6	6	6	9		

Table 4 Fitted *k* parameters and coefficients of determination in glucose titration curves.

Group	Target plasma concentration (ng/mL)	TmG	x_b	k	R^2
Vehicle		63.78	37.01	0.02846	0.9342
Tofogliflozin	13.3	61.64	13.32	0.01577	0.8992
	133	57.88	9.97	0.01447	0.8666
Phlorizin	133	75.55	33.23	0.01877	0.9035
	1333	66.23	19.64	0.01661	0.8793
	13 333	56.98	4.19	0.0146	0.8547

General Discussion

This research aimed to characterize the novel selective SGLT2 inhibitor, tofogliflozin, for the treatment of T2D in terms of efficacy, safety, and pharmacodynamics, and to clarify the physiological roles of SGLT1/2 in renal glucose reabsorption.

The evaluation of tofogliflozin efficacy, addressed in Chapter I, supports applications for the prevention and treatment of diabetic complications. Specifically, this chapter showed that long-term administration of tofogliflozin suppresses ACR and glomerular hypertrophy, and that these effects are comparable to those of a clinically approved ARB inhibitor. In addition, the reduction in hyperglycemia was apparently sufficient to prevent the loss of beta cells. More recently, long-term administration of the SGLT2 selective inhibitor, luseogliflozin, decreased systolic blood pressure (SBP) and had a renoprotective effect through a reduction in renal blood flow and an improvement of renal vascular resistance (Kojima *et al.* 2013). These findings imply that the systemic or local hemodynamic changes may contribute to the renoprotective effect of tofogliflozin.

The safety assessment of tofogliflozin, addressed in Chapter II, highlights the advantage of selective SGLT2 inhibitors over SGLT1/2 non-selective inhibitors. Namely, the increase in hepatic glucose production, induced by the glucosuric effect of tofogliflozin, was lower than with the non-selective SGLT1/2 inhibitor phlorizin. Importantly, the increase in UGE induced by phlorizin was not completely compensated, whereas that by tofogliflozin was fully counteracted. A recent study in T2D patients showed that acute administration of empagliflozin and dapagliflozin causes a significant increase in EGP and glucagon secretion in T2D patients (Ferrannini *et al.* 2014; Merovci *et al.* 2014), suggesting the findings presented in this chapter are not specific to rodents.

It’s also notable that the remained glucosuric effect by phlorizin under hypo- and normoglycemia clearly indicates the contribution ratio changes of SGLT1/2 into RGR in the substrate concentration dependent manner. The previous reports also implied that the SGLT1 may work more dominantly than SGLT2 under the low substrate concentration because of differences in affinity and capacity, using the whole-cell patch-clamp analysis in human embryonic kidney 293T cells (Hummel *et al.* 2011) or the glucose titration study in SGLT2 knock-out mice (Vallon *et al.* 2011). This finding reveals a new biological insight into the molecular mechanism of SGLT1/2 in renal glucose reabsorption, which contradicts the hypothesis that SGLT2 plays a major role in renal glucose reabsorption, independently of the tubular substrate concentration.

The pharmacodynamics of tofogliflozin, presented in Chapter III, demonstrated that the glycosuric effect was caused by reducing the threshold and enhancing the splay. Model analysis of the substrate/inhibitor interaction for renal glucose reabsorption indicated a competitive inhibition *in vivo* and *in vitro*. Consequently, excess substrate may reduce the glycosuric effect of tofogliflozin, but the controllability of the effect is likely high. These findings are consistent with the strong correlation established by PK/PD analysis between the glycosuric effect and pharmacokinetic parameters after a single oral dose in rats (Yamaguchi *et al.* 2013).

Future studies should compare the capacity of tofogliflozin and other antidiabetic agents to prevent DN and hypoglycemia. For instance, large clinical studies showed that thiazolidinediones (i.e., rosiglitazone and pioglitazone) suppress SBP and DBP, and inhibit ACR progression, through activation of the peroxisome proliferator-activated receptor gamma (PPAR gamma) (Lachin *et al.* 2011; Morikawa *et al.* 2011). A study on spontaneously hypertensive rats suggests that the renoprotective effect of pioglitazone is mediated by restoring normal insulin-stimulated production of vasoactive mediators (Potenza *et al.* 2006). These data suggest that SGLT2 inhibitors and PPAR gamma agonists possess different mechanisms of action.

Interestingly, a recent report showed that a 52-week treatment with the SGLT2 selective inhibitor canagliflozin reduced SBP significantly in pioglitazone- or metformin-treated T2D patients (Forst *et al.* 2014). Incretin mimetics (i.e., liraglutide and exenatide) also reduced SBP in T2D patients (Wang *et al.* 2013) and suppressed ACR in an animal model of T2D (Fujita *et al.* 2014). These studies suggest that a combination therapy with tofogliflozin and an incretin mimetic may deliver a more efficient renoprotective effect than tofogliflozin alone. However, hypoglycemia induces a significant compensatory increase in EGP in cases of complete SGLT1/2 inhibition. The risk of hyperglycemia may be higher with combination therapies including a non-selective SGLT1/2 inhibitor, rather than a selective SGLT2 inhibitor, because PPAR gamma agonists (Basu *et al.* 2008; Ravikumar *et al.* 2008) and incretins suppress hepatic glucose output or glucagon secretion (Egan *et al.* 2002). Therefore, safe and effective combination drug regimens must be identified using animal models and clinical studies.

In T2D models and human subjects, it is important to evaluate the long-term impact of tofogliflozin on the contribution of SGLT1/2 to renal glucose reabsorption (Chapter II), and the pharmacological characteristics (Chapter III), because diabetes is associated with an overexpression of SGLT2 in tubular epithelial cells (Osorio *et al.* 2010; Rahmoune *et al.* 2005; Tabatabai *et al.* 2009). Interestingly, Defronzo *et al.* (2013) reported that a 1-week treatment with dapagliflozin reduced the TmG, implying that a decrease in SGLT1/2 translocation to the apical membrane, or reduction in expression levels. The combination analysis described in Chapter III, including quantitative assessment of SGLT and a new *in vivo* glucose titration method, provides a more detailed analysis of the relationship between SGLT function and disease progression.

Certain issues remain unexplored. First, the impact of tofogliflozin on hemodynamic factors, and single-nephron analysis by micro-puncture, were not investigated due to technical difficulties. In addition, possible shifts in membrane localization of SGLT1/2

were also not assessed due to material difficulties regarding commercially available antibodies (Sabolic *et al.* 2012). The classical reports have shown the heterogeneity of the reabsorption in healthy or kidney disease patients using glomerular or tubular level (Lameire *et al.* 1977). In theory, the newly developed glucose titration analysis presented in Chapter III can be applied to the single nephron characterization. This approach with the various SGLT1/2 inhibitors, currently developed in clinical trials, is expected to reveal the clinical implications of heterogeneity, because competitive inhibition perturbs the heterogeneity in single nephron by changing the functional to non-functional SGLT1/2 ratio.

In summary, this research provides new insights into the physiological role of SGLT and the glucose regulation by the new selective SGLT2 inhibitor tofogliflozin. First, tofogliflozin improves glycemic control and reduces damage to the kidneys and pancreatic beta cells, suggesting that it prevents diabetic complications, such as DN. Second, this research reveals dynamic changes in the relative contributions of SGLT1/2 to renal glucose reabsorption and that highly selective inhibition of SGLT2 reduces the risk of hypoglycemia. Finally, competitive inhibition of SGLT2 promotes UGE by reducing the threshold for renal glucose reabsorption and by extending splay. Thus, tofogliflozin is a highly potent agent for diabetic care because of the favorable pharmacologic characteristics in terms of efficacy, safety, and pharmacodynamics.

Acknowledgments

I sincerely express deep gratitude to Dr. Masamichi Kurohmaru, Dr Yoshiakira Kanai, and Dr Naoki Tsunekawa (The University of Tokyo, Laboratory of Veterinary Anatomy) for their advice, support and guidance in this research.

In Chapter I, I also thank Mizuki Yamane and Tetsuya Mitsui (employees of Chugai Pharmaceutical Co., Ltd.) for their contribution to determination of plasma tofogliflozin concentration; Ryota Saito, Kasumi Takahashi, Taeko Hasegawa, Miho Nanba, and Naoto Toyota (employees of Chugai Research Institute for Medical Science, Inc.) for their assistance with the biochemical analysis of plasma and urine; Tatsuo Yata and Mio Kawai (employees of Chugai Research Institute for Medical Science, Inc.), Marii Yamamoto, Hiroyasu Muramatsu, Masao Matsuo, Dr. Nobuhiro Ban, Yasuhiro Ichida, Dr. Kenichi Ozaki, Dr. Fumihiko Ichikawa, and Kazuharu Ozawa (employees of Chugai Pharmaceutical Co., Ltd.) for their assistance with conducting the animal experiments and excellent technical assistance; and Dr. Naoshi Fukushima and Sachiya Ikeda (employees of Chugai Pharmaceutical Co., Ltd.) for critical discussions.

In Chapter II, I also thank Marii Yamamoto, Hiroyasu Muramatsu, Masakazu Sugiyama, and Aki Kito (employees of Chugai Pharmaceutical Co., Ltd.) and Mari Kinoshita, Ryuushi Takemoto, Takako Sakamoto, Mio Hiramatsu, Manabu Hirabayashi, and Eiji Kaneko (employees of Chugai Research Institute for Medical Science, Inc.) for their assistance with conducting the animal experiments; Ryota Saito, Taeko Hasegawa, Yukari Komiyama, Miho Nanba, Kasumi Takahashi, Kaori Sakamoto, and Naoto Toyota (employees of Chugai Research Institute for Medical Science, Inc.) for their assistance with determination of glucose and creatinine concentrations; and Masayuki Suzuki, Minako Takeda, Dr. Taku Fukuzawa, and Dr. Masaki Ishigai (employees of Chugai Pharmaceutical Co., Ltd.) for their helpful discussions.

In Chapter III, I also thank Ryota Saito, Kasumi Takahashi, Taeko Hasegawa, and Miho Nanba (employees of Chugai Research Institute for Medical Science, Inc.) for their assistance with the biochemical analysis of plasma and urine; Takashi Koike, Mayumi Hiranuma, Ryuushi Takemoto, and Toyokazu Matsuura (employees of Chugai Research Institute for Medical Science, Inc.) for their assistance with the pharmacokinetics study of phlorizin; Dr. Koji Yamaguchi, Dr. Motohiro Kato, and Tetsuya Mitsui (employees of Chugai Pharmaceutical Co., Ltd.) for their kind discussion concerning simulation of drug infusion; and Dr. Kiyofumi Honda, Dr. Yoshiyuki Suzuki, Dr. Yoshiki Kawabe, and Sachiya Ikeda (employee of Chugai Pharmaceutical Co., Ltd.) for critical discussions.

In writing and submitting the papers related to this research, I would like to thank all co-authors for their contribution. I would like to express deep gratitude to Dr. Masanori Fukazawa (employees of Chugai Pharmaceutical Co., Ltd.) for technical guidance in lab works, critical discussions, and corresponding authorship of these papers.

Finally, I sincerely thank my parents, sister, wife, and son for their support and encourage.

I would like to express my condolences for all animals used in this research.

References

Aljure, O. & Díez-Sampedro, A., 2010. Functional characterization of mouse sodium/glucose transporter type 3b. *American journal of physiology. Cell physiology*, 299(1), pp.C58–65.

American Diabetes Association, 2013. Standards of medical care in diabetes--2013. *Diabetes care*, 36 Suppl 1, pp.S11–66.

Arakawa, K. *et al.*, 2001. Improved diabetic syndrome in C57BL/KsJ-db/db mice by oral administration of the Na(+)-glucose cotransporter inhibitor T-1095. *British Journal of Pharmacology*, 132(2), pp.578–586.

Bailey, C.J. *et al.*, 2010. Effect of dapagliflozin in patients with type 2 diabetes who have inadequate glycaemic control with metformin: a randomised, double-blind, placebo-controlled trial. *Lancet*, 375(9733), pp.2223–2233.

Basu, R. *et al.*, 2008. Comparison of the Effects of Pioglitazone and Metformin on Hepatic and Extra-Hepatic Insulin Action in People With Type 2. *Diabetes*, 57(1), pp.24–31.

Bergeron, R. *et al.*, 2001. Effect of 5-aminoimidazole-4-carboxamide-1-beta-D-ribofuranoside infusion on in vivo glucose and lipid metabolism in lean and obese Zucker rats. *Diabetes*, 50(5), pp.1076–1082.

Bishop, J.H. *et al.*, 1978. Effects of phlorizin on glucose, water and sodium handling by the rat kidney. *The Journal of physiology*, 275, pp.467–480.

Breyer, M.D. *et al.*, 2005. Mouse models of diabetic nephropathy. *Journal of the American Society of Nephrology: JASN*, 16(1), pp.27–45.

Brodehl, J., Oemar, B.S. & Hoyer, P.F., 1987. Renal glucosuria. *Pediatric nephrology (Berlin, Germany)*, 1(3), pp.502–508.

Calado, J., Santer, R. & Rueff, J., 2011. Effect of kidney disease on glucose handling (including genetic defects). *Kidney international. Supplement*, (120), pp.S7–13.

Chao, E.C. & Henry, R.R., 2010. SGLT2 inhibition--a novel strategy for diabetes treatment. *Nature reviews. Drug discovery*, 9(7), pp.551–559.

2096 Chasis, H., Jolliffe, N. & Smith, H.W., 1933. The action of phlorizin on the excretion of
2097 glucose, xylose, sucrose, creatinine and urea by man. *The Journal of clinical*
2098 *investigation*, 12(6), pp.1083–1090.

2099 Chen, H. *et al.*, 2010. Cevoglitazar, a novel peroxisome proliferator-activated
2100 receptor-alpha/gamma dual agonist, potently reduces food intake and body
2101 weight in obese mice and cynomolgus monkeys. *Endocrinology*, 151(7),
2102 pp.3115–3124.

2103 Chen, J. *et al.*, 2010. Quantitative PCR tissue expression profiling of the human SGLT2
2104 gene and related family members. *Diabetes therapy: research, treatment and*
2105 *education of diabetes and related disorders*, 1(2), pp.57–92.

2106 Cooper, M.E., 2001. Interaction of metabolic and haemodynamic factors in mediating
2107 experimental diabetic nephropathy. *Diabetologia*, 44(11), pp.1957–1972.

2108 Defronzo, R.A. *et al.*, 2013. Characterization of Renal Glucose Reabsorption in Response
2109 to Dapagliflozin in Healthy Subjects and Subjects With Type 2 Diabetes.
2110 *Diabetes care*, 36(10), pp.3169–76.

2111 DeFronzo, R.A., Davidson, J.A. & Del Prato, S., 2012. The role of the kidneys in glucose
2112 homeostasis: a new path towards normalizing glycaemia. *Diabetes, obesity &*
2113 *metabolism*, 14(1), pp.5–14.

2114 Devenny, J.J. *et al.*, 2012. Weight loss induced by chronic dapagliflozin treatment is
2115 attenuated by compensatory hyperphagia in diet-induced obese (DIO) rats.
2116 *Obesity (Silver Spring, Md.)*, 20(8), pp.1645–1652.

2117 Dong, Y.-F. *et al.*, 2010. Aliskiren enhances protective effects of valsartan against type 2
2118 diabetic nephropathy in mice. *Journal of hypertension*, 28(7), pp.1554–1565.

2119 Dronavalli, S., Duka, I. & Bakris, G.L., 2008. The pathogenesis of diabetic nephropathy.
2120 *Nature clinical practice. Endocrinology & metabolism*, 4(8), pp.444–452.

2121 Dunn, S.R. *et al.*, 2004. Utility of endogenous creatinine clearance as a measure of renal
2122 function in mice. *Kidney international*, 65(5), pp.1959–1967.

2123 Egan, J.M. *et al.*, 2002. Glucagon-like peptide-1 augments insulin-mediated glucose
2124 uptake in the obese state. *The Journal of Clinical Endocrinology and*
2125 *Metabolism*, 87(8), pp.3768–3773.

2126 Ehrenkranz, J.R.L. *et al.*, 2005. Phlorizin: a review. *Diabetes/Metabolism Research and*
2127 *Reviews*, 21(1), pp.31–38.

2128 Ferrannini, E. *et al.*, 2014. Metabolic response to sodium-glucose cotransporter 2
2129 inhibition in type 2 diabetic patients. *Journal of Clinical Investigation*, 124(2),
2130 pp.499–508.

2131 Ferrannini, E. *et al.*, 2013. Renal glucose handling: impact of chronic kidney disease
2132 and sodium-glucose cotransporter 2 inhibition in patients with type 2 diabetes.
2133 *Diabetes care*, 36(5), pp.1260–1265.

2134 Ferrannini, E. & Solini, A., 2012. SGLT2 inhibition in diabetes mellitus: rationale and
2135 clinical prospects. *Nature reviews. Endocrinology*, 8(8), pp.495–502.

2136 Flores-Le Roux, J.A. *et al.*, 2011. Seven-year mortality in heart failure patients with
2137 undiagnosed diabetes: an observational study. *Cardiovascular Diabetology*, 10,
2138 p.39.

2139 Fonseca, V.A. *et al.*, 2013. Active- and placebo-controlled dose-finding study to assess
2140 the efficacy, safety, and tolerability of multiple doses of ipragliflozin in patients
2141 with type 2 diabetes mellitus. *Journal of diabetes and its complications*, 27(3),
2142 pp.268–273.

2143 Forbes, J.M., Fukami, K. & Cooper, M.E., 2007. Diabetic nephropathy: where
2144 hemodynamics meets metabolism. *Experimental and clinical endocrinology &*
2145 *diabetes: official journal, German Society of Endocrinology [and] German*
2146 *Diabetes Association*, 115(2), pp.69–84.

2147 Forst, T. *et al.*, 2014. Efficacy and safety of canagliflozin over 52 weeks in patients with
2148 type 2 diabetes on background metformin and pioglitazone. *Diabetes, obesity &*
2149 *metabolism*, 16(5), pp.467–477.

2150 Fujimori, Y. *et al.*, 2008. Remogliflozin etabonate, in a novel category of selective
2151 low-affinity sodium glucose cotransporter (SGLT2) inhibitors, exhibits
2152 antidiabetic efficacy in rodent models. *The Journal of pharmacology and*
2153 *experimental therapeutics*, 327(1), pp.268–276.

2154 Fujita, H. *et al.*, 2014. The protective roles of GLP-1R signaling in diabetic nephropathy:
2155 possible mechanism and therapeutic potential. *Kidney international*, 85(3),

pp.579–589.

Furler, S.M., Zelenka, G.S. & Kraegen, E.W., 1986. Development and testing of a simple algorithm for a glucose clamp. *Medical & biological engineering & computing*, 24(4), pp.365–370.

Gärtner, K., 1978. Glomerular hyperfiltration during the onset of diabetes mellitus in two strains of diabetic mice (c57bl/6j db/db and c57bl/ksj db/db). *Diabetologia*, 15(1), pp.59–63.

Gibbs, E.M. *et al.*, 1995. Glycemic improvement in diabetic db/db mice by overexpression of the human insulin-regulatable glucose transporter (GLUT4). *The Journal of clinical investigation*, 95(4), pp.1512–1518.

Guo, C. *et al.*, 2006. Mineralocorticoid receptor antagonist reduces renal injury in rodent models of types 1 and 2 diabetes mellitus. *Endocrinology*, 147(11), pp.5363–5373.

Han, S. *et al.*, 2008. Dapagliflozin, a selective SGLT2 inhibitor, improves glucose homeostasis in normal and diabetic rats. *Diabetes*, 57(6), pp.1723–1729.

Hummel, C.S. *et al.*, 2011. Glucose transport by human renal Na+/D-glucose cotransporters SGLT1 and SGLT2. *American journal of physiology. Cell physiology*, 300(1), pp.C14–21.

Hummel, C.S. *et al.*, 2012. Structural selectivity of human SGLT inhibitors. *American journal of physiology. Cell physiology*, 302(2), pp.C373–382.

International Diabetes Federation, 2013. *IDF Diabetes Atlas, 6th edn*, Brussels, Belgium: International Diabetes Federation.

Jurczak, M.J. *et al.*, 2011. SGLT2 deletion improves glucose homeostasis and preserves pancreatic beta-cell function. *Diabetes*, 60(3), pp.890–898.

Kadowaki, T. *et al.*, 2012. Tofogliflozin, a Novel and Selective SGLT2 Inhibitor Improves Glycemic Control and Lowers Body Weight in Patients with Type 2 Diabetes Mellitus Inadequately Controlled on Stable Metformin or Diet and Exercise Alone. *Diabetes*, 61 Suppl. (1), p.A22 (80–OR).

Kahn, S.E., 2003. The relative contributions of insulin resistance and beta-cell

2185 dysfunction to the pathophysiology of Type 2 diabetes. *Diabetologia*, 46(1),
2186 pp.3–19.

2187 Kanai, Y. *et al.*, 1994. The human kidney low affinity Na+/glucose cotransporter SGLT2.
2188 Delineation of the major renal reabsorptive mechanism for D-glucose. *The*
2189 *Journal of clinical investigation*, 93(1), pp.397–404.

2190 Kasichayanula, S. *et al.*, 2011. Pharmacokinetics and pharmacodynamics of
2191 dapagliflozin, a novel selective inhibitor of sodium-glucose co-transporter type 2,
2192 in Japanese subjects without and with type 2 diabetes mellitus. *Diabetes,*
2193 *obesity & metabolism*, 13(4), pp.357–365.

2194 Katsuno, K. *et al.*, 2009. Long-term treatment with sergliflozin etabonate improves
2195 disturbed glucose metabolism in KK-A(y) mice. *European journal of*
2196 *pharmacology*, 618(1-3), pp.98–104.

2197 Katsuno, K. *et al.*, 2007. Sergliflozin, a novel selective inhibitor of low-affinity sodium
2198 glucose cotransporter (SGLT2), validates the critical role of SGLT2 in renal
2199 glucose reabsorption and modulates plasma glucose level. *The Journal of*
2200 *pharmacology and experimental therapeutics*, 320(1), pp.323–330.

2201 Kharitonenkov, A. *et al.*, 2007. The metabolic state of diabetic monkeys is regulated by
2202 fibroblast growth factor-21. *Endocrinology*, 148(2), pp.774–781.

2203 Kojima, N. *et al.*, 2013. Effects of a New SGLT2 Inhibitor, Luseogliflozin, on Diabetic
2204 Nephropathy in T2DN Rats. *Journal of Pharmacology and Experimental*
2205 *Therapeutics*, 345(3), pp.464–472.

2206 Komoroski, B., Vachharajani, N., Feng, Y., *et al.*, 2009. Dapagliflozin, a novel, selective
2207 SGLT2 inhibitor, improved glycemic control over 2 weeks in patients with type 2
2208 diabetes mellitus. *Clinical pharmacology and therapeutics*, 85(5), pp.513–519.

2209 Komoroski, B., Vachharajani, N., Boulton, D., *et al.*, 2009. Dapagliflozin, a novel SGLT2
2210 inhibitor, induces dose-dependent glucosuria in healthy subjects. *Clinical*
2211 *pharmacology and therapeutics*, 85(5), pp.520–526.

2212 Kothinti, R.K. *et al.*, 2012. A novel SGLT is expressed in the human kidney. *European*
2213 *journal of pharmacology*, 690(1-3), pp.77–83.

2214 Lachin, J.M. *et al.*, 2011. Renal function in type 2 diabetes with rosiglitazone,

metformin, and glyburide monotherapy. *Clinical journal of the American Society of Nephrology: CJASN*, 6(5), pp.1032–1040.

Lameire, N.H., Lifschitz, M.D. & Stein, J.H., 1977. Heterogeneity of nephron function. *Annual review of physiology*, 39, pp.159–184.

Lenhard, J.M. *et al.*, 1999. The RXR agonist LG100268 causes hepatomegaly, improves glycaemic control and decreases cardiovascular risk and cachexia in diabetic mice suffering from pancreatic beta-cell dysfunction. *Diabetologia*, 42(5), pp.545–554.

Liang, Y. *et al.*, 2012. Effect of canagliflozin on renal threshold for glucose, glycemia, and body weight in normal and diabetic animal models. *PloS ONE*, 7(2), p.e30555.

Liu, J.J., Lee, T. & DeFronzo, R.A., 2012. Why Do SGLT2 inhibitors inhibit only 30-50% of renal glucose reabsorption in humans? *Diabetes*, 61(9), pp.2199–2204.

Lotspeich, W.D. & Woronkow, S., 1958. Some quantitative studies on phlorizin inhibition of glucose transport in the kidney. *The American journal of physiology*, 195(2), pp.331–336.

Marchetti, P. *et al.*, 2009. Goals of treatment for type 2 diabetes: beta-cell preservation for glycemic control. *Diabetes care*, 32 Suppl 2, pp.S178–183.

Martin L., 1961. Stochastic Processes in Physiology. *Proceedings of the Berkeley Symposium on Mathematical Statistics and Probability*, 4, pp.307–320.

McPhaul, J.J. & Simonaitis, J.J., 1968. Observations on the mechanisms of glucosuria during glucose loads in normal and nondiabetic subjects. *Journal of Clinical Investigation*, 47(4), pp.702–711.

Merovci, A. *et al.*, 2014. Dapagliflozin improves muscle insulin sensitivity but enhances endogenous glucose production. *The Journal of clinical investigation*, 124(2), pp.509–514.

Morikawa, A. *et al.*, 2011. Pioglitazone reduces urinary albumin excretion in renin-angiotensin system inhibitor-treated type 2 diabetic patients with hypertension and microalbuminuria: the APRIME study. *Clinical and experimental nephrology*, 15(6), pp.848–853.

2245 Moriyama, T. *et al.*, 2004. Nilvadipine attenuates mesangial expansion and glomerular
2246 hypertrophy in diabetic db/db mice, a model for type 2 diabetes. *Clinical and*
2247 *experimental nephrology*, 8(3), pp.230–236.

2248 National Kidney Foundation, 2007. KDOQI Clinical Practice Guidelines and Clinical
2249 Practice Recommendations for Diabetes and Chronic Kidney Disease. *American*
2250 *journal of kidney diseases: the official journal of the National Kidney*
2251 *Foundation*, 49(2 Suppl 2), pp.S12–154.

2252 Ohtake, Y. *et al.*, 2012. Discovery of Tofogliflozin, a Novel C-Arylglucoside with an
2253 O-Spiroketal Ring System, as a Highly Selective Sodium Glucose Cotransporter
2254 2 (SGLT2) Inhibitor for the Treatment of Type 2 Diabetes. *Journal of medicinal*
2255 *chemistry*, 55(17), pp.7828–7840.

2256 Oku, A. *et al.*, 1999. T-1095, an inhibitor of renal Na+-glucose cotransporters, may
2257 provide a novel approach to treating diabetes. *Diabetes*, 48(9), pp.1794–1800.

2258 Osorio, H. *et al.*, 2010. Effect of phlorizin on SGLT2 expression in the kidney of diabetic
2259 rats. *Journal of nephrology*, 23(5), pp.541–546.

2260 Pajor, A.M. *et al.*, 2008. Inhibitor binding in the human renal low- and high-affinity
2261 Na+/glucose cotransporters. *The Journal of pharmacology and experimental*
2262 *therapeutics*, 324(3), pp.985–991.

2263 Panchapakesan, U. *et al.*, 2013. Effects of SGLT2 Inhibition in Human Kidney Proximal
2264 Tubular Cells—Renoprotection in Diabetic Nephropathy? *PLoS ONE*, 8(2),
2265 p.e54442.

2266 Plantinga, L.C. *et al.*, 2010. Prevalence of chronic kidney disease in US adults with
2267 undiagnosed diabetes or prediabetes. *Clinical journal of the American Society of*
2268 *Nephrology: CJASN*, 5(4), pp.673–682.

2269 Polidori, D. *et al.*, 2013. Validation of a novel method for determining the renal
2270 threshold for glucose excretion in untreated and canagliflozin-treated subjects
2271 with type 2 diabetes mellitus. *The Journal of clinical endocrinology and*
2272 *metabolism*, 98(5), pp.E867–871.

2273 Poole, R.M. & Prossler, J.E., 2014. Tofogliflozin: first global approval. *Drugs*, 74(8),
2274 pp.939–944.

2275 Potenza, M.A. *et al.*, 2006. Treatment of Spontaneously Hypertensive Rats With
2276 Rosiglitazone and/or Enalapril Restores Balance Between Vasodilator and
2277 Vasoconstrictor Actions of Insulin With Simultaneous Improvement in
2278 Hypertension and Insulin Resistance. *Diabetes*, 55(12), pp.3594–3603.

2279 Qi, Z. *et al.*, 2005. Characterization of susceptibility of inbred mouse strains to diabetic
2280 nephropathy. *Diabetes*, 54(9), pp.2628–2637.

2281 Rahmoune, H. *et al.*, 2005. Glucose transporters in human renal proximal tubular cells
2282 isolated from the urine of patients with non-insulin-dependent diabetes.
2283 *Diabetes*, 54(12), pp.3427–3434.

2284 Ravikumar, B. *et al.*, 2008. Pioglitazone Decreases Fasting and Postprandial
2285 Endogenous Glucose Production in Proportion to Decrease in Hepatic
2286 Triglyceride Content. *Diabetes*, 57(9), pp.2288–2295.

2287 Rieselbach, R.E. *et al.*, 1967. Glucose Titration Studies in Patients with Chronic
2288 Progressive Renal Disease*. *Journal of Clinical Investigation*, 46(2), pp.157–163.

2289 Rossetti, L., Smith, D., *et al.*, 1987. Correction of hyperglycemia with phlorizin
2290 normalizes tissue sensitivity to insulin in diabetic rats. *The Journal of clinical*
2291 *investigation*, 79(5), pp.1510–1515.

2292 Rossetti, L., Shulman, G.I., *et al.*, 1987. Effect of chronic hyperglycemia on in vivo
2293 insulin secretion in partially pancreatectomized rats. *Journal of Clinical*
2294 *Investigation*, 80(4), pp.1037–1044.

2295 Rüster, C. & Wolf, G., 2006. Renin-angiotensin-aldosterone system and progression of
2296 renal disease. *Journal of the American Society of Nephrology: JASN*, 17(11),
2297 pp.2985–2991.

2298 Sabolic, I. *et al.*, 2012. Expression of Na+-D-glucose cotransporter SGLT2 in rodents is
2299 kidney-specific and exhibits sex and species differences. *AJP: Cell Physiology*,
2300 302(8), pp.C1174–C1188.

2301 Santer, R. *et al.*, 2003. Molecular analysis of the SGLT2 gene in patients with renal
2302 glucosuria. *Journal of the American Society of Nephrology: JASN*, 14(11),
2303 pp.2873–2882.

2304 Santer, R. & Calado, J., 2010. Familial renal glucosuria and SGLT2: from a mendelian

2305 trait to a therapeutic target. *Clinical journal of the American Society of*
2306 *Nephrology: CJASN*, 5(1), pp.133–141.

2307 Schernthaner, G. *et al.*, 2013. Canagliflozin compared with sitagliptin for patients with
2308 type 2 diabetes who do not have adequate glycemic control with metformin plus
2309 sulfonylurea: a 52-week randomized trial. *Diabetes care*, 36(9), pp.2508–2515.

2310 Senador, D. *et al.*, 2009. Cardiovascular and autonomic phenotype of db/db diabetic
2311 mice. *Experimental physiology*, 94(6), pp.648–658.

2312 Shankel, S.W., Robson, A.M. & Bricker, N.S., 1967. On the mechanism of the splay in
2313 the glucose titration curve in advanced experimental renal disease in the rat.
2314 *The Journal of clinical investigation*, 46(2), pp.164–172.

2315 Sha, S. *et al.*, 2011. Canagliflozin, a novel inhibitor of sodium glucose co-transporter 2,
2316 dose dependently reduces calculated renal threshold for glucose excretion and
2317 increases urinary glucose excretion in healthy subjects. *Diabetes, obesity &*
2318 *metabolism*, 13(7), pp.669–672.

2319 Soler, M.J., Riera, M. & Batlle, D., 2012. New experimental models of diabetic
2320 nephropathy in mice models of type 2 diabetes: efforts to replicate human
2321 nephropathy. *Experimental diabetes research*, 2012, p.616313.

2322 Sugaru, E. *et al.*, 2006a. Enhanced effect of combined treatment with SMP-534
2323 (antifibrotic agent) and losartan in diabetic nephropathy. *American journal of*
2324 *nephrology*, 26(1), pp.50–58.

2325 Sugaru, E. *et al.*, 2006b. SMP-534 ameliorates progression of glomerular fibrosis and
2326 urinary albumin in diabetic db/db mice. *American journal of physiology. Renal*
2327 *physiology*, 290(4), pp.F813–820.

2328 Suzuki, M. *et al.*, 2012. Tofogliflozin, a potent and highly specific sodium/glucose
2329 cotransporter 2 inhibitor, improves glycemic control in diabetic rats and mice.
2330 *The Journal of Pharmacology and Experimental Therapeutics*, 341(3),
2331 pp.692–701.

2332 Tabatabai, N.M. *et al.*, 2009. Enhanced expressions of sodium-glucose cotransporters in
2333 the kidneys of diabetic Zucker rats. *Diabetes Research and Clinical Practice*,
2334 83(1), pp.e27–30.

2335 Tahara, A. *et al.*, 2012. Pharmacological profile of ipragliflozin (ASP1941), a novel
2336 selective SGLT2 inhibitor, in vitro and in vivo. *Naunyn-Schmiedeberg's archives*
2337 *of pharmacology*, 385(4), pp.423–436.

2338 Tesch, G.H. & Lim, A.K.H., 2011. Recent insights into diabetic renal injury from the
2339 db/db mouse model of type 2 diabetic nephropathy. *American journal of*
2340 *physiology. Renal physiology*, 300(2), pp.F301–310.

2341 The DCCT Research Group, 1993. The effect of intensive treatment of diabetes on the
2342 development and progression of long-term complications in insulin-dependent
2343 diabetes mellitus. The Diabetes Control and Complications Trial Research
2344 Group. *The New England journal of medicine*, 329(14), pp.977–986.

2345 Thomas, M.C. & Atkins, R.C., 2006. Blood pressure lowering for the prevention and
2346 treatment of diabetic kidney disease. *Drugs*, 66(17), pp.2213–2234.

2347 Ueta, K. *et al.*, 2006. Reduction of renal transport maximum for glucose by inhibition of
2348 NA(+)-glucose cotransporter suppresses blood glucose elevation in dogs.
2349 *Biological & pharmaceutical bulletin*, 29(1), pp.114–118.

2350 UKPDS Group, 1998. Intensive blood-glucose control with sulphonylureas or insulin
2351 compared with conventional treatment and risk of complications in patients
2352 with type 2 diabetes (UKPDS 33). UK Prospective Diabetes Study (UKPDS)
2353 Group. *Lancet*, 352(9131), pp.837–853.

2354 Usberti, M. & Andreucci, V.E., 1976. Relationship of glomerular filtration rate and
2355 hypoalbuminaemia to renal glucose reabsorption. *Proceedings of the European*
2356 *Dialysis and Transplant Association. European Dialysis and Transplant*
2357 *Association*, 12, pp.174–182.

2358 Vallon, V. *et al.*, 2013. Knockout of Na-glucose transporter SGLT2 attenuates
2359 hyperglycemia and glomerular hyperfiltration but not kidney growth or injury
2360 in diabetes mellitus. *American journal of physiology. Renal physiology*, 304(2),
2361 pp.F156–167.

2362 Vallon, V. *et al.*, 2011. SGLT2 mediates glucose reabsorption in the early proximal
2363 tubule. *Journal of the American Society of Nephrology: JASN*, 22(1),
2364 pp.104–112.

Vallon, V., 2011. The proximal tubule in the pathophysiology of the diabetic kidney. *American journal of physiology. Regulatory, integrative and comparative physiology*, 300(5), pp.R1009–1022.

Vallon, V., Blantz, R.C. & Thomson, S., 2003. Glomerular hyperfiltration and the salt paradox in early [corrected] type 1 diabetes mellitus: a tubulo-centric view. *Journal of the American Society of Nephrology: JASN*, 14(2), pp.530–537.

Vallon, V. & Thomson, S.C., 2012. Renal function in diabetic disease models: the tubular system in the pathophysiology of the diabetic kidney. *Annual Review of Physiology*, 74, pp.351–375.

Wagner, J.D. *et al.*, 2010. A selective peroxisome proliferator-activated receptor alpha agonist, CP-900691, improves plasma lipids, lipoproteins, and glycemic control in diabetic monkeys. *The Journal of pharmacology and experimental therapeutics*, 333(3), pp.844–853.

Wang, B. *et al.*, 2013. Blood pressure-lowering effects of GLP-1 receptor agonists exenatide and liraglutide: a meta-analysis of clinical trials. *Diabetes, Obesity and Metabolism*, 15(8), pp.737–749.

Washburn, W.N. & Poucher, S.M., 2013. Differentiating sodium-glucose co-transporter-2 inhibitors in development for the treatment of type 2 diabetes mellitus. *Expert opinion on investigational drugs*, 22(4), pp.463–486.

Weekley, L.B., Deldar, A. & Tapp, E., 2003. Development of renal function tests for measurement of urine concentrating ability, urine acidification, and glomerular filtration rate in female cynomolgus monkeys. *Contemporary topics in laboratory animal science / American Association for Laboratory Animal Science*, 42(3), pp.22–25.

Wilding, J.P.H. *et al.*, 2009. A study of dapagliflozin in patients with type 2 diabetes receiving high doses of insulin plus insulin sensitizers: applicability of a novel insulin-independent treatment. *Diabetes care*, 32(9), pp.1656–1662.

Wilding, J.P.H. *et al.*, 2012. Long-term efficacy of dapagliflozin in patients with type 2 diabetes mellitus receiving high doses of insulin: a randomized trial. *Annals of internal medicine*, 156(6), pp.405–415.

Wright, E.M., Loo, D.D.F. & Hirayama, B.A., 2011. Biology of human sodium glucose transporters. *Physiological reviews*, 91(2), pp.733–794.

Wright, E.M., Turk, E. & Martin, M.G., 2002. Molecular basis for glucose-galactose malabsorption. *Cell Biochemistry and Biophysics*, 36(2-3), pp.115–121.

Yamaguchi, K. *et al.*, 2013. In vitro-in vivo correlation of the inhibition potency of sodium-glucose cotransporter inhibitors in rat: a pharmacokinetic and pharmacodynamic modeling approach. *The Journal of pharmacology and experimental therapeutics*, 345(1), pp.52–61.

Yamaguchi, K. *et al.*, 2011. Pharmacokinetic and pharmacodynamic modeling of the effect of an sodium-glucose cotransporter inhibitor, phlorizin, on renal glucose transport in rats. *Drug metabolism and disposition: the biological fate of chemicals*, 39(10), pp.1801–1807.

Yamamoto, K. *et al.*, 2011. TS-071 is a novel, potent and selective renal sodium-glucose cotransporter 2 (SGLT2) inhibitor with anti-hyperglycaemic activity. *British journal of pharmacology*, 164(1), pp.181–191.

Zanardi, T.A. *et al.*, 2012. Pharmacodynamics and Subchronic Toxicity in Mice and Monkeys of ISIS 388626, a Second-Generation Antisense Oligonucleotide That Targets Human Sodium Glucose Cotransporter 2. *The Journal of pharmacology and experimental therapeutics*, 343(2), pp.489–496.

Zhang, L. *et al.*, 2010. Dapagliflozin treatment in patients with different stages of type 2 diabetes mellitus: effects on glycaemic control and body weight. *Diabetes, obesity & metabolism*, 12(6), pp.510–516.

Zhao, F.-Q. & Keating, A.F., 2007. Functional properties and genomics of glucose transporters. *Current genomics*, 8(2), pp.113–128.